View metadata, citation and similar papers at core.ac.uk
brought to you by CORE
provided by Multimedia ONline ARchiv CHemnitz

Spectroelectrochemistry of Intrinsically Conducting Furan-Thiophenes Copolymers

von der Fakultät für Naturwissenschaften der Technischen Universität Chemnitz
genehmigte Dissertation zur Erlangung des akademichen Grades

doctor rerum naturalium
(Dr. rer. nat.)

Vorgelegt von
M. Sc. Fadi Alakhras
geboren am 05.07.1979 in Libyen

eingereicht am 20.09.2007

Gutachter: Prof. Dr. Rudolf Holze
Prof. Dr. Stefan Spange
Prof. Dr. Lothar Dunsch

Tag der Verteidigung: 29.09.2008

Bibliographische Beschreibung und Referat

Fadi Alakhras

Spectroelectrochemistry of Intrinsically Conducting Furan-Thiophenes Copolymers

Die elektrochemische Copolymerisation von Furan und Thiophen oder 3-Chlorothiophen wurde erfolgreich realisiert in einer Elektrolytlösung von Bortrifluorid-Diethylether + Ethylether (Verhältnis 1:2) bei konstantem Elektrodenpotenzial. Die Zugabe von Trifluoroessigsäure (TFA) (10 Vol-%) zu Bortrifluorid-Diethylether + Ethylether (Verhältnis 1:2) erniedrigte das Oxidationspotenzial der Monomere; die Polymerisationsgeschwindigkeit erhöhte sich, da TFA die Ionenleitfähigkeit des Elektrolyts vergrößert.

Die Homopolymere zeigen nur einen Redoxpeak, verursacht durch Polymeroxidation und -reduktion. Die elektrochemische Copolymerisation wird bei verschiedenen Potenzialen und mit unterschiedlichen Thiophen- oder 3-Chlorothiophenkonzentrationen untersucht. Die Copolymere zeigen ein Redoxpeakpaar, dessen Position sich wesentlich von der der Homopolymere unterscheidet. Mit zunehmendem Polymerisationspotenzial und/oder zunehmender Konzentration an Thiophen- oder 3-Chlorothiophen werden auch mehr Thiophen- oder 3-Chlorothiopheneinheiten in den Copolymerfilm eingebaut. Ein Elektropolymerisationmechanismus wird für die Copolymere vermutet und die Copolymere weisen eine recht gute Langzeitstabilität der Redoxaktivität nach Zyklen in Acetonitril auf.

In situ UV-Vis-Spektren der Homo- und Copolymerfilme wurden gemessen und λ_{1max}, welches dem $\pi \rightarrow \pi^*$- Übergang entspricht, wurde bestimmt. Der optische Übergang bei λ_{2max} vom Valenzband in das höhere Bipolaronband wurde ebenfalls bestimmt. Die Bandlücke für die Homo- und Copolymerfilme beim direkten Übergang wurde von der Kante im Absorptionsspektrum abgeschätzt. Die elektrochemische Thermodynamik für die Homo- und Copolymerfilme deutet darauf hin, dass jeweils ein Elektron von den Polymersegmenten, bestehend aus 4 Monomereinheiten, entfernt wird.

Die untersuchten leitfähigen Filme zeigen einen Leitfähigkeitssprung mit einer stabilen Leitfähigkeit bis $E_{Ag/AgCl}$= 2 V. Diese Leitfähigkeitsänderung ist reversibel. Polyfuran hat verglichen mit Polythiophen eine geringere Leitfähigkeit und die Leitfähigkeit von Poly(3-chlorothiophen) ist rund eine Zehnerpotenz niedriger als die von Polythiophen. Da das *in situ* Leitfähigkeitsverhalten der Copolymere nicht die Summe der einzelnen Homopolymere bildet, kann man ausschließen, dass es sich bei den abgeschiedenen Copolymeren um Blockcopolymere handelt.

Mit Hilfe der FTIR-Spektroskopie wurden Schwingungsspektren der Homo- und Copolymerfilme aufgenommen. Die Ergebnisse zeigen, dass es zur α-α'-Verknüpfung zwischen den Radikalkationen während der Copolymerisation kommt, was charakteristisch ist für α-substituierte fünfgliedrige heterozyklische Verbindungen. Der Mechanismus der elektrochemischen Degradation von Furan-Thiophen-Copolymeren wird ebenfalls mit Hilfe der gemessenen Spektren beschrieben.

Die *in situ* Resonanz-Raman-Spektroskopie ergab, dass die spektroskopischen Eigenschaften der Copolymere zwischen denen der Homopolymere lagen. Bei höheren Polymerisationspotenzialen und höheren Konzentrationen an Thiophen oder 3-Chlorothiophen werden mehr Thiophen- oder 3-Chlorothiopheneinheiten in die Copolymerketten eingebaut. Es ist offensichtlich, dass die Ramanspektren der Copolymere wesentlich komplexer sind als die der Homopolymere, wodurch die Auswertung erschwert wird. Dennoch erinnern die Ramanspektren der Copolymere an die der Homopolymere.

Die spektroelektrochemischen Eigenschaften der Copolymere haben bestätigt, dass deren Charakteristika zwischen denen der Homopolymere liegen, was deutlich macht, dass die Oxidation von Monomeren möglich ist und dass die Copolymerketten demnach aus Furan- und Thiophen- bzw. 3-Chlorothiopheneinheiten bestehen können.

Schlüsselwörter: Spektroelektrochemie, Elektropolymerisation, Zyklische Voltammetrie, Copolymere, Polyfuran, Polythiophen, Poly(3-chlorothiophen).

Abstract

Fadi Alakhras

Spectroelectrochemistry of Intrinsically Conducting Furan-Thiophenes Copolymers

Electrochemical copolymerization of furan and thiophene or 3-chlorothiophene was successfully realized in a solvent system consisting of boron trifluoride ethyl ether (BFEE) + ethyl ether (EE) (ratio 1:2) at constant electrode potential. The addition of trifluoroacetic acid (TFA) (10 % by volume) to BFEE + EE (ratio 1:2) decreased the oxidation potential of the monomers; the polymerization rate was also accelerated because TFA increases the ionic conductivity of the electrolyte.

The homopolymers have only one redox peak caused by polymer oxidation and reduction. Electrochemical copolymerization both at different potentials and with different thiophene or 3-chlorothiophene concentrations is investigated. The copolymers show one anodic/cathodic peak couple that appears at a position quite different from the positions observed with homopolymers. More thiophene or 3-chlorothiophene units are incorporated into the copolymer film with an increasing polymerization potential of the copolymer and/or with an increasing concentration of thiophene or 3-chlorothiophene in the feed. An electropolymerization mechanism of copolymers has been proposed, and the copolymers show a fairly good long-term stability of the redox activity after cycling in acetonitrile.

In situ UV-Vis spectra of the homo- and copolymer films were measured and λ_{1max} which corresponds to the $\pi \rightarrow \pi^*$ transition is determined. The optical transition with λ_{2max} from the valence band into the higher bipolaron band is also assigned. The band gap (E_g) for homo- and copolymer films from a direct interband transition is estimated from the absorption edge of the spectrum. The redox thermodynamics of the homo- and copolymer films suggest that one electron is removed from polymer segments containing four monomer units.

The studied conducting films show a single conductivity change with a stable conductivity up to $E_{Ag/AgCl}$= 2 V. The conductivity of these films is almost restored

when the potential shift direction is reversed. Polyfuran compared to polythiophene, has a lower conductivity and the conductivity of poly(3-chlorothiophene) is around one order of magnitude lower than that of polythiophene. The *in situ* conductivity properties of the copolymers are not the sum of those of the individual homopolymers. This result may eliminate the possibility that the copolymers can be considered as block copolymers.

Vibrational spectra of homo- and copolymer films investigated in this study have been obtained using FTIR spectroscopy. The results indicate that α-α' coupling of radical cations has taken place in the copolymerization. This is a characteristic of α-substituted five-membered heterocyclic compounds. The electrochemical degradation mechanism of furan-thiophene copolymers is also described using the obtained spectra.

The *in situ* resonance Raman spectroscopy of the copolymers shows spectroscopic properties intermediate between those of homopolymers. At higher polymerization potentials and at higher concentrations of thiophene or 3-chlorothiophene in the feed more thiophene or 3-chlorothiophene units are incorporated into the copolymer chains. It is obvious that the Raman spectra of the copolymers are more complex than those of homopolymers, which makes the assignment difficult. However, the *in situ* Raman spectra of the copolymers are reminiscent of those of the homopolymers.

The spectroelectrochemical properties of the copolymers confirmed that the copolymers show intermediate characteristics between the homopolymers, implying that oxidation of monomers is possible and the copolymer chains may accordingly be composed of furan and thiophene or 3-chlorothiophene units.

Keywords: Spectroelectrochemistry, Electropolymerization, Cyclic voltammetry, Copolymers, Polyfuran, Polythiophene, Poly(3-chlorothiophene).

Die vorliegende Arbeit wurde in der Zeit von Mai 2005 bis Mai 2007 unter Leitung von Prof. Dr. Rudolf Holze am Lehrstuhl für Physikalische Chemie/Elektrochemie der Technischen Universität Chemnitz durchgeführt.

Acknowledgements

I would like to express my deepest appreciation, gratitude and special grateful to my supervisor Prof. Dr. Rudolf Holze for his considerable assistance, advice and guidance during this work.

I am deeply grateful to my colleagues, with whom I spent a precious time, for their excellent suggestions and contributions to the success of this work.

I would also like to thank the staff members and employees at Chemnitz University of Technology for giving me all the facilities to carry out this work.

Great thanks are owed to my family for their sustainable support, encouragement, and care during this period of time.

Dedication

To my Parents

The two candles that always enlighten my life

To the soul of my beloved Grandfather Abdel Rahim

Fadi

Table of Contents

Bibliographische Beschreibung und Referat 2

Abstract 3

Zeitraum, Ort der Durchführung 5

Acknowledgments 6

Dedication 7

Table of contents 8

List of abbreviations 11

1 Introduction 13

1.1 Conducting Polymers 13

1.2 The Structure of Conducting Polymers 14

1.3 The Mechanism of Conduction 16

1.4 Polyfuran 17

1.5 Polythiophenes 19

1.6 Conducting Copolymers 20

1.7 The Synthesis of Conducting Polymers 21

1.7.1 Chemical Synthesis 21

1.7.2 Electrochemical Synthesis 21

1.8 The Effects of Boron trifluoride-ethyl ether as a Solvent 23

1.9 Characterization of Conducting Polymers 24

1.9.1 Electrochemical Measurements 24

1.9.2 Spectroscopic Measurements 25

1.9.3 Conductivity Measurements 26

1.10 Applications of Conducting Polymers 27

1.11 Aim and Scope of the Work 27

2 Experimental 30

2.1 Chemicals 30

2.2 Electropolymerization and Cyclic Voltammetry 30

2.3 *In situ* UV-Visible Spectroscopy and Redox Thermodynamics 31

2.4 *In situ* Conductivity Measurements 31

2.5 Fourier Transform Infrared (FTIR) Spectroscopy 32

2.6 The *In situ* Resonance Raman Spectroscopy 32

3 Results and Discussion 33

3.1 Electrochemistry of Homo- and Copolymer Films 33

3.1.1 Electropolymerization 33

3.1.2 Cyclic Voltammetry 36

3.1.3 The Proposed Mechanism of the Electrochemical Formation of Furan-Thiophene Copolymers 46

3.1.4 The Stability of Redox Activity of Furan-Thiophene Copolymers 48

3.2 *In situ* UV-Visible Spectroscopy 51

3.2.1 The *In situ* UV-Visible Spectroscopy of Homo- and Copolymer Films 51

3.2.2 Redox Thermodynamics 66

3.3 *In situ* Conductivity Measurements 69

3.4 Fourier Transform Infrared Spectroscopy 79

3.4.1 The FTIR Spectroscopy of Homo- and Copolymer Films 79

3.4.2 The Electrochemical Degradation Mechanism of Furan-Thiophene Copolymers 87

3.5 The *In situ* Resonance Raman Spectroscopy 93

Summary 119

Future work 123

References 124

List of publications 134

Selbstständigkeitserklärung 135

Curriculum Vitae 136

List of Abbreviations

Ag/AgCl	silver/silver chloride electrode
$AlCl_3$	aluminim chloride
A_{ox}	absorbance of oxidized film
A_{red}	absorbance of reduced film
BFEE	boron trifluoride ethyl ether
BrTh	3-bromothiophene
BTh	3-butylthiophene
$CaCl_2$	copper (II) chloride
CTh	3-chlorothiphene
CV	cyclic voltammogram
E^o	standard electrode potential
$E_{Ag/AgCl}$	electrode potential (*v*s Ag/AgCl in acetonitrile)
EE	ethyl ether
E_g	band gap
E_{pa}	anodic peak potential
E_{pc}	cathodic peak potential
E_{pol}	polymerization potential
E_{SCE}	electrode potential (*v*s SCE)
ESD	electrostatic discharge
eV	electron volt
$FeCl_3$	ferric chloride
FTIR	fourier-transform infrared
HOMO	highest occupied molecular orbital
ICP	intrinsically conducting polymers
ITO	indium doped tin oxide
KBr	potassium bromide
LEDs	light emitting diodes
LUMO	lowest unoccupied molecular orbital
$NaClO_4$	sodium perchlorate

NMR	nuclear magnetic resonance
PA	polyacetylene
PAni	polyaniline
PCTh	poly(3-chlorothiophene)
PPP	poly(p-phenylene)
PPy	polypyrrole
Pt electrode	platinum electrode
PTh	polythiophene
SA	sulfuric acid
SCE	saturated calomel electrode
TBATFB	tetrabutylammonium tetrafluoroborate m
TFA	trifluoroacetic acid
UV-Vis	ultraviolet-visible
λ_{max}	wavelength at band maximum
δ	in-plane deformation
γ	out-of-plane deformation
ν	stretching
ω	out-of-plane bending

Introduction

Most common polymers are non-conductive. They are used not only for structural purposes, but for electrical isolation as well. Electrically conductive particles like carbon black and metal fibers are sometimes added to a polymer to form a conductive polymer blend. These blends are often called extrinsically conducting polymers and may be used in applications where electrostatic discharge (ESD) must be prevented. In contrast, the intrinsically conducting polymers or ICPs described in this thesis possess electronic conduction abilities within their own molecular structure. The conductive behavior of these ICPs has a strong resemblance to semi-conductors and is likewise governed by charge carrier shortage. A significant difference with metallic semiconductors is the lack of long-distance three-dimensional ordering, as the polymer chains have a limited length.

1.1 Conducting Polymers

The chemistry Nobel Prize in the year 2000 went to Alan Heeger, Alan MacDiarmid, and Hideki Shirakawa "for the discovery and development of electrically conductive polymers." The three winners established that polymer plastics can be made to conduct electricity if alternating single and double bonds link their carbon atoms, and electrons are either removed through oxidation or introduced through reduction. Normally the electrons in the bonds remain localized and cannot carry an electric current, but when the team "doped" the material with strong electron acceptors such as iodine, the polymer began to conduct nearly as well as a metal, with a conductivity 10^{11} times higher than pure polyacetylene (PA) [1-2]. Although polyacetylene exhibits a very high conductivity in the doped form, the material is not stable against oxygen or humidity and it is intractable. For these reasons, much work has been devoted to synthesizing soluble and stable polyacetylenes [3-4]. Unfortunately, these substituted derivatives exhibit electrical conductivities that are much lower than the parent polymer. The discovery of polyacetylene led to the search for new structures that could lead to new and improved polymer properties.

Several polymers have been found to show the same behavior as polyacetylene, including polypyrrole (PPy), polythiophene (PTh) and polyaniline (PAni). These polymers all show conjugation in their molecular structures, which is the basis for their conductive behavior. These ICPs are particularly important because they exhibit good electric conductivity and chemical stability in the ambient atmosphere, and they have revealed numerous areas of application such as materials for battery electrodes [5], gas sensors [6], chemical sensors [7-14], biosensors [15-18], ion sieving [19], corrosion protection [20], and microwave shielding [21].
These conducting polymers differ from polyacetylene in that they have a nondegenerate ground state because of the energetic nonequivalence of their two limiting mesomeric forms, aromatic and quinoid, their high environmental stability, and their structural versatility, which allows modulation of their electronic and electrochemical properties by manipulation of the monomer structure [22].

1.2 The Structure of Conducting Polymers

All materials can be divided into three main groups: insulators, semiconductors and metals. These are differentiated by their ability to conduct electron flow (current). Conducting polymers constitute a class of materials that possess properties of both organic polymers and inorganic conductors or semiconductors [23]. These materials can be defined as organic polymers in which the monomeric units are covalently linked [24]. The best known property of these conjugated polymers is their ability to conduct electric current after being partly oxidized or reduced [25].

The polymers that display electron conduction all have a system of conjugated π bonds, sometimes interspersed with atoms such as nitrogen, sulfur and oxygen. Table 1 provides structure of some common conducting polymers [26-31].

Table 1. Names and structures of the most common studied conducting polymers.

Polymer	Structure	Polymer	Structure
Polypyrrole	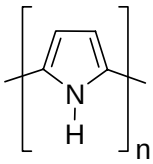	Polyindole	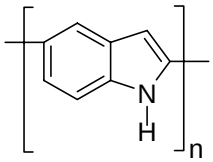
Polythiophene	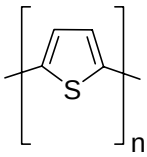	Polyaniline	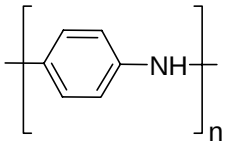
Polyfuran	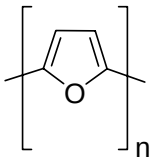	Polyazulene	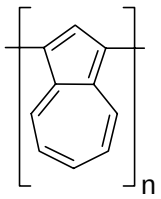
Polyselenophene	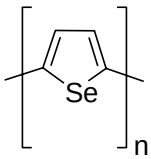	Poly *Para*-phenylene	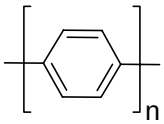

It was originally believed that the mechanism of conduction in polymeric materials was electron transport through the system of conjugated multiple bonds. With the bonds in a single plane and the π orbitals parallel, the orbitals of π electrons overlap to form a single delocalized cloud of π electrons over the entire molecules. This theory was based on the observation that the bond lengths in conjugated systems were intermediate between the values of single and double bonds. A more recent explanation of the mechanism of conduction in polymeric materials is presented in section 1.3.

1.3 The Mechanism of Conduction

Electronically conducting polymers are extensively conjugated molecules, and they are believed to possess a spatially delocalized band-like electronic structure. Conduction occurs when an electron is promoted from the valence band to the conduction band, but this can not occur when the bands are either empty or full [32]. The energy difference between the highest occupied band (valence band) and the lowest unoccupied band (conduction band) is called the band gap. If the band gap is small, the thermal excitation can be enough to give rise to conductivity. This is what happens in conventional semiconductors. Conducting polymers are different in that they conduct without having either a partially empty or partially filled band [32]. Fig. 1 represents the band structure in an electronically conducting polymer.

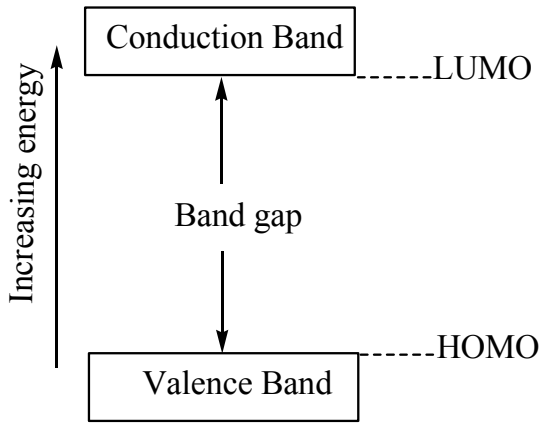

Fig. 1. Band structure in an electronically conducting polymer.

The electronic ground state of conducting polymers is that of an insulator. The conductivity of these polymers is transformed through the process of doping [33]. The doping is usually quantitative, and can be carried out chemically by either exposure of the polymer to the dopant, or by electrochemical oxidation or reduction [33]. These dopants work by acting as charge transfer agents. They are positioned interstitially between the polymer chains and donate charges to, or accept charges from the polymer backbone.

When a π electron is removed from the polymer backbone, it becomes a radical cation (polaron) that is delocalized over several monomeric units. When a second electron is removed from the polymer, two individual polarons or one bipolaron can form [34]. Because the formation of bipolarons is energetically more favorable than the separated polaronic states, bipolarons are spread over the polymer. Polarons and bipolarons are mobile in an electric field and they are the charge carriers responsible for electrical conduction in polymer chains. The positively charged defects (polaron and bipolaron) on polythiophene are depicted in Fig. 2.

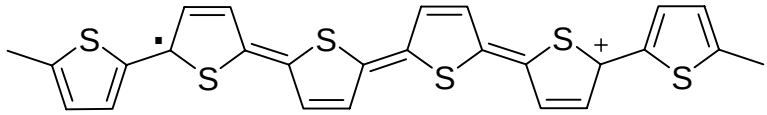

(A)

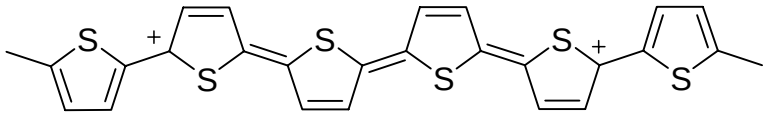

(B)

Fig. 2. The positively charged defects on polythiophene: (A) polaron, (B) bipolaron.

1.4 Polyfuran

Among conducting polymers with an extended π-electron system, polyfuran is interesting because of its possible technological applications as a humidity sensor [35]. Polyfuran is very sensitive to humidity, and its electrical resistivity decreases considerably and reversibly upon contact with moisture. In addition to this, polyfuran can be used as an optoelectronic device, since upon doping the color changes from yellow-brown to black-brown [36].

Polyfuran is among the most ill-defined of conjugated polymers compared to polypyrrole and polythiophene. The synthesis of polyfuran films was first mentioned in 1982 by Tourillon and Garnier, the reported polymer exhibited low electrical conductivity ranging from 10^{-5} to 10^{-3} S cm^{-1} [27]. It was claimed that polyfuran has been

obtained previously by electrochemical polymerization of furan, but the high voltage required for the electropolymerization (1.8-2.5 V) results in irreversible oxidation of the polymer [37]. With another method, polyfuran was prepared by electrochemical reduction of 2,5-dibromofuran in acetonitrile using $[Ni(bipy)_3]^{2+}$ as a catalyst. The polymer obtained only in trace amount on the cathode was in its neutral insulating form [38]. Gleins and Benz tried to use terfuran as the starting monomer to lower the oxidation potential. The obtained polymer had an electrical conductivity of $2*10^{-3}$ S cm^{-1} when doped with $CF_3SO_3^-$. Although the oxidation potential was lowered by this method (~1.5 V), the resultant polymer contained a large amount of saturated rings as evidenced by infrared spectrometry [39].

More recently, furan has been electropolymerized in acetonitrile at potentials E_{SCE} = 2.1-2.3 V using $NaClO_4$ as an electrolyte [40]. The obtained film showed ill-defined cyclic voltammograms compared to those obtained by Glenis et al. and by Zotti et al. It was obvious that the polymer underwent irreversible oxidation and contained a large amount of saturated rings or ring-opened components at such high potentials.

Polyfuran and poly(2-methylfuran) were prepared by controlled potential electrolysis in acetonitrile at room temperature. The electrical conductivity of polyfuran is decreased by a factor of four when the methyl group is present in the α-position. The temperature effect on the rate of polymerization of furan was studied with cyclic voltammetry technique and an increase in the initial rate of polymerization was observed with increasing temperature. The mechanism of electrochemical polymerization was investigated with *in situ* electron spin resonance spectroscopy. The spectrum of furan indicated that the radical cation formed after electron transfer couples immediately which is followed by elimination of H^+, indicating that polymerization occurs by α-α' mechanism [41].

Free-standing polyfuran films have been successfully synthesized by electrochemical polymerization of furan at low potential ($E_{Ag/AgCl}$ = 1.2 V) in a binary solvent system containing boron trifluoride-ethyl ether and additional ethyl ether. The polymer shows good mechanical properties, and its electrical conductivity is around 10^{-2} S cm^{-1} [42].

Raman spectra of polyfuran were first reported by Hernandez et al. [43, 44], and the bands related to neutral polyfuran were assigned based on theoretical calculations. However, it was found that the Raman spectral features of doped polyfuran were similar to those of neutral films, except for the difference in their signal-to-noise ratios. In a combined experimental and theoretical study of the Raman spectra of electrosynthesized polyfuran in dedoped and doped state it was found that the spectral features of polyfuran are strongly dependent on its doping level. Thus, the second component of polyfuran was the oxidized species of the polymer [45].

1.5 Polythiophenes

The advantageous properties of polythiophene derivatives have been reviewed by a number of workers [46-50]. Polythiophene and its derivatives have acquired tremendous technological potentials in electrocatalysis [51, 52], the fabrication of molecular electronic devices [53], solid state batteries [54], chemically modified electrodes [55], and biosensors [56–58]. This is mainly due to the remarkable solid state properties of polythiophenes including high conductivity (10^2 S/cm), stability in both air and moisture, structural versatility and wide electrochemical potential windows, which can make it less susceptible to overoxidation and therefore to degradation.

Polythiophene and its derivatives are unique in that they may be prepared both anodically and cathodically. Anodic preparation of polythiophene was first mentioned by Tourillon et al. in connection with their oxidation experiments on aromatic oligomers and monomers [27], whereas the cathodic preparation of polythiophene involves the electroreduction of the complex (2-bromo-5-thienyl) triphenylnickel dibromide in acetonitrile [59]. Shi, Jin, and Xue decreased the polymerization potential of thiophene to about $E_{Ag/AgCl}$ = 1.0 V by performing the electropolymerization of thiophene in trifluroborate-ethyl ether (BFEE) solution [60, 61]. With the lower potential, they prepared flexible polythiophene films with strong mechanical properties.

Much interest has been generated in the studies of substituted polythiophenes in view of the fact that introduction of substitutions in the monomers influences the properties of the resulting polymers significantly.

A wide range of substituted thiophene-based polymers has gained popularity and importance in conducting polymer research [62-64]. However, only few articles have focused on poly(3-halide thiophene)s [65-69]. Poly(3-chlorothiophene) (PCTh) was synthesized electrochemically from 3-chloro-2-trimethylsilylthiophene [69] and only one short communication concerning direct oxidation of 3-chlorothiophene has been reported [66].

Since the oxidation of 3-chlorothiophene requires a very high potential in neutral solvents (E_{SCE} = 2.18 V), poly(3-chlorothiophene) films were synthesized electrochemically by direct oxidation of 3-chlorothiophene (CTh) in mixed electrolytes of boron trifluoride diethyl etherate (BFEE) and trifluoroacetic acid (TFA) or sulfuric acid (SA) [70, 71]. The addition of TFA or SA to BFEE can further decrease the oxidation potential of the monomer and improve the quality of the polymer film [72, 73].

1.6 Conducting Copolymers

Copolymerization and blending are important methods of modifying the properties of individual polymers. For example, Berggren et al. reported on light emitting diodes (LEDs) with variable colors from blends of polythiophene derivatives [74]. By blending polymers with different emission and charge-transport characteristics, light-emitting diodes can be fabricated in which the emission color is controlled by the operating voltage. Thus, copolymers and composites of heterocyclic compounds may be useful in practical applications.

Li et al. successfully copolymerized 3-butylthiophene (BTh) and 3-bromothiophene (BrTh) on stainless steel electrodes [75]. The resulting poly(BTh-co-BrTh) films were flexible with a tensile strength of 18.3 MPa. Electrochemical copolymerization of furan and 3-methyl thiophene was performed potentiostatically in a binary solvent system consisting of boron trifluoride-ethyl ether and additional ethyl ether (ratio 2:1). The obtained copolymer was characterized by cyclic voltammetry, infrared spectroscopy and electrical conductivity. The copolymerization was carried out at $E_{Ag/AgCl,\ 0.1\ M\ KCl}$ = 1.2 V, the polymer had an electrical conductivity of 0.36 S cm^{-1}[76]. Wan et al. also found that the composition of the copolymer varies with the applied electrochemical polymerization potential and the monomer feed ratio. The higher the applied potential, the more furan units are incorporated into the copolymer film, while the

higher the concentration of the pyrrole, the more pyrrole units are incorporated into the copolymer film [77].

1.7 The Synthesis of Conducting Polymers

Synthesis of the ICPs was done using two principal methods: classical organic synthesis "chemical" and electrochemical synthesis. A synopsis of each synthesis procedure is given in this section. Each method has its advantages and disadvantages. The chemical synthesis can be used to produce significantly more polymer than the electrochemical method. However, the classic procedure uses much more solvent and reagents, is more time-consuming (days), and is more difficult to accomplish. The electrochemical synthesis is fast (minutes) and easy to implement; nevertheless, the quantity of polymer produced using the current instrumentation is very small. Other advantages of the electrochemical procedure will be presented later in this section.

1.7.1 Chemical Synthesis

Among the chemical polymerization techniques, oxidative methods represent the least expensive and most widely exploited means by which conjugated polymers can be prepared [78]. Oxidative chemical polymerizations are accomplished by exposing the monomer to a two-electron stoichiometric amount of oxidizing agent, resulting in the formation of the polymer in its doped and conducting state. Isolation of the neutral polymer is achieved by exposing the material to a strong reducing agent such as ammonium hydroxide or hydrazine. Heterocyclic monomers, such as thiophene and its derivatives, are typically polymerized in the presence of anhydrous $FeCl_3$ [79] although other Lewis acids can also be used [80]. Furthermore, benzene can be polymerized to form PPP by adding $AlCl_3/CuCl_2$ [81].

1.7.2 Electrochemical Synthesis

Electropolymerization is a standard oxidative method for preparing electrically conducting conjugated polymers. Smooth, polymeric films can be efficiently electrosynthesized onto conducting substrates where their resultant electrical and optical

properties can be probed easily by several electrochemical and coupled *in situ* techniques. Electropolymerization involves the oxidation of a monomer dissolved in a supporting electrolyte solution by applying an external potential to form reactive radical cations (also known as the monomer oxidation potential) (Fig. 3).

After the initial oxidation, two routes for polymer formation are possible. In the first pathway, a monomer radical cation can couple with neutral monomer, and after a second oxidation and loss of two protons, it forms a neutral dimer [82]. The second route involves the coupling of two radical cations followed by the loss of two protons to yield neutral dimer [83, 84]. Then the neutral dimer is oxidized and the process is repeated until an electroactive polymer film is deposited onto the conducting substrate. Because of the oxidative nature of electropolymerizations, the deposited polymer is typically in its oxidized state, thus necessitating the presence of a supporting electrolyte to compensate the positive charges along the polymer backbone.

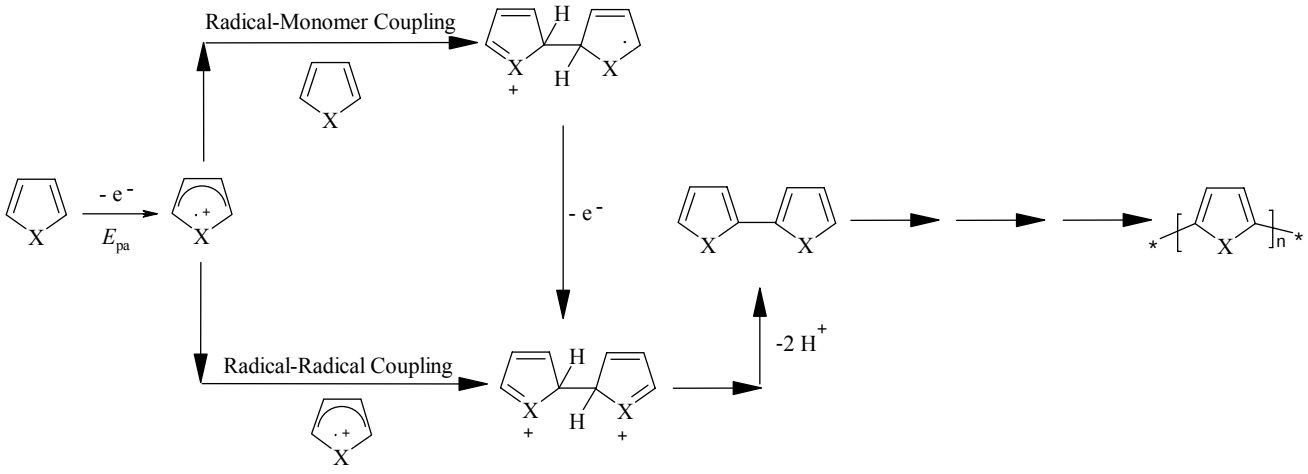

Fig. 3. Proposed mechanism for the electrochemical polymerization of five-membered heterocycles.

The efficiency of the polymerization is dictated by the ease with which electrons can be removed from the monomer and by the stability of the resultant radical cation. Electron-rich monomers, such as thiophene and pyrrole, are able to lose an electron more easily, and are also able to stabilize the resultant radical cation through resonance across the π electron system better than relatively electron-poor compounds

such as benzene. Upon electropolymerization, stable electroactive polymers derived from electron-rich heterocycles can be formed. Despite the facile nature of electrochemical polymerization, this method possesses the major limitation of yielding insoluble materials, precluding the analysis of primary structure by traditional analytical techniques. Because of this limitation, chemical polymerization methods have gained popularity for synthesizing novel soluble conjugated polymers.

1.8 The Effects of Boron trifluoride-ethyl ether as a Solvent

BFEE is a coordination compound between boron trifluoride and diethyl ether in 1:1 equivalent proportion. The conductivity of BFEE is $2.97*10^{-4}$ S/cm at 25^{o}C [85]. BFEE solution is a strong Lewis acid. It is widely used as a catalyst in electrochemical polymerization of aromatic monomers. BFEE can exist in diethyl ether as a polar molecule, $[(C_2H_5)_3O^+]BF_4^-$, which furnishes a conducting medium [86]. This solution is also electrochemically stable over a wide potential range.

Shi et al. used freshly distilled BFEE (without adding any other solvent) as a medium for anodic oxidative polymerization of various aromatic monomers such as naphthalene, thiophene, benzene, and their derivatives [60-61, 72, 86-89]. It has been proposed that the potential-lowering effect of BFEE on the electropolymerization of thiophene results from the interaction of BFEE and thiophene rings, thus lowering the aromatic resonance energy of the rings. The polymer films obtained had well-defined conjugated structures and good mechanical properties.

Boron trifluoride-ethyl ether (BFEE) complex was also chosen as a binary system to lower the oxidation potential of furan [77]. The significant decrease in the oxidation potential of furan in the strongly acidic medium can be rationalized in two ways: firstly, furan forms a complex with the strong acid, thereby reducing the resonance stabilization of the aromatic ring and shifting the oxidation potential to less anodic potentials. Secondly, the increased acidity of the solvent imparts a greater stability to the cation radical, which in turn promotes the electrooxidation and subsequent polymerization. However, the resonance energy of furan is so low that it acts more like a conjugated diene than like a heteroaromatic molecule, which makes it sensitive to acids. Additional polymerization occurred immediately and nonconjugated polymer was

precipitated when furan was directly added to BFEE. Thus ethyl ether was added to adjust the acidity of BFEE and the undesirable polymerization was suppressed [42].

Since the orientation of the polymeric nuclei with respect to the metal surface is very attractive for the study of conduction mechanisms and for the developments of high conductivities and mechanical properties, the BFEE system has proved by surface enhanced Raman spectroscopy to be a good medium not only in the electrosynthesis of high quality conducting polymers, but also in the study of conduction mechanisms [90-91].

1.9 Characterization of Conducting Polymers

The general drawbacks of electrochemical preparation are that the polymers are produced in rather small amounts and tend to be insoluble, making characterization with conventional analytical techniques, such as NMR spectroscopy and size exclusion chromatography, difficult if not impossible. The homo- and copolymer films synthesized electrochemically in this project are characterized by several spectroelectrochemical techniques as discussed below.

1.9.1 Electrochemical Measurements

The arsenal of electrochemical methods that can be applied to the study of conducting polymer films deposited on a conducting surface is fairly broad and it has been thoroughly reviewed. Among these methods, cyclic voltammetry (CV), due to its simplicity and versatility, has become increasingly popular as a mean to study redox states. The electrode potential at which a polymer undergoes reduction or oxidation can be rapidly located by CV. Furthermore, CV reveals information regarding the stability of the product during multiple redox cycles. Since the rate of potential scan is variable, both fast and slow reactions can be followed.

1.9.2 Spectroscopic Measurements

Spectroscopy is the study of the interaction between radiation (electromagnetic radiation, or light) and matter. The matter can be atoms, molecules, atomic or molecular ions, or solids. Spectroscopy is often used in physical and analytical chemistry for the identification of substances through the spectrum emitted from or absorbed by them. The spectroscopic techniques that have been used in this project are briefly decribed as follows:

UV-Vis spectroscopy probes the electronic transitions of molecules as they absorb light in the UV and visible regions of the electromagnetic spectrum. Any species with an extended system of alternating double and single bonds will absorb UV light, and anything with color absorbs visible light, making UV-Vis spectroscopy applicable to a wide range of samples especially in conjugated systems. The absorption maximum λ_{1max} assigned to the $\pi \rightarrow \pi^*$ transition is measured with the polymer films in their neutral state, whereas the absorption maximum λ_{2max} assigned to an intraband transition from the valence band into the upper bipolaron band of the polymer in its oxidized state is also determined. The band gap (E_g) for the homo- and copolymer films from a direct interband transition can as well be estimated from the absorption edge of the spectrum.

FTIR Spectroscopy is one of the most common spectroscopic techniques used by organic and inorganic chemists. The main goal of FTIR spectroscopic analysis is to determine the chemical functional groups in the sample, to assess its purity, and sometimes to identify it. Infrared radiation is that part of the electromagnetic spectrum between the visible and microwave regions. Infrared radiation is absorbed by organic molecules and converted into energy of molecular vibration, either stretching or bending. An electrochemical degradation mechanism of furan-thiophene copolymers in acetonitrile and aqueous solution is proposed depending on FTIR spectroscopy. Furthermore α-α' coupling of radical cations which has taken place in the copolymerization has been depicted by using this technique.

Raman spectroscopy is a spectroscopic technique used in condensed matter physics and chemistry to study vibrational, rotational, and other low-frequency modes

(plasmons and superconducting gas excitations) in a system. When light is scattered from a molecule most photons are elastically scattered. The scattered photons have the same energy (frequency) and, therefore, wavelength, as the incident photons. However, a small fraction of light (approximately 1 in 10^7 photons) is scattered at optical frequencies different from, and usually lower than, the frequency of the incident photons. The process leading to this inelastic scatter is the termed the Raman effect. Raman scattering can occur with a change in vibrational, rotational or electronic energy of a molecule. Chemists are concerned primarily with the vibrational Raman effect. The difference in energy between the incident photon and the Raman scattered photon is equal to the energy of a vibration of the scattering molecule.

The advantage of the Raman spectroscopy arises from the resonance enhancement of the Raman signals. The electrochemically doping method is almost ideally suited for the studies of doping induced changes in Raman spectra of polythiophene and polyfuran. Taking into account the oxidative nature of the doping and strong resonance effects observed in Raman spectroelectrochemistry, it is very advantageous to correlate the Raman studies with cyclic voltammetry and UV-Visible spectroelectrochemistry [92].

1.9.3 Conductivity Measurements

Conductivity measurement is an important step to characterize conducting polymers. It depends upon how the polymers were processed and manipulated. The conductivity measurements can be carried out either *ex situ* (two or four-probe method) or *in situ*.

A new *in situ* electrochemical conductivity technique which is much easier to handle and which uses a two-band gap electrode has been developed in our laboratory [93]. This technique has been frequently used for electrochemically synthesized conducting polymers [94]. In addition, the differences of doping state or electrolyte solution composition can be seen through changes in electrical conductivity for many polymer films prepared electrochemically.

1.10 Applications of Conducting Polymers

The extended π-systems of conjugated polymer are highly susceptible to chemical or electrochemical oxidation or reduction. These alter the electrical and optical properties of the polymer, and by controlling this oxidation and reduction, it is possible to precisely control these properties. It is even possible to switch from a conducting state to an insulating state. There are four main fields of application for these polymers as shown in Fig. 4 [95].

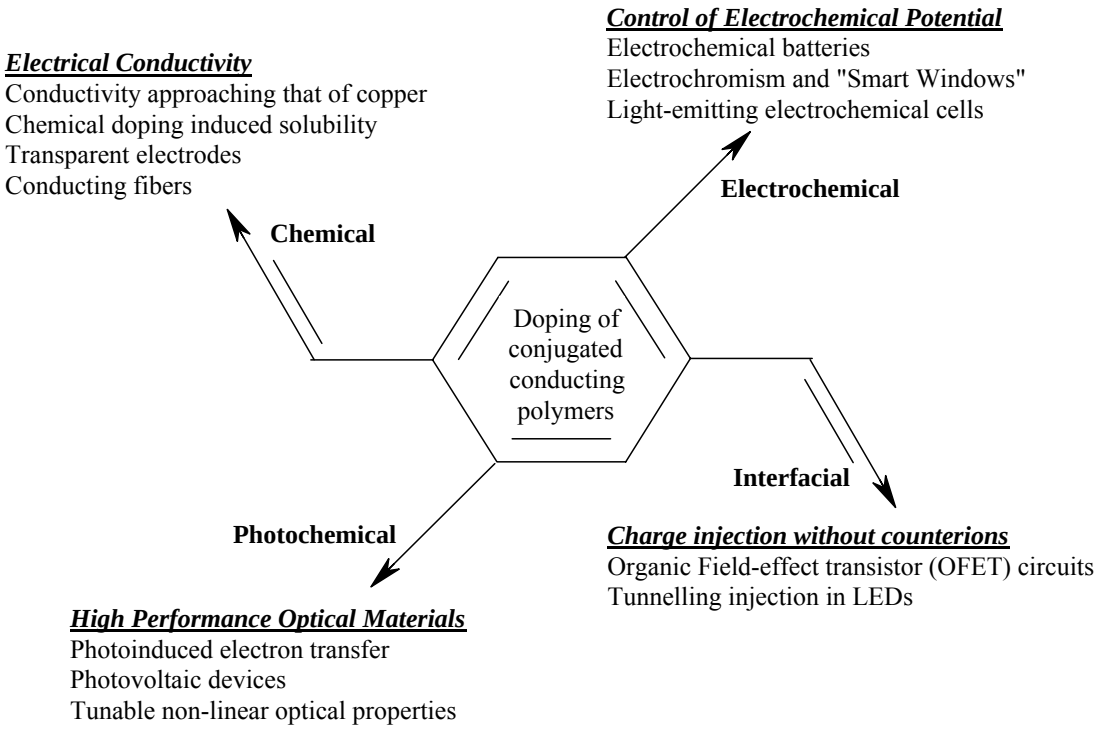

Fig. 4. Applications of conducting polymers in diverse fields.

1.11 Aim and Scope of the Work

Electronically conducting polymers, in particular those based on monomers such as pyrrole, thiophene, aniline and their substituted relatives have many potential applications. However, the stability of conducting polymers seems to be a major limiting factor in their practical applications. Thus, their degradation properties under different conditions have been studied extensively [96]. Most degradation studies have

been focused on the overoxidation of conventional conducting polymers, such as polypyrrole [97, 98], polythiophene [99, 100], and polyaniline [101, 102].
The search for conjugated polymers with small band gaps has been of particular interest [103] because of their expected pronounced nonlinear optical properties [104] and transparency in the visible region combined with high electrical conductivity [105]; they are considered for the fabrication of light emitting diodes operating in the infrared region [106]. Significant synthetic efforts have been made towards these polymers [107-109], showing that the band gap can be reduced to below 1 eV while sustaining good stability.

Polyfuran has a relatively large band gap of 2.35 eV [39], compared with polythiophene 2.0 eV [110], and polyacetylene 1.48 eV [111]. This relatively high band gap leads to doping problems; the commonly used polymers are stable in *p*-doped but not in *n*-doped form, in addition to this, the neutral form of the polymer is an insulator. A smaller band gap could help solve these problems.
The polymerization of furan, due to its lower aromaticity and drastic conditions needed for polymerization, is difficult to perform, and a number of saturated rings in the polymer chains are obtained. Hence, less attention has been paid to the study of the properties and potential applications of polyfuran.

The basic aim of this work is to prepare the homopolymers and furan-thiophenes copolymers by electropolymerization of furan, thiophene, and 3-chlorothiophene at constant electrode potential.
The homopolymers and copolymers have been studied using spectroelectrochemical techniques beyond cyclic voltammetry, in particular *in situ* UV-Vis spectroscopy, infrared spectroscopy and finally *in situ* Resonance Raman spectroscopy. *In situ* conductivity measurements have also been investigated.

The influence of the applied polymerization potential and the monomer feed ratio on the properties of the copolymers is discussed. A mechanism of the electrochemical formation of furan-thiophene copolymers has additionally been proposed. The stability of the redox activity of furan-thiophene copolymers was investigated and compared with previously prepared polyfuran films.
Electrochemical copolymerization may result in modification of the relatively large band gap of polyfuran, so small band gap polymers based on furan-thiophenes co-

polymers were attempted taking into account the results of *in situ* UV-Vis spectroscopy.

An electrochemical degradation mechanism of furan-thiophene copolymers in acetonitrile and aqueous solution has also been studied depending on FTIR spectroscopy data.

The electrical resistivity measurements of homo- and copolymer films were carried out and the relation between the resistivity and the concentration of thiophene in the electropolymerization solutions has been investigated.

Additionally, the *in situ* Resonance Raman spectroscopic measurements have been correlated with the results of cyclic voltammetry and *in situ* UV-Visible spectroscopy to investigate the doping/dedoping and resonance effects in the Raman spectra.

The redox thermodynamics of homo- and copolymer films were determined using the Nernst plots constructed from absorbance measurements performed *in situ* at various doping levels.

The effect of chlorine atom on the electrochemical polymerization potential of 3-chlorothiophene has been studied and consequently the spectroelectrochemical properties of furan-3-chlorothiophene copolymers have been compared with those of furan-thiophene films.

The results obtained and presented in this work demonstrate that the materials furan and thiophene may be combined for the development of new type of polymers, poly(furan-co-thiophene) having impressive features in terms of conductivity and stability. Taking this into consideration, these materials appear suitable for technological applications.

Experimental

2.1 Chemicals

Furan (Aldrich, 99 %), thiophene (Fluka, 98 %), and 3-chlorothiophene (Aldrich, 98 %) were distilled under nitrogen just prior to use. Ethyl ether (EE) (Acros) was dried and distilled in the presence of sodium. Boron trifluoride-ethyl ether (BFEE) (Acros, 48 % BF_3) was used as received. Tetrabutylammonium tetrafluoroborate (TBATFB) (Aldrich, 99 %) was dried under vacuum at 80^{o}C for 24 hours. Trifluoroacetic acid (TFA) (Riedel-deHaën, 99 %) and acetonitrile (Merck, anhydrous, < 10 ppm H_2O) were used without further purification.

2.2 Electropolymerization and Cyclic Voltammetry

Electropolymerization of furan and thiophene was performed potentiostatically in a BFEE + EE (ratio 1:2) solution containing 0.1 **M** TBATFB as well, whereas electropolymerization of furan and 3-chlorothiophene was performed potentiostatically in a BFEE + EE (ratio 1:2) and TFA (10 % by volume) solution containing 0.1 **M** TBATFB in addition. Electropolymerization has been carried out in a one-compartment three-electrode cell at room temperature at constant electrode potential for two minutes. The constant electrode potential for the preparation of copolymer films was chosen according to the threshold polymerization potential of the homopolymers. A platinum sheet electrode (approximate surface area 1.5 cm^2) was used as working electrode; a non-aqueous Ag/AgCl electrode filled with acetonitrile containing 0.1 **M** TBATFB saturated with AgCl as reference electrode. After polymerization the film was washed with acetonitrile to remove any traces of mono- and oligomers.

Cyclic voltammetry of the homo- and copolymer films was carried out in a monomer free acetonitrile solution containing 0.1 **M** TBATFB as supporting electrolyte. Before each experiment the solution was deareated by bubbling with N_2. The reference electrode potential was verified frequently with respect to an aqueous saturated calomel electrode because the employed non-aqueous reference electrode system is prone to potential drift [112]. A custom built potentiostat interfaced with a standard

PC via an ADDA-converter card operating with custom developed software was used to record cyclic voltammograms (CVs).

2.3 *In situ* UV-Visible Spectroscopy and Redox Thermodynamics

UV-Vis spectra were recorded for homo- and copolymer films deposited on an optically transparent ITO-glass electrode (Merck) as working electrode in the supporting electrolyte solution in a standard 10 mm cuvette using a Shimadzu UV 2101-PC instrument (resolution 0.1 nm); a cuvette with the same solution and uncoated ITO glass was placed in the reference beam.
The CVs of homo- and copolymer films are used to determine the suitable range of electrode potentials for UV-Vis experiments. The absorption maximum λ_{1max} assigned to the $\pi \rightarrow \pi^*$ transition is measured with the polymer in its neutral state. The absorption maximum λ_{2max} assigned to an intraband transition from the valence band into the upper bipolaron band of the polymer in its oxidized state. The electrode potential where the UV-Vis-spectrum was measured depended on the type of polymer, it was always positive to the polymer oxidation peak as observed in the respective CVs of homo- and copolymer films. Because maxima are weak and shift considerably as a function of electrode potential all numbers are approximate only.

The ratio of the concentration of oxidized and reduced sites [O]/[R] was determined by using $[O]/[R] = (A_{red}\text{-}A)/(A\text{-}A_{ox})$, where A is the absorbance at a given applied potential, A_{ox} the absorbance of the fully oxidized film, and A_{red} that of the fully reduced state [113].

2.4 *In situ* Conductivity Measurements

For the *in situ* conductivity measurements, the homo- and copolymer films were deposited on a two-band Pt electrode in a one-compartment three-electrode cell. For conductivity measurements this electrode was connected to a specially designed electrical circuit supplying 10 mV of dc voltage across the two Pt strips [93, 94].

2.5 Fourier Transform Infrared (FTIR) Spectroscopy

A platinum sheet electrode (approximate surface area 1.5 cm^2) was used as working electrode. The deposited pristine film was scraped off from the electrode and dried. After cyclic voltammetry scans, the film was also scraped off and dried. FTIR spectra of the homo- and copolymer films using KBr-discs were recorded on a Perkin Elmer FTIR 1000 spectrometer at 2 cm^{-1} resolution (eight scans).

2.6 The *In situ* Resonance Raman Spectroscopy

A platinum disc electrode (2×5 mm) embedded in epoxy resin was used as working electrode. The platinum disc electrode was polished with diamond polishing paste down to 0.3 μm and then to 0.05 μm with aqueous alumina slurry. Raman spectra of homo- and copolymer films were recorded using an ISA T64000 spectrometer connected to a liquid nitrogen-cooled spectraview 2D CCD detection system. The spectra were measured using 647.1 nm exciting laser light provided by Coherent Innova 70 series ion laser; the laser power was always maintained at 70 mW to avoid destruction of the samples.

Results and Discussion

3.1 Electrochemistry of Homo- and Copolymer Films

3.1.1 Electropolymerization

Furan and Thiophene

CVs of a platinum working electrode in the polymerization solution containing the monomers are given in Fig. 5. The background electrolyte is electrochemically silent in the whole potential range (curve D).

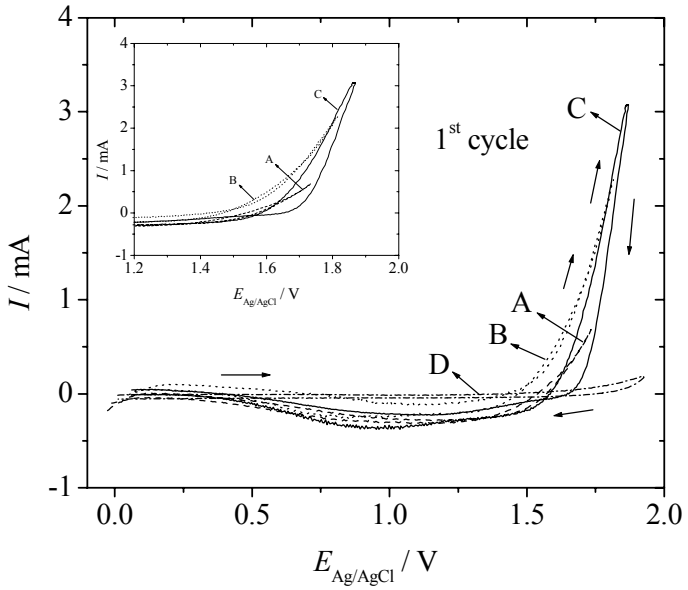

Fig. 5. CVs of (A) 0.1 **M** furan, (B) 0.1 **M** furan and 0.1 **M** thiophene, (C) 0.1 **M** thiophene, (D) no monomer in 0.1 **M** TBATFB in BFEE + EE (ratio 1:2). dE/dt = 100 mV/s.

The polymerization threshold (the lowest potential needed to sustain growth of a polymer layer) of furan is $E_{Ag/AgCl}$ = 1.45 V (curve A) and of thiophene $E_{Ag/AgCl}$ = 1.65 V (curve C). The small difference between the oxidation potentials of the two monomers suggests a large probability of copolymerization of the two monomers. Curve B

was obtained when a current-potential curve was taken in a solution containing 0.10 **M** furan and 0.10 **M** thiophene. However, the superposition of curve A and curve C does not simply add up to curve B. The current of curve B is smaller than that for thiophene and larger than that for furan. This might be caused by changes in the electrochemical environment such as electrode roughness or by the lowered electric conductivity of the formed polymer film accompanying the incorporation of furan rings into the copolymer chain [77, 76]. The oxidation potential of the mixture of furan and thiophene is around $E_{Ag/AgCl}$ = 1.50-1.60 V, which is between the oxidation potentials of the two monomers, implying that oxidation of both monomers is likely, the copolymer chains may accordingly be composed of furan and thiophene units [76].

Furan and 3-Chlorothiophene

The anodic polymerization curves in the polymerization solution containing the monomers are displayed in Fig. 6. The onset of oxidation of furan is initiated at $E_{Ag/AgCl}$ = 1.35 V (curve A) and of 3-chlorothiophene at $E_{Ag/AgCl}$ = 1.55 V (curve C), whereas the oxidation potential of the mixture of furan and 3-chlorothiophene is around $E_{Ag/AgCl}$ = 1.40-1.50 V, which is between the oxidation potentials of the two monomers. The addition of TFA (10 % by volume) to BFEE + EE (ratio 1:2) decreased the oxidation potential of the monomers; the polymerization rate was also accelerated because TFA increases the ionic conductivity of the electrolyte [71]. Furthermore the small difference between the oxidation potentials of the two monomers suggests a large probability of copolymerization and the copolymer chains may accordingly be composed of furan and 3-chlorothiophene units.

According to the normally accepted mechanism, the polymerization of 3-chlorothiophenes is initiated by electrochemical generation of the radical cations of the monomer. After this step, two radicals are coupled to a dimer and then two protons are eliminated. This is a reversible chemical procedure [114]. While with an increase of TFA content in the electrolyte a high proton concentration would suppress the reaction rate [115]. On the contrary, this reaction is also favored by rapid generation of radical cations [46]. The chlorine atom is electron withdrawing thus decreases the stability of the radical cations generated in the polymerization solution. Consequently, the total polymerization rate is controlled by the factors described above. Ac-

cording to the electrochemical kinetics, at a given applied potential (E), the polymerization rate is exponential to the potential difference (E-$E°$) of E and the oxidation potential of the monomer ($E°$). It is known that BFEE exists in diethyl ether as a polar molecule, $[(C_2H_5)_3O^+]BF_4^-$ [86], and the existence of a small amount of water complexes BF_3 into $H^+[BF_3OH]^+$, which furnishes a conducting medium [70]. However, the conductivity of pure BFEE is relatively low (960 μS cm^{-1}). The addition of a small amount of TFA (10%) into BFEE can increase the conductivity of the electrolyte significantly (4500 μS cm^{-1}) [70]. It also should be noted here that the addition of TFA into BFEE may lead to the formation of π complexes between the monomer and the strong acid [116]. These two factors result in a decrease of the oxidation potential of 3-chlorothiphene ($E°$) as described above.

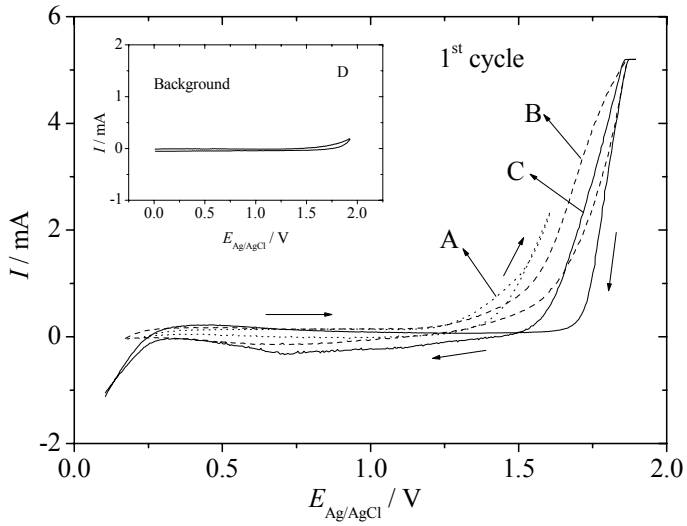

Fig. 6. CVs of (A) 0.1 **M** furan, (B) 0.1 **M** furan and 0.1 **M** 3-chlorothiophene, (C) 0.1 **M** 3-chlorothiophene, (D) no monomer in 0.1 **M** TBATFB in BFEE + EE (ratio 1:2) and TFA (10 % by volume). dE/dt = 100 mV/s.

3.1.2 Cyclic Voltammetry

Homo- and Copolymer Films of Furan and Thiophene

Fig. 7(A, C) shows the CVs of polyfuran and polythiophene in the acetonitrile-based electrolyte solution. For polyfuran, there is a broad anodic peak at $E_{Ag/AgCl}$ = ~ 0.50 V caused by polymer oxidation and a corresponding broad cathodic peak around $E_{Ag/AgCl}$ = ~ 0.46 V due to polymer reduction. The difference in the peak potentials of 0.04 V indicates a high reversibility of the associated redox processes. For polythiophene, the respective peaks are at $E_{Ag/AgCl}$ = ~ 1.38 V and at $E_{Ag/AgCl}$ = ~ 1.15 V, with a difference of 0.23 V. The redox processes of polythiophene are less close to reversibility, as the peak separation is larger than observed with polyfuran. These differences and the broad, poorly defined current waves are commonly observed in the electrochemistry of intrinsically conducting polymers based on a number of factors including the diffusion of the dopant ions inside and outside the film and the change of the conformation of the polymer chain during the redox processes [39, 42].

Copolymerization is carried out under potentiostatic conditions. Fig. 7(B) shows a typical cyclic voltammogram of a copolymer obtained from a BFEE + EE (ratio 1:2) solution containing 0.10 **M** furan and 0.10 **M** thiophene prepared at $E_{Ag/AgCl}$ = 1.60 V. It is impossible to record the CVs of the homopolymers and the copolymer in the same potential range because overoxidation of polyfuran will influence the film response and as a result ill-defined CVs as shown in Fig. 7(D) (polyfuran scanned between $E_{Ag/AgCl}$ = 0.0 - 1.65 V) will be obtained. The copolymer is more stable and less affected by overoxidation presumably due to the existence of thiophene units in the copolymer chains which may increase the stability of the copolymer.
Only one anodic/cathodic peak couple appears with the copolymer film at a position quite different from the positions observed with polyfuran and polythiophene. The appearance of one redox peak indicates uniform redox properties. In addition, it is noteworthy that both the cathodic and the anodic currents are higher than those found with the homopolymers. This implies that the electrochemical activity (redox capacity) of the copolymer is higher after the same time of electropolymerization.

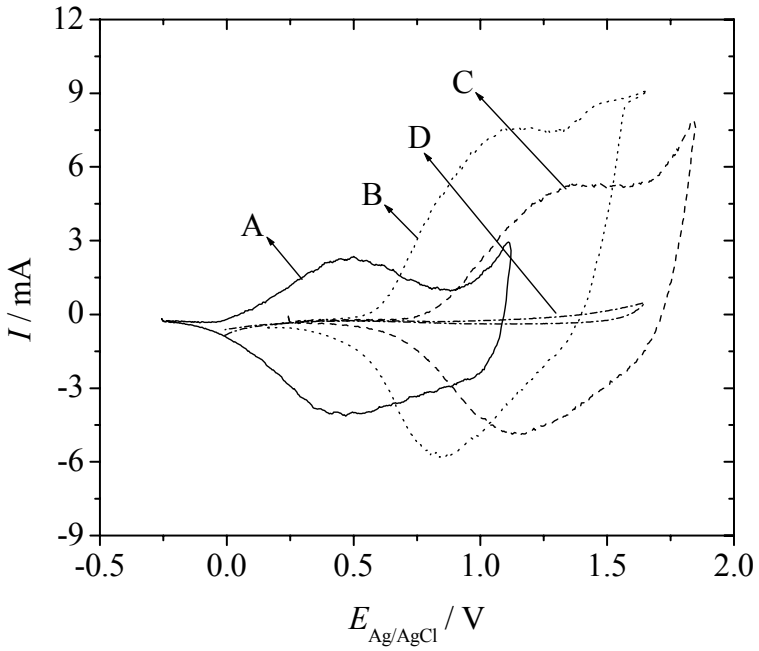

Fig. 7. CVs recorded in a solution of acetonitrile + 0.10 **M** TBATFB (A) polyfuran deposited at $E_{Ag/AgCl}$ = 1.45 V in a BFEE + EE (ratio 1:2) containing 0.1 **M** furan, (B) copolymer deposited at $E_{Ag/AgCl}$ = 1.60 V in a BFEE + EE (ratio 1:2) solution containing 0.1 **M** furan and 0.1 **M** thiophene, (C) polythiophene deposited at $E_{Ag/AgCl}$ = 1.65 V in a BFEE + EE (ratio 1:2) containing 0.1 **M** thiophene, (D) polyfuran scanned in extended scan range from $E_{Ag/AgCl}$ = 0.0 - 1.65 V; dE/dt = 100 mV/s.

Electrochemical copolymerization both at different potentials and with different thiophene concentrations was investigated. Fig. 8 shows CVs of the copolymers obtained with electropolymerization in solutions containing 0.1 **M** furan and 0.1 **M** thiophene at potentials ranging from $E_{Ag/AgCl}$ = 1.5 to 1.7 V. The redox peak potential of the copolymers shifts to higher potentials with an increasing polymerization potential of the copolymer. When prepared at $E_{Ag/AgCl}$ = 1.5 V, the copolymer shows an anodic peak at $E_{Ag/AgCl}$ = 1.0 V and a cathodic peak at $E_{Ag/AgCl}$ = 0.77 V, whereas the copolymer prepared at $E_{Ag/AgCl}$ = 1.7 V shows an anodic peak at $E_{Ag/AgCl}$ = 1.27 V and a cathodic peak at $E_{Ag/AgCl}$ = 1.01 V. The former peak pair is closer to that of polyfuran,

while the latter is closer to that of polythiophene. This indicates that more thiophene units are incorporated into the copolymer with increasing preparation potential.

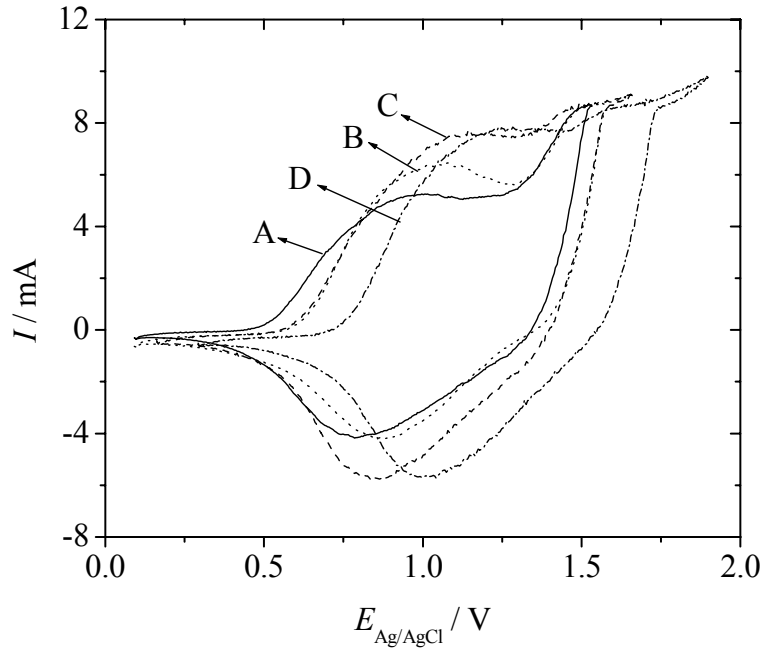

Fig. 8. CVs recorded in a solution of acetonitrile + 0.10 **M** TBATFB of copolymers deposited at $E_{Ag/AgCl}$ = (A) 1.5 V, (B) 1.55 V, (C) 1.6 V, (D) 1.7 V in a BFEE + EE (ratio 1:2) solution containing furan:thiophene (mole ratio 1:1). dE/dt = 100 mV/s.

The electrochemical characteristics of both the homopolymers and copolymers displayed in Figs. 7 and Fig. 8 indicate that keeping the potential of electrosynthesis of copolymers formed in mixed solutions near the threshold potential for electropolymerization of furan may result in the furan-based copolymers and vice versa.

When the furan/thiophene feed ratio is changed from 1:1 to 4:1 (0.1 **M** / 0.025 **M**) CVs as shown in Fig. 9(A) are obtained; at a ratio of 8:1 (0.1 **M** / 0.0125 **M**) CVs shown in Fig. 9(B) result. Only one redox peak couple appears, and the positive shift of the redox peak with increasing preparation potentials is again observed. When comparing the cyclic voltammograms of the copolymers prepared at the same polymerization potential in these different solutions, it is observed that lower concentration

of thiophene leads to a negative shift of the redox peak potentials of the copolymer. This implies that more thiophene units are incorporated into the copolymer film when the concentration of thiophene increases (see Fig. 10).

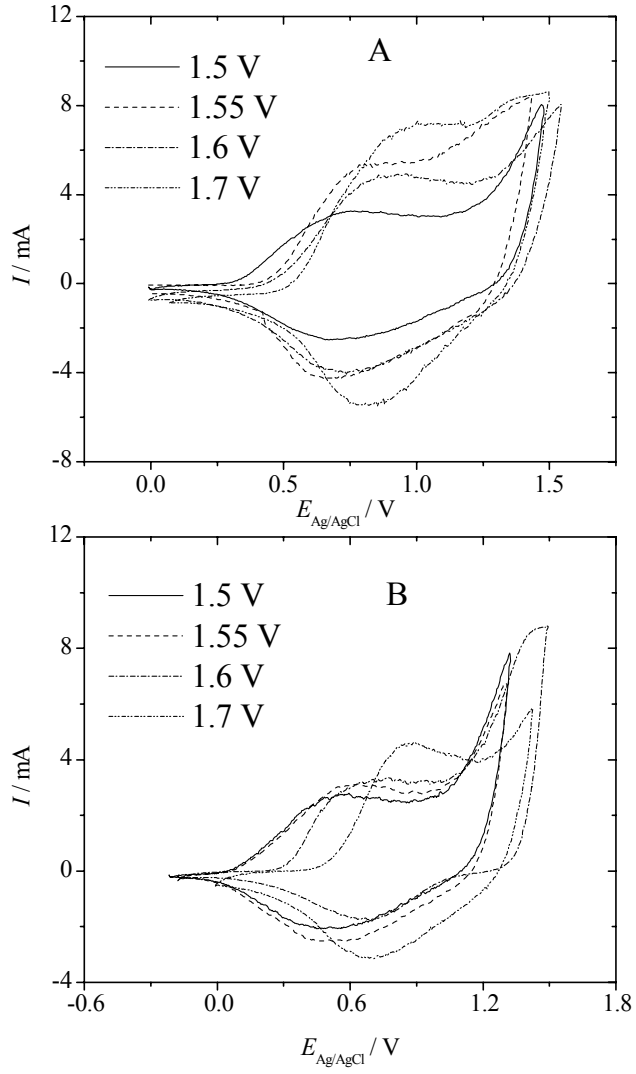

Fig. 9. CVs recorded in acetonitrile + 0.10 **M** TBATFB solution of copolymers deposited at ranging $E_{Ag/AgCl}$ = 1.5 - 1.7 V respectively in a BFEE + EE (ratio 1:2) solution containing furan:thiophene mole ratio (A) 4:1, (B) 8:1. dE/dt = 100 mV/s.

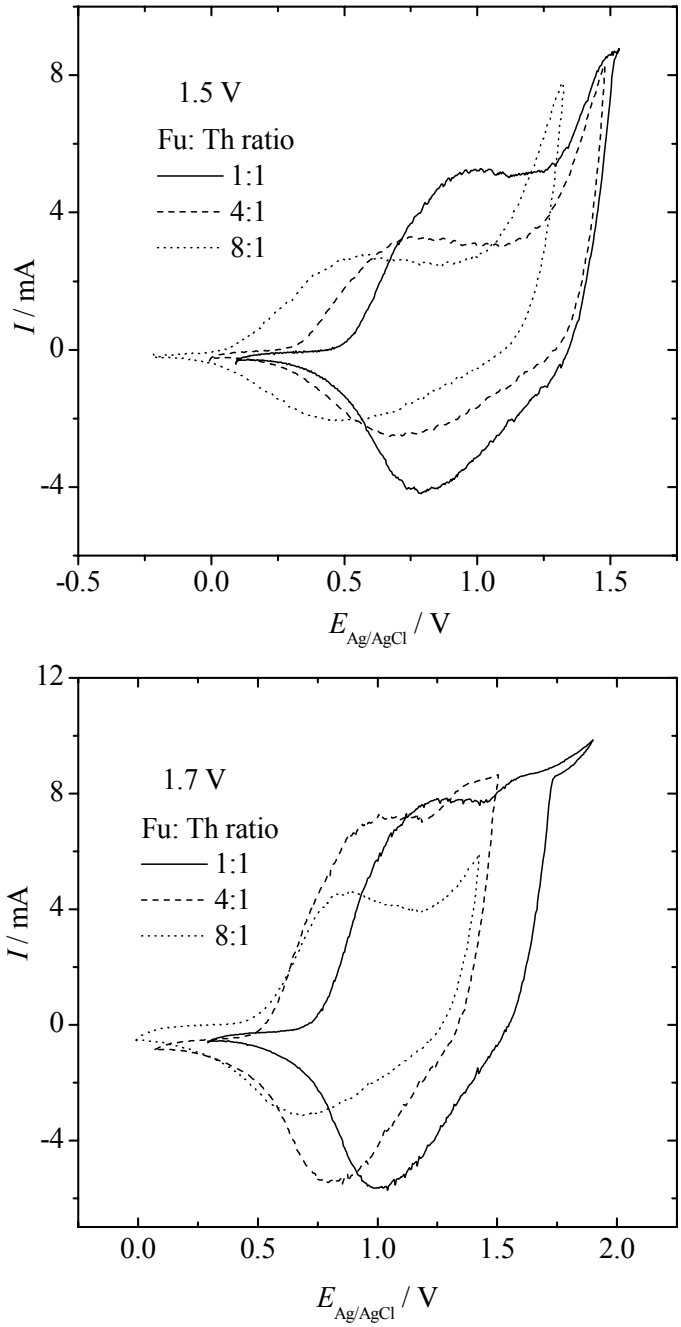

Fig. 10. CVs recorded in acetonitrile + 0.10 **M** TBATFB solution of copolymers deposited at $E_{Ag/AgCl}$ = 1.5, 1.7 V respectively in a BFEE + EE (ratio 1:2) solution containing furan:thiophene (mole ratio 1:1, 4:1, 8:1). dE/dt = 100 mV/s.

The peak potential values of the copolymers prepared at different potentials from these three different solutions are listed in Table 2, the peak potentials of the homopolymers are added for comparison.

Table 2. Peak potentials of the copolymers prepared at various electropolymerization potentials E_{pol} from BFEE + EE (ratio 1:2) solutions containing different monomer feed ratios. Peak potentials of homopolymers are added for comparison.

Fu/Th (Mole ratio)	E_{pol} = 1.50 V		E_{pol} = 1.55 V		E_{pol} = 1.60 V		E_{pol} = 1.70 V		Polyfuran E_{pol} = 1.45 V		Polythiophene E_{pol} = 1.65 V	
	E_{pa}/V	E_{pc}/V	E_{pa}/V	E_{pc}/V	E_{pa}/V	E_{pc}/V	E_{pa}/V	E_{pc}/V	E_{pa}/V	E_{pc}/V	E_{pa}/V	E_{pc}/V
1:1	1.00	0.77	1.06	0.87	1.14	0.84	1.27	1.01				
4:1	0.76	0.67	0.82	0.65	0.92	0.72	1.04	0.89	0.50	0.46	1.38	1.15
8:1	0.54	0.50	0.65	0.44	0.75	0.67	0.89	0.69				

In Fig. 11 the relationship between the anodic peak current and the concentration of thiophene in the electropolymerization solutions is linear (linear fit) especially at higher concentrations (0.025 - 0.1 **M**).

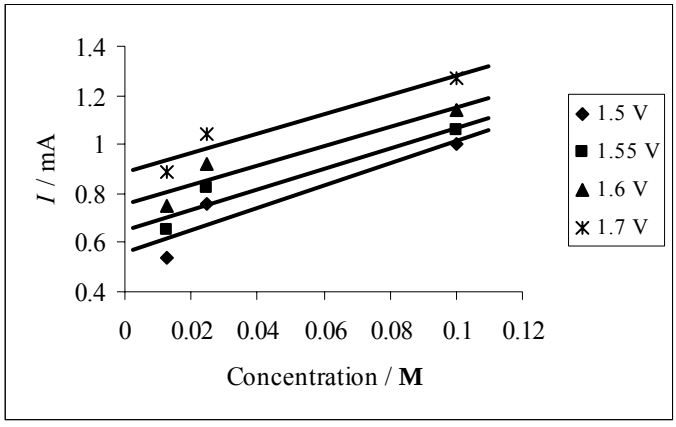

Fig. 11. Dependence of anodic peak current of copolymers deposited at $E_{Ag/AgCl}$ = 1.5 - 1.7 V respectively on concentration of thiophene in mixed solutions.

All the above results indicate that the electrochemical properties of the copolymers depend not only on the electrochemical polymerization potential but also on the monomer feed ratio. Presumably the dependence of the electrochemical properties of the copolymer on the electropolymerization potential and monomer feed ratio reflects the composition and perhaps even the structure of the copolymers.

Fig. 12 shows CVs at dE/dt = 25, 50, and 100 mV/s of copolymer films deposited at $E_{Ag/AgCl}$ = 1.5 V in a solution containing furan/thiophene (ratio 1:1). The inset depicts the dependency of the anodic peak currents on the square root of the scan rate. The plot yields a straight line indicating that the electrochemical processes are diffusion-controlled, and the redox couple is attached to the electrode [39, 70]. For a diffusion-controlled process the straight line should pass through the origin, but in the case of conducting polymers deviations from the ideal behavior may arise from contributions such as double-layer charging which can disturb the zero intercept [117].

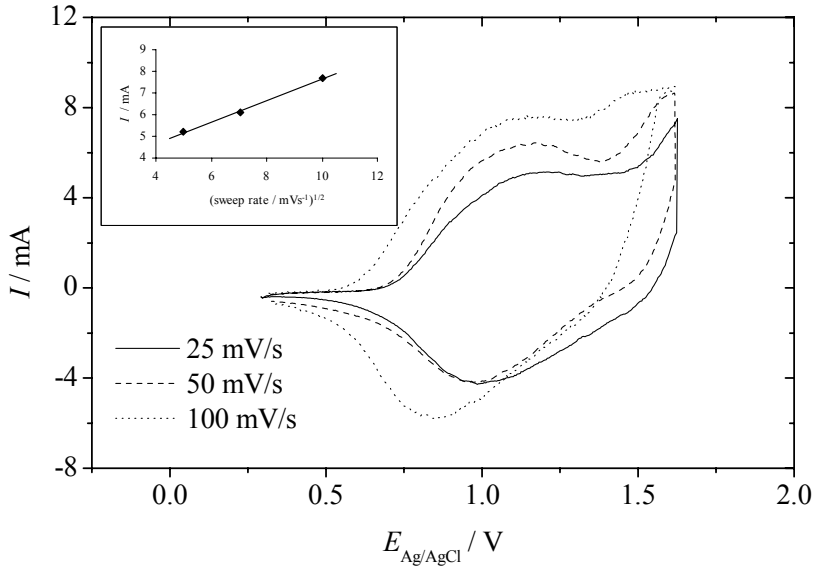

Fig. 12. CVs recorded in a solution of acetonitrile + 0.10 **M** TBATFB of copolymer films deposited at $E_{Ag/AgCl}$ = 1.50 V in a BFEE + EE (ratio 1:2) solution containing 0.1 **M** furan and 0.1 **M** thiophene, dE/dt = 25, 50, and 100 mV/s.

Homo- and Copolymer Films of Furan and 3-Chlorothiophene

The CVs of polyfuran, copolymer and poly(3-chlorothiophene) in the acetonitrile-based supporting electrolyte solution are shown in Fig. 13. For polyfuran, there is a broad anodic peak at $E_{Ag/AgCl}$ = ~ 0.57 V caused by polymer oxidation and a corresponding broad cathodic peak around $E_{Ag/AgCl}$ = ~ 0.43 V due to polymer reduction with a peak potential difference of 0.14 V. For poly(3-chlorothiophene), the respective peaks are at $E_{Ag/AgCl}$ = ~ 1.40 V and at $E_{Ag/AgCl}$ = ~ 1.24 V, with a difference of 0.16 V. The difference and the broad, poorly defined current waves are still observed and attributed to a number of factors which have been explained previously. Substituted polythiophenes prepared from nonsymmetric monomers usually show broad redox waves in their CVs [118]. This phenomenon is ascribable to the presence of coupling defects distributed statistically, which results in a series of energetically nonequivalent chain segments.

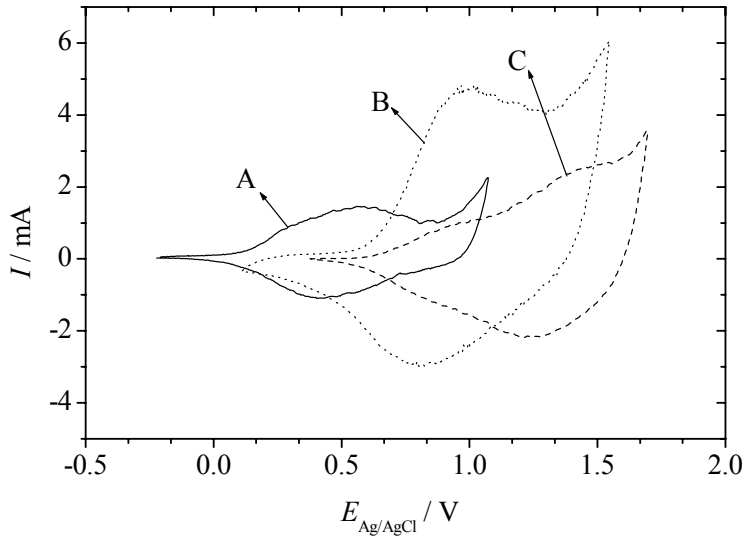

Fig. 13. CVs recorded in a solution of acetonitrile + 0.10 **M** TBATFB (A) polyfuran deposited at $E_{Ag/AgCl}$ = 1.35 V in a BFEE + EE (ratio 1:2) and TFA (10 % by volume) solution containing 0.1 **M** furan, (B) copolymer deposited at $E_{Ag/AgCl}$ = 1.7 V in a BFEE + EE (ratio 1:2) and TFA (10 % by volume) solution containing 0.1 **M** furan and 0.0125 **M** 3-chlorothiophene, (C) poly(3-chlorothiophene) deposited at $E_{Ag/AgCl}$ = 1.55 V in a BFEE + EE (ratio 1:2) and TFA (10 % by volume) solution containing 0.1 **M** 3-chlorothiophene. dE/dt = 100 mV/s.

The copolymer which is obtained from a BFEE + EE (ratio 1:2) and TFA (10 % by volume) solution containing 0.10 **M** furan and 0.0125 **M** 3-chlorothiophene deposited at $E_{Ag/AgCl}$ = 1.70 V shows in its typical CV only one anodic/cathodic peak couple at a position quite different from the positions observed with the homopolymers. The appearance of one redox peak indicates uniform redox properties. In addition, it is noteworthy that both the cathodic and the anodic currents are higher than those found with the homopolymers. This implies that the electrochemical activity (redox capacity) of the copolymer is higher after the same time of electropolymerization.

Electrochemical copolymerization both at different potentials and with different thiophene concentrations has been investigated. Fig. 14(A) shows CVs of the copolymers obtained with electropolymerization in solutions containing 0.1 **M** furan and 0.1 **M** 3-chlorothiophene at $E_{Ag/AgCl}$ = 1.5 and 1.7 V. The redox peak potential of the copolymers shifts to higher potentials with an increasing polymerization potential of the copolymer. This indicates that more 3-chlorothiophene units are incorporated into the copolymer with increasing preparation potential.

When the furan/3-chlorothiophene feed ratio is changed from 1:1 to 8:1 (0.1 **M** / 0.0125 **M**) CVs as shown in Fig. 14(B) are obtained. Only one redox peak couple appears and when comparing the CVs of the copolymers prepared at the same polymerization potential in these different solutions it is observed that lower concentration of thiophene leads to a negative shift of the redox peak potentials of the copolymer. This implies that more 3-chlorothiophene units are incorporated into the copolymer film when the concentration of 3-chlorothiophene is increased.

The electrochemical characteristics of the homopolymers and copolymers displayed in Figs. 13 and Fig. 14(B) indicate that keeping the potential of electrosynthesis of copolymers formed in mixed solutions near the threshold potential for electropolymerization of furan may result in the furan-based copolymers and vice versa.

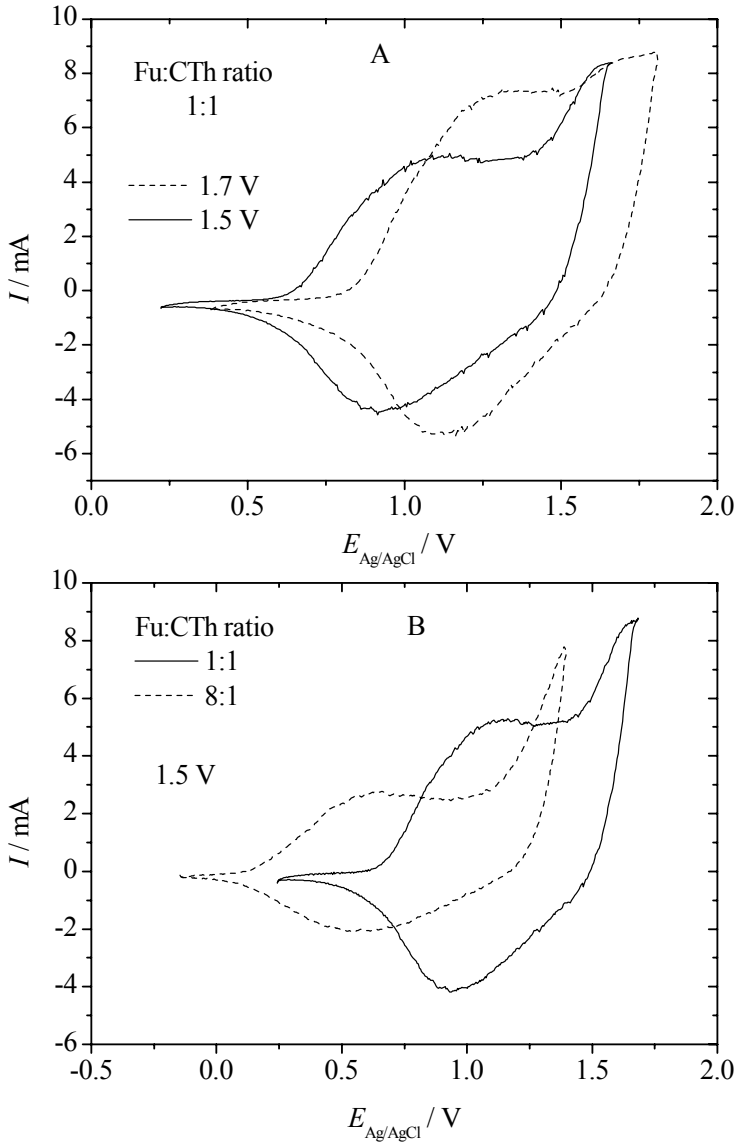

Fig. 14. A: CVs recorded at dE/dt = 100 mV/s in acetonitrile + 0.10 **M** TBATFB solution of copolymers deposited at $E_{Ag/AgCl}$ = 1.5 V and 1.7 V in a BFEE + EE (ratio 1:2) and TFA (10 % by volume) solution containing furan/3-chlorothiophene (mole ratio 1:1);

B: deposited at $E_{Ag/AgCl}$ = 1.5 V in a BFEE + EE (ratio 1:2) and TFA (10 % by volume) solution containing furan/3-chlorothiophene (mole ratio 1:1 and 8:1).

The peak potential values of the copolymers prepared at different potentials from these three different solutions are listed in Table 3, the peak potentials of the homopolymers are added for comparison.

Table 3. Peak potentials of the copolymers prepared at $E_{Ag/AgCl}$ = 1.50 and 1.70 V from BFEE + EE (ratio 1:2) and TFA (10 % by volume) solutions containing different monomer feed ratios. Peak potentials of homopolymers are added for comparison.

Fu/ClTh (Mole ratio)	E_{pol} = 1.50 V		E_{pol} = 1.70 V		PFu E_{pol} = 1.35 V		PClTh E_{pol} = 1.55 V	
	E_{pa}/V	E_{pc}/V	E_{pa}/V	E_{pc}/V	E_{pa}/V	E_{pc}/V	E_{pa}/V	E_{pc}/V
1:1	1.10	0.92	1.30	1.11	0.57	0.43	1.40	1.24
8:1	0.62	0.60	0.97	0.80				

3.1.3 The Proposed Mechanism of the Electrochemical Formation of Furan-Thiophene Copolymers

The electropolymerization mechanism of copolymers is presumably even more complex than that of homopolymers [46]. Fig. 15 shows a proposed mechanism for the electropolymerization of furan and thiophene [41, 119] based on already known coupling reactions of aromatic compounds [46, 120-121]. The first electrochemical step (E) is the oxidation of the monomer (1) into its radical cation. The second step involves the coupling of two radicals (2) to produce a dihydrodimer (3) dication that leads to a dimer (4) after the loss of two protons and rearomatization. This rearomatization constitutes the driving force of the chemical step (C). At the applied electrode potential the dimer (4), which is more easily oxidized than the monomer, is present in its radical form (5) and undergoes further coupling with a monomeric radical (6). Electropolymerization then proceeds through successive electrochemical and chemical steps according to a general E(EC)n mechanism until the oligomer becomes in-

soluble in the electrolyte solution and precipitates onto the electrode surface; soluble oligomers were observed to stray away from the electrode at the beginning of the polymerization.

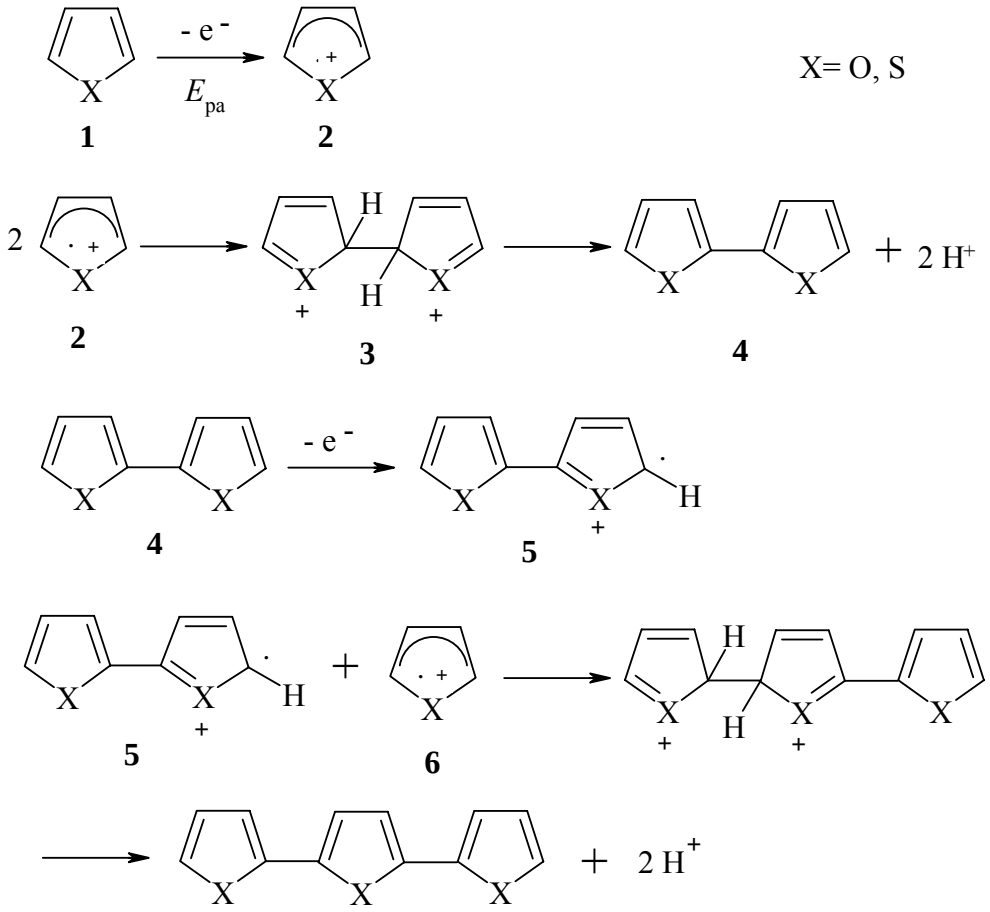

Fig. 15. Proposed mechanism of the electropolymerization of furan-thiophene copolymers.

For thiophene, a cation radical-monomer coupling mechanism was also assumed to explain the observed polymerization rate increase brought about by added bithiophene or terthiophene [121].

3.1.4 The Stability of Redox Activity of Furan-Thiophene Copolymers

Furan-thiophene copolymers show a fairly good long-term stability of the redox activity after cycling in organic solvents such as acetonitrile as compared with polyfuran films [42] as shown in Fig. 16. This applies also to the other copolymers studied in this project prepared at different feed ratios and/or polymerization potentials. The peak separation of anodic and cathodic peak potential is still small which indicates an almost reversible redox reaction. The retention of the redox activity of furan-thiophene copolymers after cycling in dry acetonitrile for 100 times is about 60 %. As shown in the inset the anodic peak current decreases as the number of potential cycles increases, indicating a decrease of the redox activity.

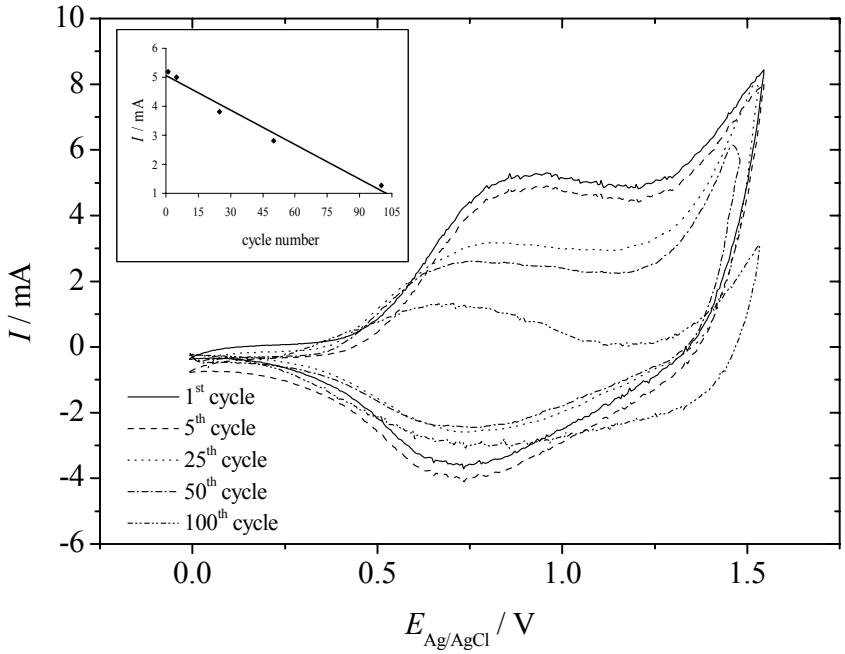

Fig. 16. 1st, 5th, 25th, 50th, and 100th CV recorded in acetonitrile+ 0.10 **M** TBATFB solution of copolymer deposited at $E_{Ag/AgCl}$ = 1.60 V in a BFEE + EE (ratio 1:2) solution containing furan:thiophene, mole ratio 4:1. dE/dt = 100 mV/s.

However, when furan-thiophene copolymer is cycled in an aqueous solution, the redox activity is almost totally lost since it shows a very large anodic peak current around 1.36 V, but no associated cathodic peak (see Fig. 17). This process is independent of the pH value of the aqueous solution indicating that water molecules instead of protons or hydroxyl ions are involved in this degradation process [122].

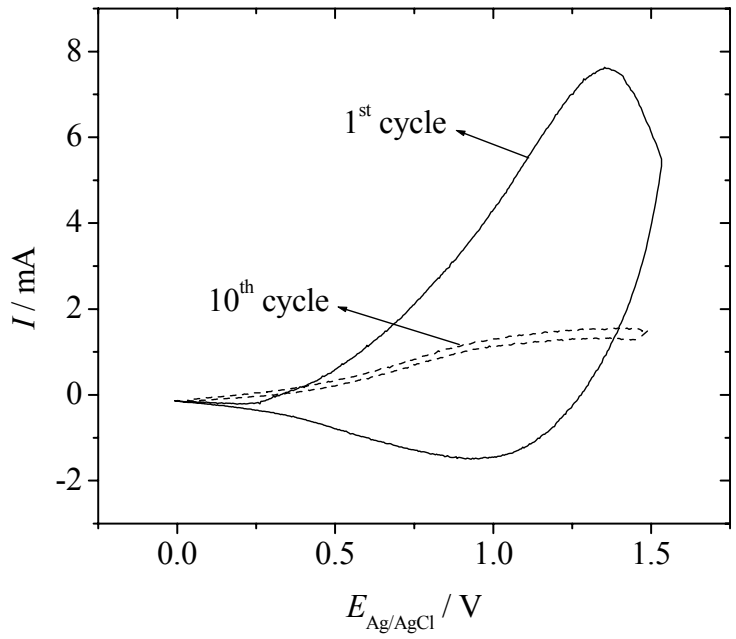

Fig. 17. 1st and 10th CV recorded in aqueous solution containing 0.10 **M** NaTFB of copolymer deposited at $E_{Ag/AgCl}$ = 1.60 V in a BFEE + EE (ratio 1:2) solution containing furan:thiophene, mole ratio 4:1. dE/dt = 100 mV/s.

Fig. 18 shows the retention of the redox activity of a furan-thiophene copolymer in wet acetonitrile solution; the volume ratio of acetonitrile to water is set to 100:1. About 20 % of the redox activity of the copolymer remains after 100 cycles indicating that the loss rate of redox activity increases with the amount of water in acetonitrile. The associated loss of redox capacity during the oxidation process may be caused by the destruction of conjugated structures [39].

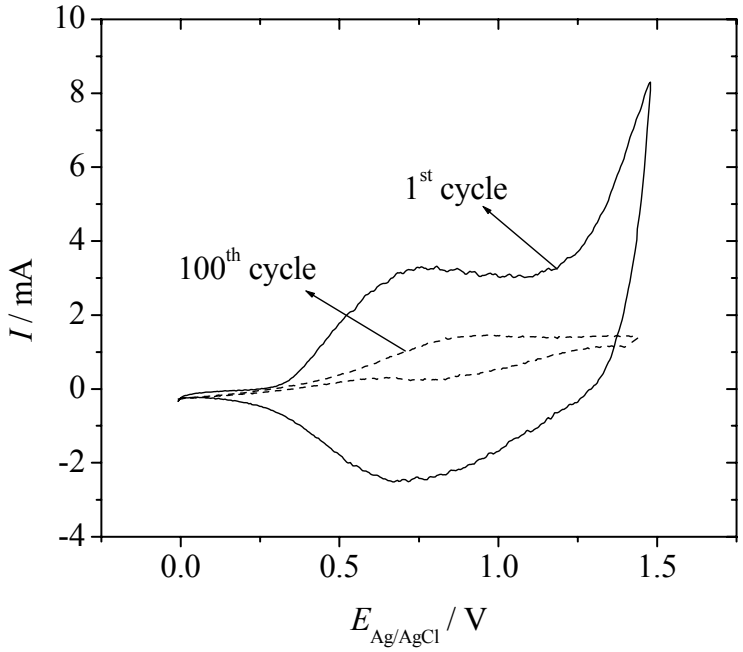

Fig. 18. 1st and 100th CV recorded in acetonitrile/H_2O (volume ratio 100:1)+ 0.10 **M** TBATFB solution of copolymer deposited at $E_{Ag/AgCl}$ = 1.60 V in a BFEE + EE (ratio 1:2) solution containing furan:thiophene, mole ratio 4:1. dE/dt = 100 mV/s.

3.2 *In situ* UV-Visible Spectroscopy

3.2.1 The *In situ* UV-Visible Spectroscopy of Homo- and Copolymer Films

Homo- and Copolymer Films of Furan and Thiophene

The *in situ* UV-Vis absorption spectra of polyfuran and polythiophene are displayed for reference in Fig. 19 and Fig. 21 respectively. Polyfuran shows a broad absorption band around 405 nm in the neutral state. This broad absorption band with λ_{1max}, which lies between 380 nm (3.27 eV) and 540 nm (2.29 eV), corresponds to the $\pi \rightarrow \pi^*$ transition, the width indicates the coexistence of both long and short effective conjugation lengths in the polyfuran films.

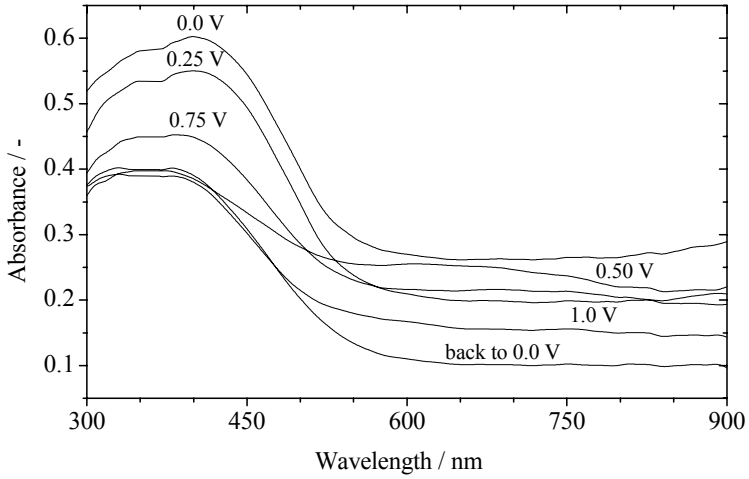

Fig. 19. *In situ* UV-Vis spectra recorded at different applied potentials in a solution of acetonitrile + 0.1 **M** TBATFB of polyfuran prepared at $E_{Ag/AgCl}$ = 1.45 V from BFEE + EE (ratio 1:2) solution containing 0.1 **M** furan and 0.1 **M** TBATFB.

In an extended system the band gap (E_g) can be defined as the difference between the lowest energy in the conduction band and the highest energy in the valence band. According to the zero-order approximation, this is equal to the lowest excitation energy, which can be obtained from the onset value at the lower energy edge of the optical absorption spectra [123, 124]. E_g for polyfuran from a direct interband transi-

tion can be estimated from the absorption edge (~ 535 nm) of the spectrum to be about 2.32 eV very close to the value reported in the literature [39].

When an electron is removed from the top of the valance band of a conjugated polymer, such as polyfuran or polythiophene, a vacancy (hole or radical cation) not completely delocalized is created as would be expected from classical band theory. Only partial delocalization occurs, extending over several monomer units, causing them to deform structurally. According to solid-state physics, a radical cation which is partially delocalized over some polymer segments is called a small polaron. It stabilizes itself by polarizing the medium around it [126, 127].

The presence of a polaron on the chain introduces two localized electronic levels in the gap; a singly occupied bonding polaron state above the valence band edge and an empty antibonding polaron state below the conduction band edge [128]. The location of the antibonding polaron state is a bit away from the conduction band edge than the location of the bonding state from the valence band edge. This asymmetric location arises because of the different oxygen/ sulfur orbital contributions to the valence and conduction band [128]. Furthermore, the possibility of three optical transitions below the band gap transition in a slightly doped conjugated polymer can be attributed as follows: the first absorption can be related to a transition from the valence band to the bonding polaron state, the second one is associated with a transition from the bonding to the antibonding polaron state, and the third one corresponds to a transition from the valence band to the antibonding polaron state [128].

When a second electron is taken out of the chain, the energetically favorable species is a spinless bipolaron which also extends over several monomer units. The geometry relaxation is stronger than in the polaron case; the geometry within the bipolaron is more quinoid-like than with the polaron, consequently the empty bipolaron electronic levels in the gap are more a way from the band edges than in the polaron case [129]. The presence of bipolarons on polymer chains result in the possibility of two optical transitions below the band gap transition: from the valence band to the lower bipolaron level and from the valence band to the upper bipolaron level. At heavily doped polymer, the overlap between the bipolaron states leads to the formation of two wide bipolaron bands in the gap. The band gap for polyfuran has widened

from 2.32 eV in the neutral state to 2.47 eV in the doped state. This is due to the fact that the bipolaron states coming in the gap are taken from the valence and conduction band edges [129].

The passage from the undoped to the doped state of polyfuran is accompanied by weakening as well as a blue shift of the absorption band in the visible and shifting into NIR upon further oxidation. The optical transition with λ_{2max} from the valence band into the upper bipolaron band (the upper subgap state) is located at 685 nm (1.81 eV), (see Fig. 20), this assignment has been previously suggested [39, 128, 129].

In the polymer, furan/ thiophene units have positive charges, which are balanced by a variety of so-called dopant anions. Anions are expelled from the polymer film (undoping) when a negative potential is applied to the films, thus transforming it to the reduced state. Conversely, when a positive potential is applied to oxidize the neutral film (doping), anions are taken up [25, 130]. Polaron, bipolaron energy levels, conduction and valance bands as well as optical transitions for polyfuran and polythiophene are shown in Fig. 20.

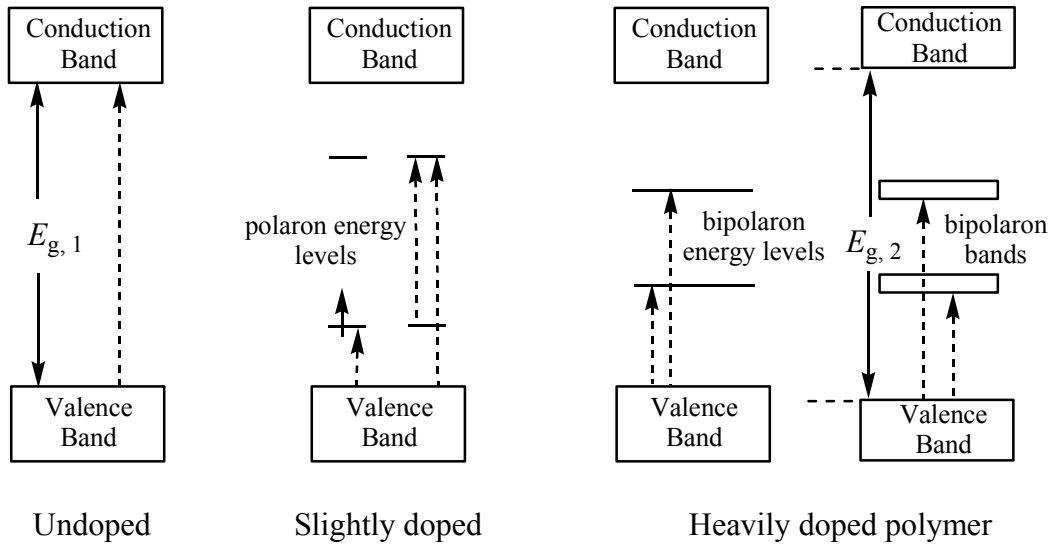

Fig. 20. Polaron, bipolaron energy levels, conduction, valence, bipolaron bands as well as optical transitions in polyfuran and polythiophene. $E_{g,1}$: band gap of neutral polymer, $E_{g,2}$: band gap of heavily doped polymer

Polythiophene exhibits an absorption maximum at 447 nm in the neutral state. This broad absorption band corresponds to the $\pi \rightarrow \pi^*$ transition, the width implies again the coexistence of both long and short effective conjugation lengths. Upon oxidation, this absorption almost vanishes; instead a very broad feature raises around 775 nm (1.60 eV) with its maximum λ_{2max} shifting into the NIR upon further oxidation. E_g for polythiophene for the direct interband transition can be deduced from the energy of the absorption edge (~ 590 nm) of the spectrum at about 2.10 eV which is in agreement with literature data [39, 42]. In the band gap, bipolaron bands are formed and the upper one is located 1.60 eV above the valence band. The band gap has also widened from 2.10 eV in the neutral state to 2.41 eV in the doped state.

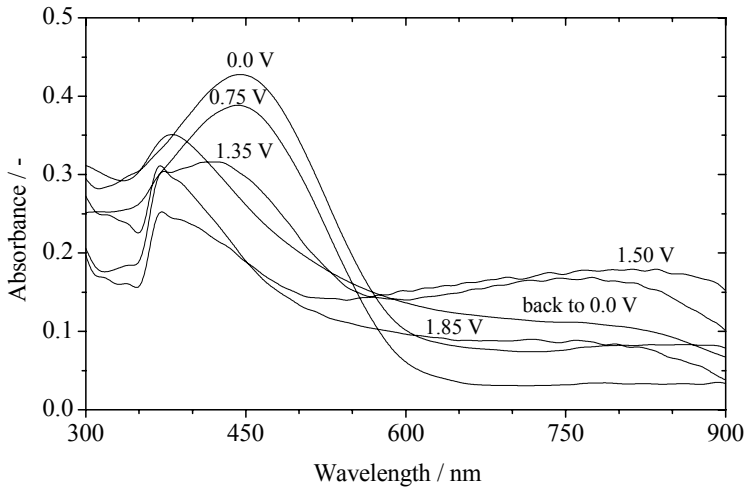

Fig. 21. *In situ* UV-Vis spectra recorded at different applied potentials in a solution of acetonitrile + 0.1 **M** TBATFB of polythiophene prepared at $E_{Ag/AgCl}$ = 1.65 V from BFEE + EE (ratio 1:2) solution containing 0.1 **M** thiophene and 0.1 **M** TBATFB.

The absorption bands and band gaps of polyfuran and polythiophene are listed in Table 4.

Table 4. Absorption bands and band gaps of polyfuran and polythiophene.

Homopolymer	λ_{1max}		λ_{2max}		Band gap	
	nm	eV	nm	eV	nm	eV
Polyfuran	405	3.06	685	1.81	535	2.32
Polythiophene	447	2.77	775	1.60	590	2.10

In situ UV-Vis spectra both at different electrode potentials and with different thiophene concentrations in the polymerization solution were investigated. Fig. 22 (A-D) shows the *in situ* UV-Vis spectra of the copolymers obtained from BFEE + EE (ratio 1:2) solution containing 0.10 **M** furan and 0.10 **M** thiophene at potentials ranging from $E_{Ag/AgCl}$ = 1.5 to 1.7 V respectively.

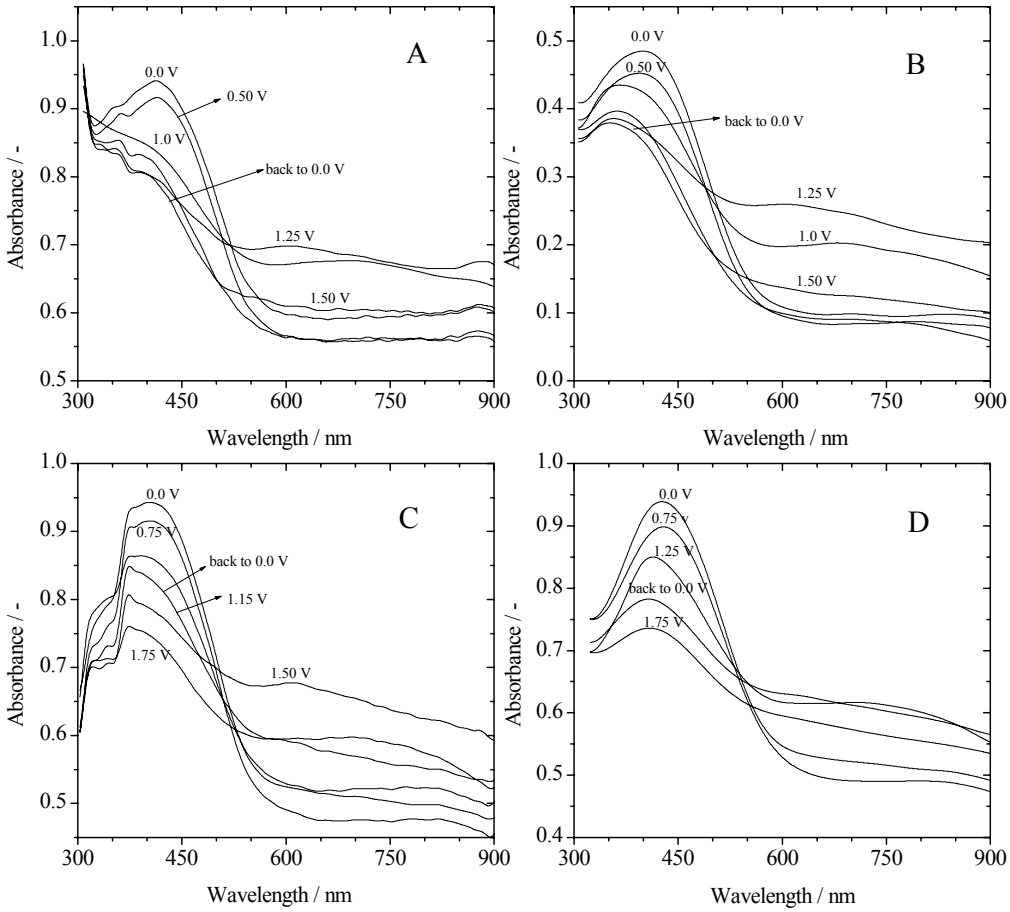

Fig. 22. *In situ* UV-Vis spectra recorded at different applied potentials in a solution of acetonitrile + 0.1 **M** TBATFB of copolymers prepared at $E_{Ag/AgCl}$ = (A) 1.5 V, (B) 1.55 V, (C) 1.6 V, (D) 1.7 V from BFEE + EE (ratio 1:2) solution containing 0.1 **M** furan, 0.1 **M** thiophene, and 0.1 **M** TBATFB.

The copolymers have a broad absorption band in the neutral state corresponding to the $\pi \rightarrow \pi^*$ transition indicating the coexistence of units of both long and short effective conjugation lengths containing furan and thiophene monomer units. A remarkable characteristic of the UV-Vis spectra is the shift of the broad absorption band in the neutral state of the copolymers to higher wavelengths with increasing preparation potential of the copolymer. When prepared at $E_{Ag/AgCl}$ = 1.5 V, the copolymer shows an absorption band around 415 nm which is in the vicinity of the absorption band of pure polyfuran; when prepared at $E_{Ag/AgCl}$ = 1.7 V, the copolymer shows an absorption band at 430 nm which is closer to pure polythiophene. This indicates that more thiophene units are incorporated into the copolymer with an increasing preparation potential.

The same behavior is still observed upon oxidation, which means that absorption assigned to the $\pi \rightarrow \pi^*$ transition almost vanishes; a very broad feature rises (λ_{2max}) instead with its maximum shifting into NIR upon further oxidation, which is attributed to polaron/bipolaron transitions between band gap states. Conceivable polaron and bipolaron structures in copolymers are shown in Fig. 23.

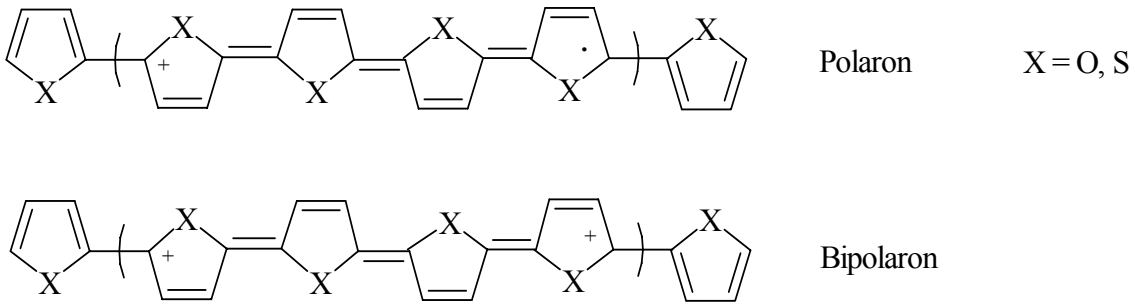

Fig. 23. Possible polarons and bipolarons in copolymers.

E_g for the copolymers prepared at potentials ranging from $E_{Ag/AgCl}$ = 1.5 to 1.7 V from a direct interband transition can also be estimated from the absorption edge (~548 - 575 nm) of the spectrum, being about 2.26 - 2.16 eV respectively, which is less than that for polyfuran. The absorption bands and band gaps of copolymers obtained from BFEE + EE (ratio 1:2) solution containing 0.10 **M** furan and 0.10 **M** thiophene at potentials ranging from $E_{Ag/AgCl}$ = 1.5 to 1.7 V are listed in Table 5.

Table 5. Absorption bands and band gaps of copolymers obtained from BFEE + EE (ratio 1:2) solutions containing 0.10 **M** furan and 0.10 **M** thiophene at potentials ranging from $E_{Ag/AgCl}$ = 1.5 to 1.7 V.

Polymerization potential $E_{Ag/AgCl}$	λ_{1max}		λ_{2max}		Band gap	
	nm	eV	nm	eV	nm	eV
1.5	415	2.99	704	1.76	548	2.26
1.55	418	2.97	710	1.75	556	2.23
1.6	423	2.93	728	1.70	558	2.22
1.7	430	2.89	737	1.68	575	2.16

When the furan/thiophene feed ratio changed from 1:1 to 4:1 (Fig. 24) and to 8:1 (Fig. 25), the following characteristics still exist in the UV-Vis spectra: the appearance of a broad absorption band in the neutral state and the blue shift of the absorption band in the visible region observed upon oxidation and the appearance of absorption features in the near IR region.

When comparing the UV-Vis spectra of the copolymers prepared at the same polymerization potential in these different solutions, it is observed that a lower concentration of thiophene leads to a blue shift of the absorption band of the copolymer obtained. A copolymer prepared in a solution containing furan/thiophene (ratio 1:1) prepared at $E_{Ag/AgCl}$ = 1.6 V shows an absorption band around 423 nm, whereas a copolymer obtained in a solution containing furan/thiophene (ratio 4:1) shows an absorption band around 417 nm. Finally the copolymer prepared in a solution containing furan/thiophene (ratio 8:1) shows an absorption band around 413 nm. This implies that more thiophene units are incorporated into the copolymer film when the concentration of thiophene is increased.

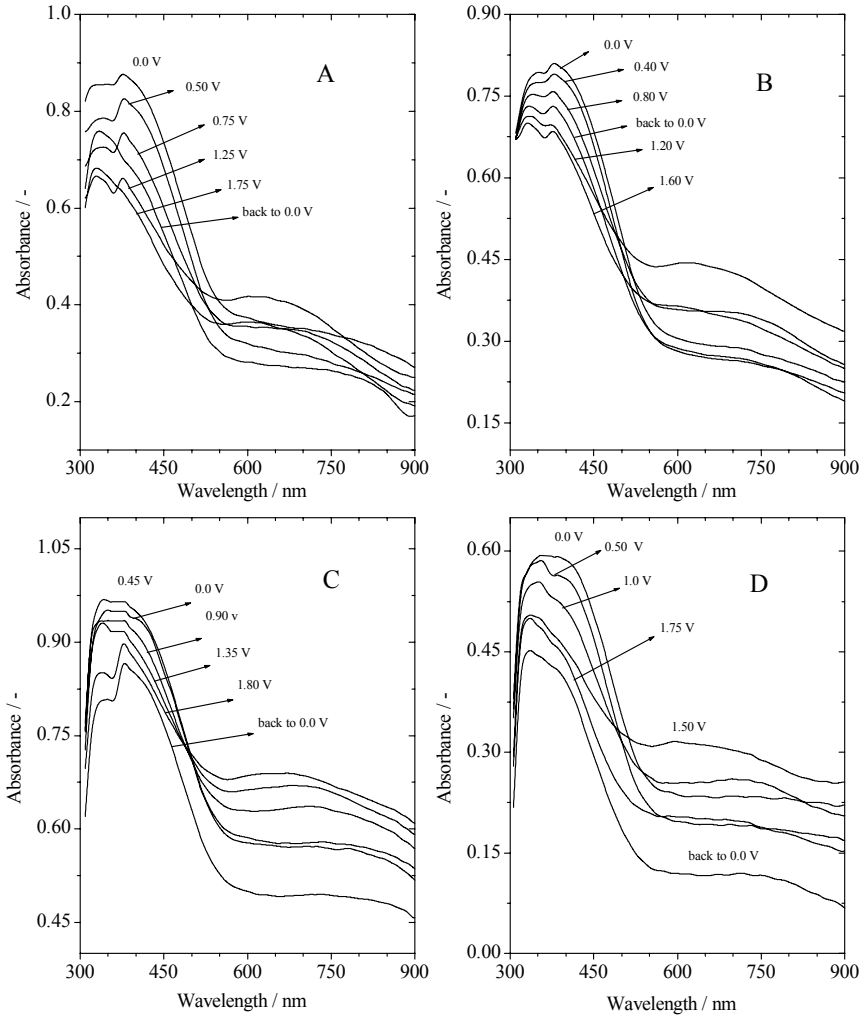

Fig. 24. *In situ* UV-Vis spectra recorded at different applied potentials in a solution of acetonitrile + 0.1 **M** TBATFB of copolymers prepared at $E_{Ag/AgCl}$ = (A)1.5 V, (B) 1.55 V, (C) 1.6 V, (D) 1.7 V from BFEE + EE (ratio 1:2) solution containing 0.1 **M** furan, 0.025 **M** thiophene, and 0.1 **M** TBATFB.

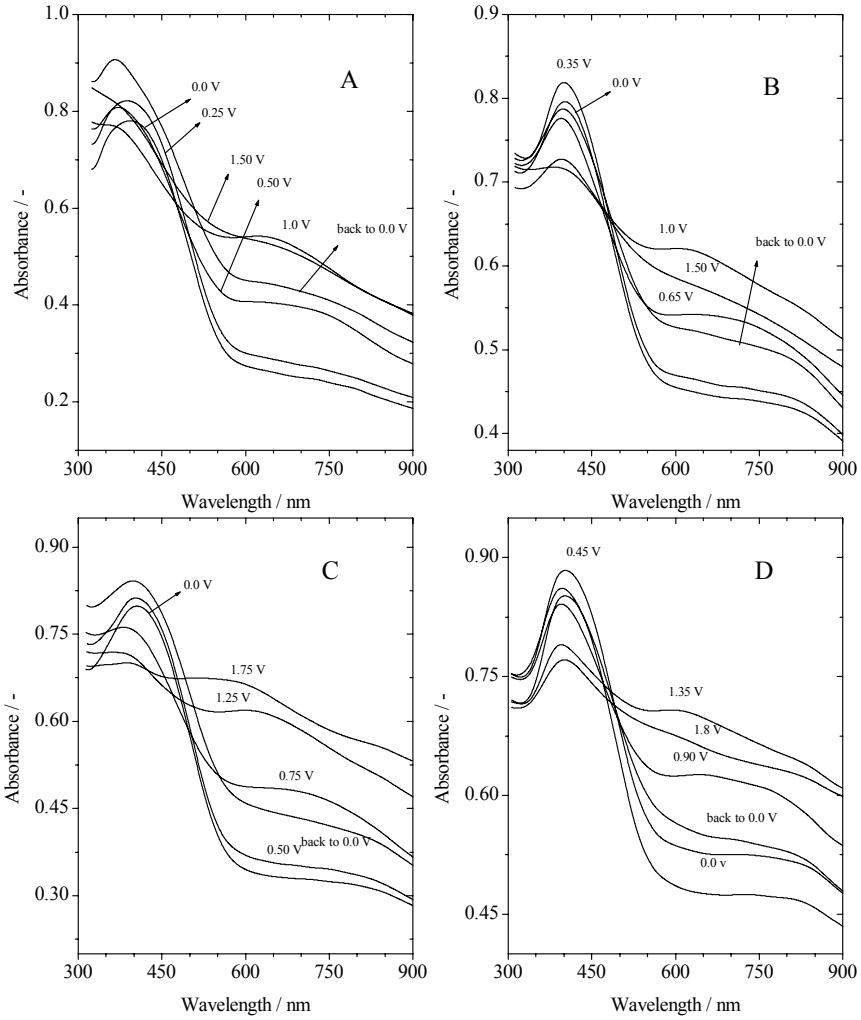

Fig. 25. *In situ* UV-Vis spectra recorded at different applied potentials in a solution of acetonitrile + 0.1 **M** TBATFB of copolymers prepared at $E_{Ag/AgCl}$ = (A) 1.5 V, (B) 1.55 V, (C) 1.6 V, (D) 1.7 V from BFEE + EE (ratio 1:2) solution containing 0.1 **M** furan, 0.0125 **M** thiophene, and 0.1 **M** TBATFB.

The absorption bands and band gaps of the copolymers prepared at different polymerization potentials from these different solutions are listed in Table 6 and 7.

Table 6. Absorption bands and band gaps of copolymers obtained from BFEE + EE (ratio 1:2) solution containing furan/thiophene (mole ratio 4:1) at potentials ranging from $E_{Ag/AgCl}$ = 1.5 to 1.7 V.

Polymerization potential $E_{Ag/AgCl}$	λ_{1max}		λ_{2max}		Band gap	
	nm	eV	nm	eV	nm	eV
1.5	411	3.02	690	1.79	545	2.28
1.55	413	3.00	708	1.75	556	2.23
1.6	417	2.98	722	1.72	552	2.25
1.7	420	2.95	728	1.70	542	2.29

Table 7. Absorption bands and band gaps of copolymers obtained from BFEE + EE (ratio 1:2) solution containing furan/thiophene (mole ratio 8:1) at potentials ranging from $E_{Ag/AgCl}$ = 1.5 to 1.7 V.

Polymerization potential $E_{Ag/AgCl}$	λ_{1max}		λ_{2max}		Band gap	
	nm	eV	nm	eV	nm	eV
1.5	408	3.04	722	1.72	550	2.26
1.55	411	3.02	700	1.77	543	2.29
1.6	413	3.00	715	1.74	548	2.26
1.7	415	2.98	718	1.73	555	2.23

The initial spectrum for the homo- and copolymers is not reached perfectly upon reduction, which implies incomplete reversibility of oxidation/reduction of the polymers. This might be caused by partial destruction of conjugated structures in the polymer chains [39, 131].

Homo- and Copolymer Films of Furan and 3-Chlorothiophene

Polyfuran (Fig. 26) shows a broad absorption band around 407 nm in the neutral state. This broad absorption band with λ_{1max} corresponds to the $\pi \rightarrow \pi^*$ transition, the width indicates the coexistence of both long and short effective conjugation lengths in the polyfuran films.

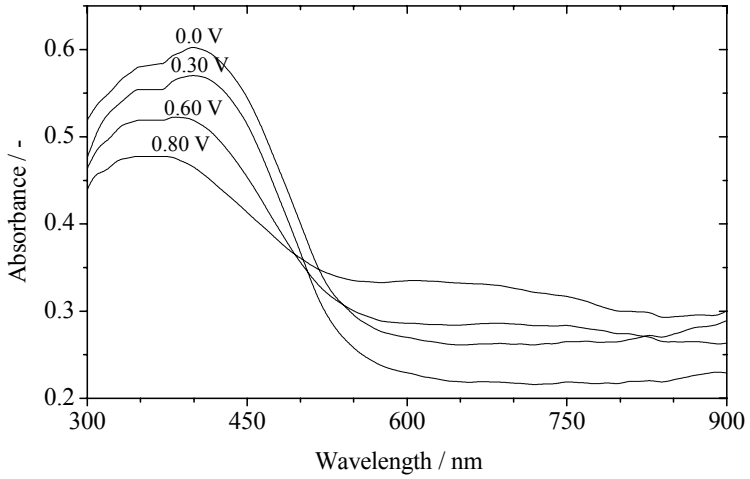

Fig. 26. *In situ* UV-Vis spectra recorded at different applied potentials in a solution of acetonitrile + 0.1 **M** TBATFB of polyfuran prepared at $E_{Ag/AgCl}$ = 1.35 V from BFEE + EE (ratio 1:2) and TFA (10 % by volume) solution containing 0.1 **M** furan and 0.1 **M** TBATFB.

According to the zero-order approximation, E_g for polyfuran from a direct interband transition can be estimated from the absorption edge (~ 530 nm) of the spectrum to be about 2.34 eV very close to the value reported in the literature [39] and previously prepared in this project (see page 52).

The passage from the undoped to the doped state is accompanied by weakening as well as a blue shift of the absorption band in the visible and shifting into NIR upon further oxidation. The optical transition with λ_{2max} from the valence band into the upper bipolaron band (the upper subgap state) is located at 680 nm (1.82 eV) above the valence band.

Poly(3-chlorothiophene) exhibits an absorption maximum at 440 nm in the neutral state (see Fig. 27). This broad absorption band corresponds to the $\pi \rightarrow \pi^*$ transition, the width implies again the coexistence of both long and short effective conjugation lengths. Upon oxidation, this absorption almost vanishes; instead a very broad feature raises around 770 nm (1.61 eV) with its maximum λ_{2max} shifting into the NIR upon further oxidation.

E_g for poly(3-chlorothiophene) for the direct interband transition between the highest occupied electronic levels (upper valance band edge) and the lowest unoccupied levels (lower conduction band edge) can be deduced from the energy of the absorption edge (~ 580 nm) of the spectrum at about 2.14 eV. In the band gap, lower and upper polaron/bipolaron states are formed, the upper bipolaron band is located 1.61 eV above the valence band.

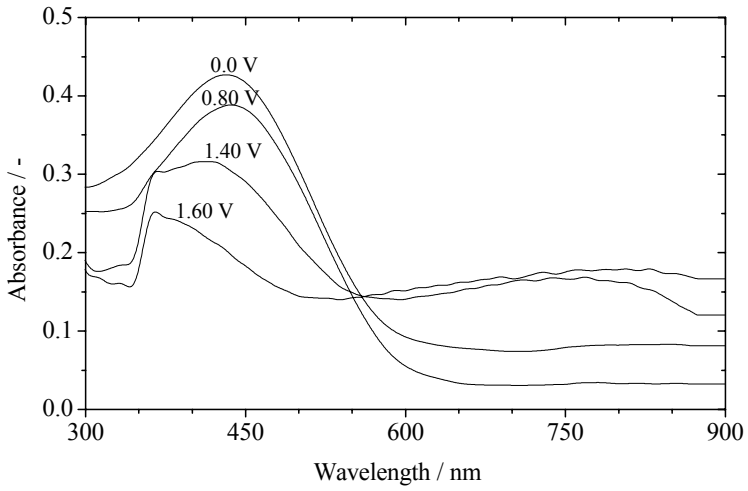

Fig. 27. *In situ* UV-Vis spectra recorded at different applied potentials in a solution of acetonitrile + 0.1 **M** TBATFB of poly(3-chlorothiophene) prepared at $E_{Ag/AgCl}$ = 1.55 V from BFEE + EE (ratio 1:2) and TFA (10 % by volume) solution containing 0.1 **M** 3-chlorothiophene and 0.1 **M** TBATFB.

The absorption bands and band gaps of polyfuran and poly(3-chlorothiophene) are listed in Table 8.

Table 8. Absorption bands and band gaps of polyfuran and poly(3-chlorothiophene).

Homopolymer	λ_{1max}		λ_{2max}		Band gap	
	nm	eV	nm	eV	nm	eV
Polyfuran	407	3.05	680	1.82	530	2.34
Poly(3-chlorothiophene)	440	2.82	770	1.61	580	2.14

As the steric hindrance of the substituents at the 3-positions is a major factor interrupting the coplanarity of adjacent thiophene rings, which in turn leads to a loss of inter-ring conjugation [132, 133], one would expect the π-conjugation length in the 3-substituted polymers to be reduced remarkably with bulkier halogen substituents. The slight difference between the band gap in PCTh and that in PTh which is around 0.04 eV shows that Cl substituents do not influence the inter-ring π-conjugation significantly as the inter-ring twist angle is relatively small in the solid state [134].

Fig. 28 shows the *in situ* UV-Vis spectra of the copolymers obtained from a solution of BFEE + EE (ratio 1:2) and TFA (10 % by volume) containing furan/3-chlorothiophene (mole ratio 1:1 and 8:1) at deposition potentials $E_{Ag/AgCl}$ = 1.7 and 1.5 V respectively. The copolymers have a broad absorption band in the neutral state corresponding to the π → π* transition indicating the coexistence of both long and short effective conjugation lengths containing furan and 3-chlorothiophene monomer units. A remarkable characteristic of the UV-Vis spectra is the shift of the broad absorption band in the neutral state of the copolymers to higher wavelengths with increasing preparation potential of the copolymer. This indicates that more 3-chlorothiophene units are incorporated into the copolymer with increasing preparation potential. Upon oxidation, the absorption assigned to the π→ π* transition almost vanishes, instead a very broad feature rises (λ_{2max}) with its maximum shifting into NIR upon more oxidation which is attributed to polaron/bipolaron transitions between band gap states. E_g for the copolymers prepared at potentials $E_{Ag/AgCl}$ = 1.5 and 1.7 V from a direct interband transition can also be estimated from the absorption edge (~550, 575 nm) of the spectrum, being about 2.26, 2.16 eV respectively which is less than observed with polyfuran.

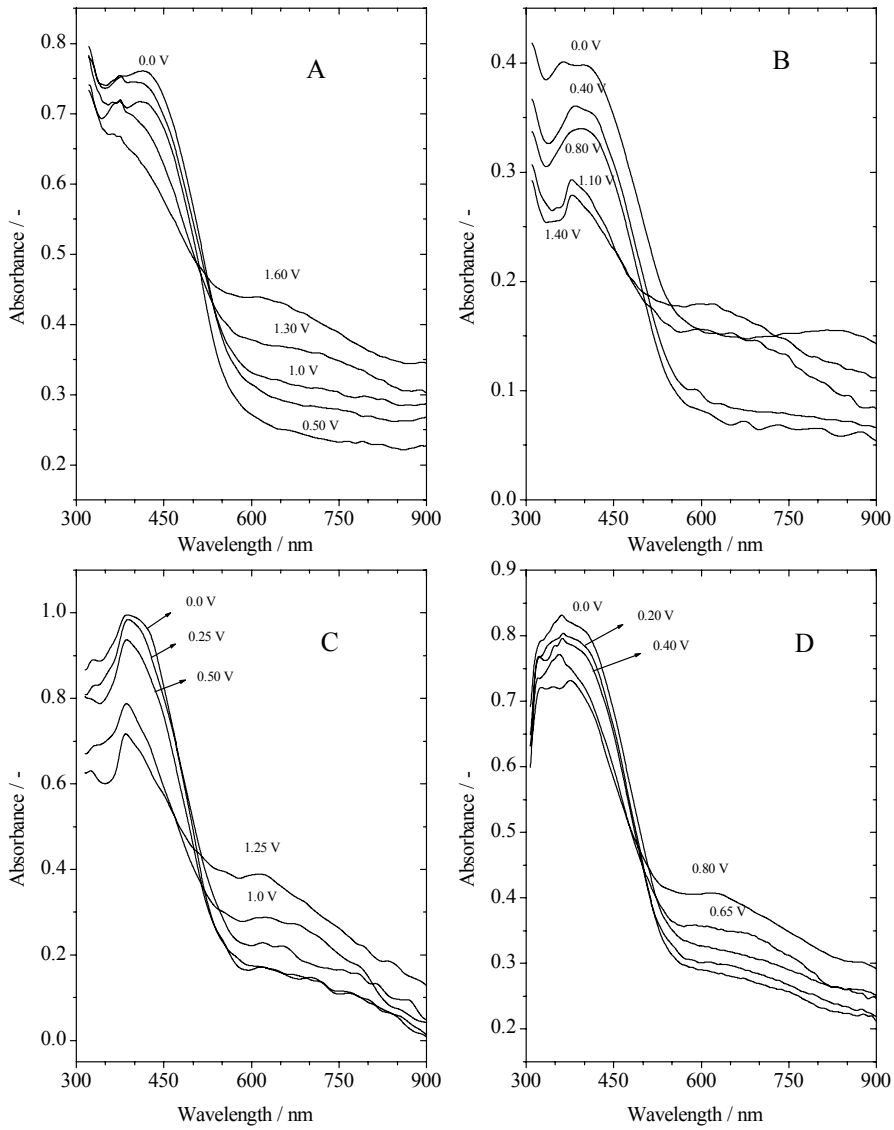

Fig. 28. *In situ* UV-Vis spectra recorded at different applied potentials in a solution of acetonitrile + 0.1 **M** TBATFB of copolymers deposited at $E_{Ag/AgCl}$ (A) 1.7 V, (B) 1.5 V in a BFEE + EE (ratio 1:2) and TFA (10 % by volume) containing furan/3-chlorothiophene (mole ratio 1:1), (C) 1.7 V, (D) 1.5 V in a BFEE + EE (ratio 1:2) and TFA (10 % by volume) containing furan/3-chlorothiophene (mole ratio 8:1)

When the furan/3-chlorothiophene feed ratio changed from 1:1 to 8:1, the following characteristics still exist in the UV-Vis spectra: the appearance of a broad absorption band in the neutral state and the blue shift of the absorption band in the visi-

ble region observed upon oxidation and the appearance of absorption features in the near IR region. When comparing the UV-Vis spectra of the copolymers prepared at the same polymerization potential in these different solutions, it is observed that a lower concentration of 3-chlorothiophene leads to a blue shift of the absorption band of the copolymer obtained. This implies that more 3-chlorothiophene units are incorporated into the copolymer film when the concentration of 3-chlorothiophene is increased. The absorption bands and band gaps of the copolymers prepared at different polymerization potentials from these different solutions are listed in Table 9 and 10.

Table 9. Absorption bands and band gaps of copolymers obtained from BFEE + EE (ratio 1:2) and TFA (10 % by volume) solutions containing 0.10 **M** furan and 0.10 **M** 3-chlorothiophene at potentials $E_{Ag/AgCl}$ = 1.5 and 1.7 V.

Polymerization potential $E_{Ag/AgCl}$	λ_{1max}		λ_{2max}		Band gap	
	nm	eV	nm	eV	nm	eV
1.5	415	2.99	705	1.76	550	2.26
1.7	431	2.88	720	1.72	575	2.16

Table 10. Absorption bands and band gaps of copolymers obtained from BFEE + EE (ratio 1:2) and TFA (10 % by volume) solution containing furan/3-chlorothiophene (mole ratio 8:1) at potentials $E_{Ag/AgCl}$ = 1.5 and 1.7 V.

Polymerization potential $E_{Ag/AgCl}$	λ_{1max}		λ_{2max}		Band gap	
	nm	eV	nm	eV	nm	eV
1.5	410	3.03	690	1.80	540	2.30
1.7	420	2.95	700	1.77	555	2.24

3.2.2 Redox Thermodynamics

In a Nernstian system a plot of E versus log([0]/[R]) will yield a straight line with a slope of 0.059/n and an intercept of E^{o} (where the concentrations of oxidized and reduced species are equal) [113]. It is understood that conducting polymer systems are not Nernstian, but this technique offers a useful way of comparing the thermodynamic properties of similar polymers.

Fig. 29(A, B) shows the plots corresponding to the oxidation process of the polymer potential as a function of the logarithm of [O]/[R] for the homopolymers.

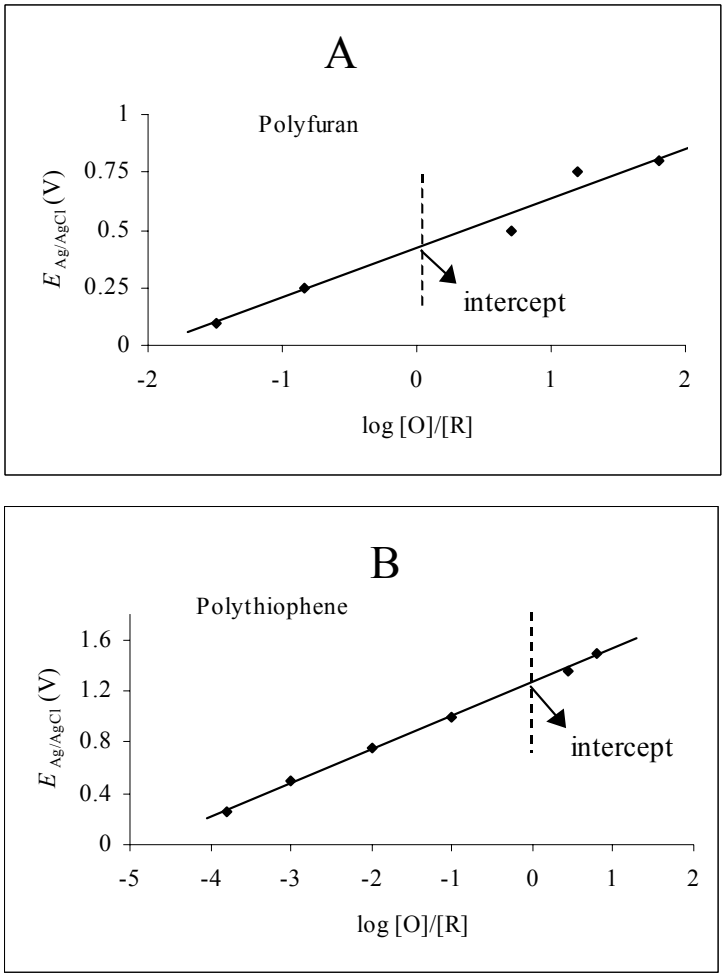

Fig. 29. Nernstian plots corresponding to the oxidation process recorded in a solution of acetonitrile + 0.1 **M** TBATFB of (A) polyfuran, (B) polythiophene.

These plots show a linear fit with an intercept (E^{o}) of 0.42 V and 1.27 V for polyfuran and polythiophene respectively, whereas the slopes are 216 mV/log unit and 264 mV/log unit suggesting that one electron is removed from the polymer segments containing four monomer units [39, 135].

In addition, it is noteworthy that the standard electrode potentials of the copolymers increase with an increasing preparation potential and they also increase when the concentration of thiophene increases as well as indicated in Table 11. These results concur with our results of cyclic voltammetry. Furthermore, there is a correlation between the standard electrode potential and the oxidation potential of the copolymers, which is clearly depicted in Fig. 30.

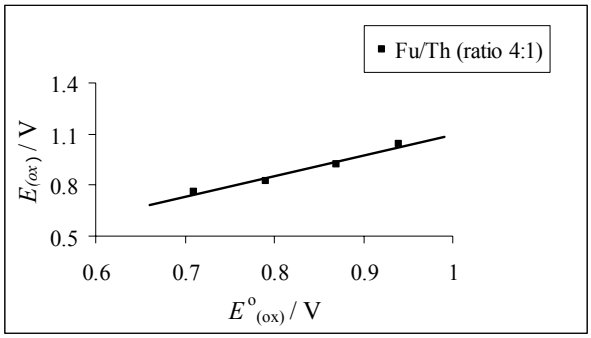

Fig. 30. Correlation between standard electrode potential and oxidation potential of copolymer obtained from BFEE + EE (ratio 1:2) solution containing furan/thiophene (mole ratio 4:1) at potentials from $E_{Ag/AgCl}$ = 1.5-1.7 V.

Table 11. Redox thermodynamic results of copolymer films.

Fu/Th (Mole Ratio)	E_{pol} = 1.50 V		E_{pol} = 1.55 V		E_{pol} = 1.60 V		E_{pol} = 1.70 V	
	$E^{0}_{(ox)}$ /V	slope$_{(ox)}$ mV/log unit	$E^{0}_{(ox)}$ /V	slope$_{(ox)}$ mV/log unit	$E^{0}_{(ox)}$ /V	slope$_{(ox)}$ mV/log unit	$E^{0}_{(ox)}$ /V	slope$_{(ox)}$ mV/log unit
1:1	0.96	252	0.98	260	1.20	262	1.22	274
4:1	0.71	237	0.79	248	0.87	254	0.94	268
8:1	0.44	203	0.61	219	0.74	224	0.85	234

There is also a correlation between the standard electrode potential and the slope of the plots for the copolymers (see Table 11 and Fig. 31): The oxidation of copolymers with higher standard potential requires more energy [113].

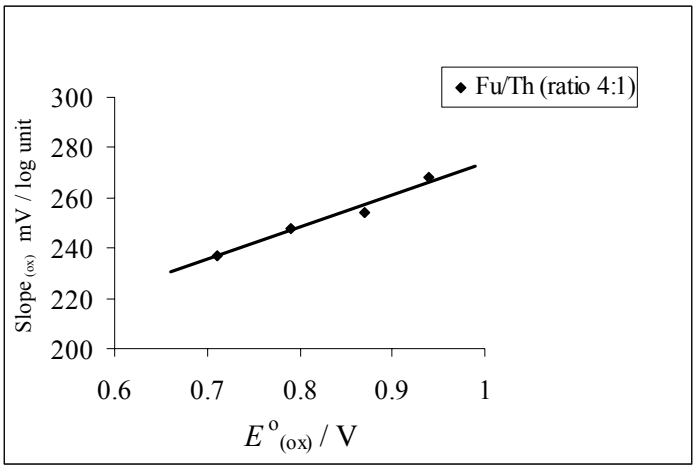

Fig. 31. Correlation between standard electrode potential and slope of the plots of a copolymer obtained from BFEE + EE (ratio 1:2) solution containing furan/thiophene (mole ratio 4:1) at potentials from $E_{Ag/AgCl}$ = 1.5-1.7 V.

Although the slope of the oxidation process of the copolymers decreases from 274 mV/log unit to 203 mV/log unit, it remains in every case significantly larger than the 59 mV/log unit expected for a simple monoelectronic redox couple. Non-Nernstian behaviour has been already observed in the redox process of conducting polymers [136-139], and it has been attributed to the charge storage mechanism in conjugated materials [113, 140].

3.3 *In situ* Conductivity Measurements

Homo- and Copolymer Films of Furan and Thiophene

Polyfuran deposited potentiostatically at $E_{Ag/AgCl}$= 1.45 V shows a single conductivity change by three orders of magnitude starting around $E_{Ag/AgCl}$= 0.1 V (Fig. 32). When the potential shift is reversed from 1.2 to - 0.2 V, the resistivity is almost restored. The conductivity almost the same after 0.8 V with a constant value up to $E_{Ag/AgCl}$= 1.2 V.

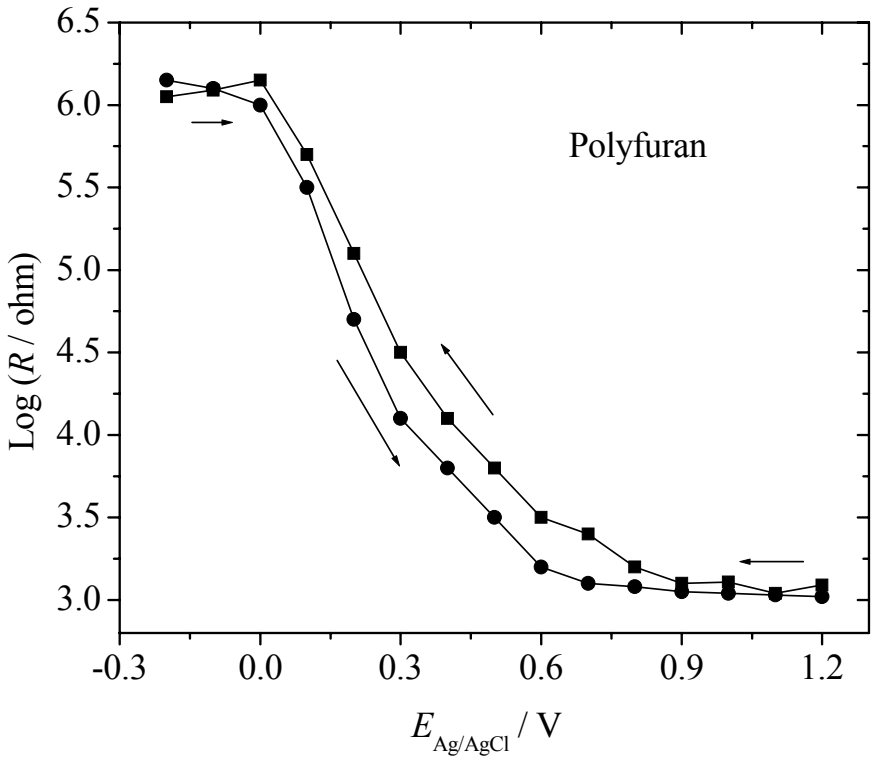

Fig. 32. Resistivity versus electrode potential data in a solution of acetonitrile + 0.1 **M** TBATFB of polyfuran.

The lower electrical conductivity of polyfuran may be attributed to the shorter conjugation length compared with polythiophene and polypyrrole, which can be seen from its UV-Vis spectra [42]. Another reason is that the degradation and ring opening reaction cannot be totally suppressed in the polymerization solution, and nonconjugated regions, even though in small amounts, exist in the polymer chains. As a consequence, the existence of high and low electrical conductivity domains in the film restricts the charge carrier migration in the polymer [40, 141].

The resistivity versus the applied potential plot of polythiophene deposited potentiostatically at $E_{Ag/AgCl}$= 1.65 V is displayed in Fig. 33. Polythiophene shows a single change in resistivity. When the applied potential was increased, the resistivity decreased sharply by two orders of magnitude after $E_{Ag/AgCl}$= 0.7 V with a highly stable conductivity up to $E_{Ag/AgCl}$= 2 V. These observations for polythiophene have been previously reported [131]. In a potential scan back from 2.0 to 0.0 V the resistivity is almost completely restored.

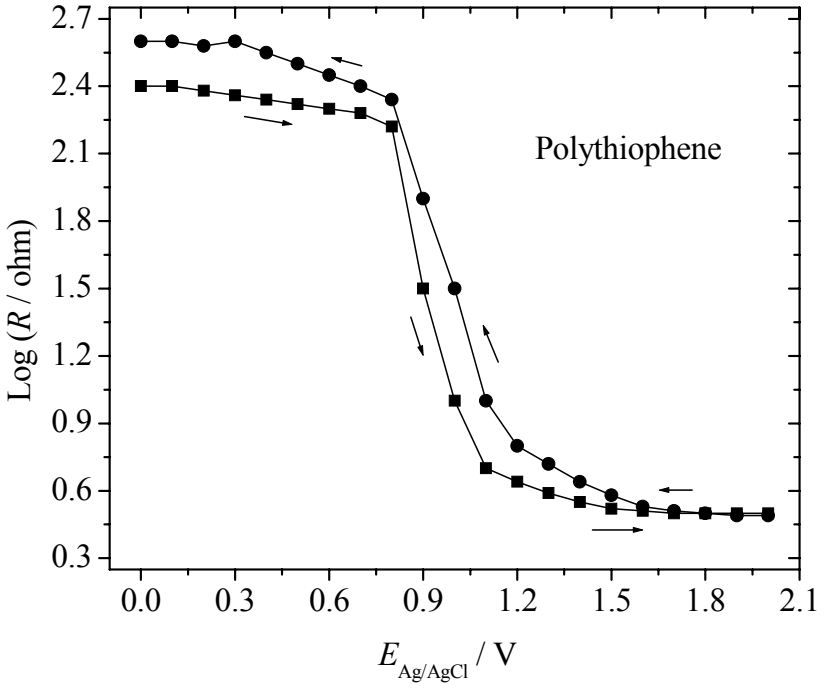

Fig. 33. Resistivity versus electrode potential data in a solution of acetonitrile + 0.1 **M** TBATFB of polythiophene.

In situ conductivity measurements both at different electrode potentials and with different thiophene concentrations in the polymerization solution have been performed. Fig. 34(A-D) shows the resistivity versus the applied electrode potential of the copolymers obtained from BFEE + EE (ratio 1:2) solution containing furan/thiophene (mole ratio 1:1) at potentials ranging $E_{Ag/AgCl}$ = 1.5-1.7 V respectively.

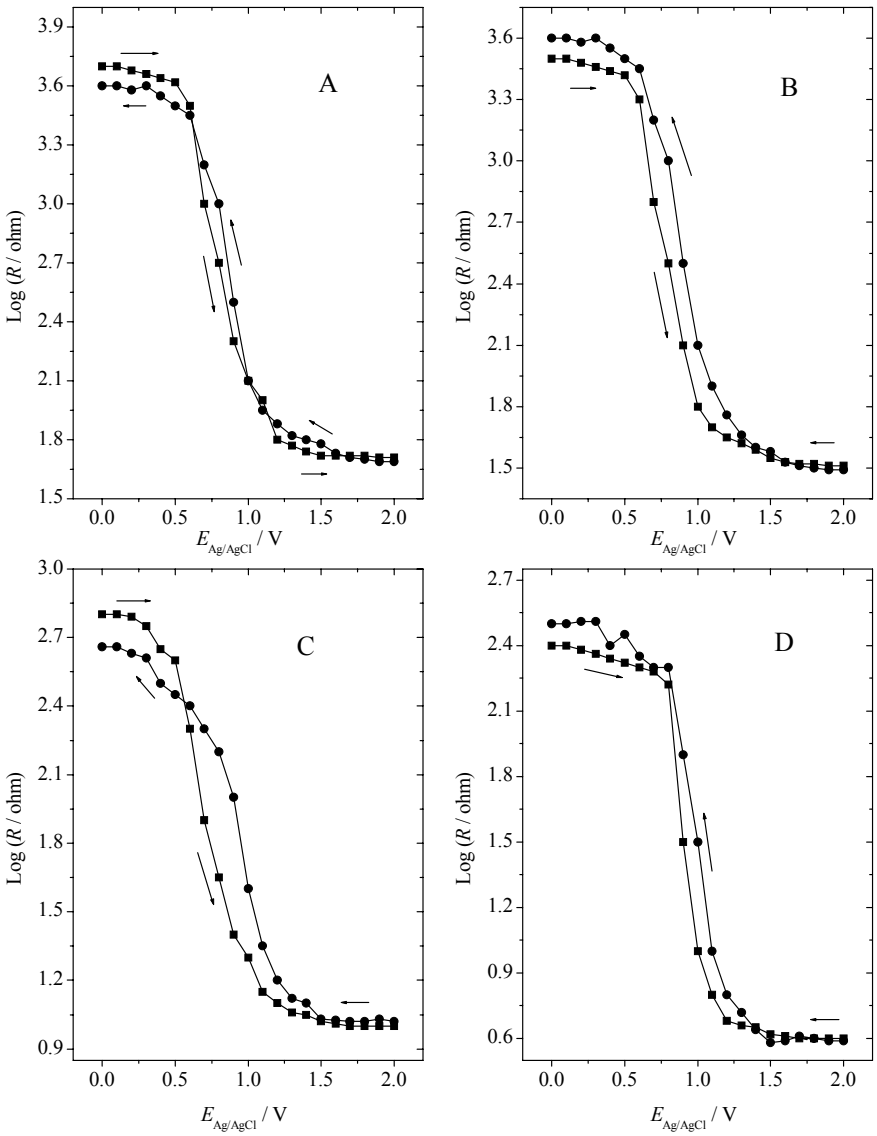

Fig. 34. Resistivity versus electrode potential data in a solution of acetonitrile + 0.1 **M** TBATFB of copolymers obtained from BFEE + EE (ratio 1:2) solution containing furan/thiophene (mole ratio 1:1) at potentials $E_{Ag/AgCl}$ = (A) 1.5 V, (B) 1.55 V, (C) 1.6 V, (D) 1.7 V.

Like the homopolymers, the copolymers (A-D) show a single change in resistivity. For copolymer (D), when the applied potential is increased, the resistivity decreases sharply at $E_{Ag/AgCl}$ = 0.8 V with a stable conductivity up to $E_{Ag/AgCl}$= 2 V. Furthermore, its conductivity is close to that of polythiophene and higher than that of polyfuran by 2.4 orders of magnitude. The resistivity is almost completely restored when the potential is shifted back from 2.0 to 0.0 V.

Reminiscent of copolymer (D), the same changes can be observed with copolymer (A). However, compared to polyfuran, its conductivity is by 1.3 orders of magnitude higher. This indicates that more thiophene units are incorporated into the copolymer chains with an increasing preparation potential.

When the furan/thiophene feed ratio is changed from 1:1 to 4:1 (Fig. 35) the same interesting features still exist, i.e. copolymers show a single change in resistivity, when the applied potential is increased, the resistivity decreased and the resistivity is almost restored when the potential is shifted back to 0.0 V.

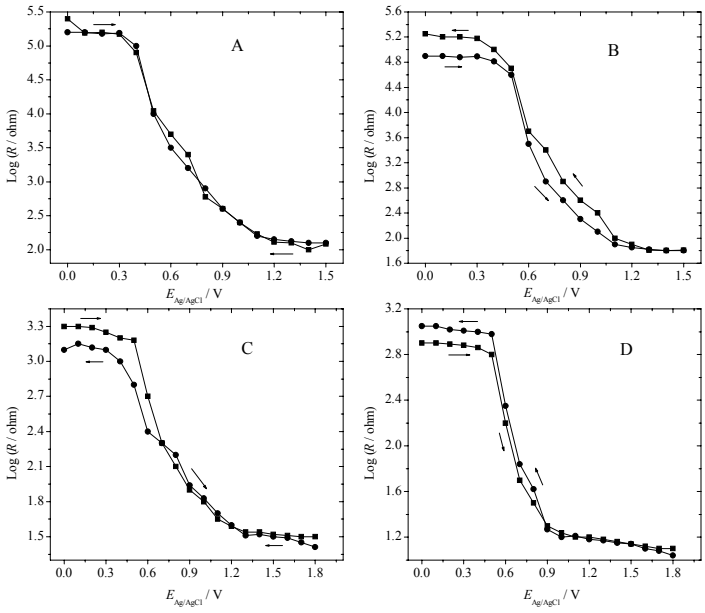

Fig. 35. Resistivity versus electrode potential data in a solution of acetonitrile + 0.1 **M** TBATFB of copolymers obtained from BFEE + EE (ratio 1:2) solution containing furan/thiophene (mole ratio 4:1) at potentials $E_{Ag/AgCl}$ = (A) 1.5 V, (B) 1.55 V, (C) 1.6 V, (D) 1.7 V.

When the furan/thiophene feed ratio is changed from 1:1 to 8:1 the same interesting features mentioned above still exist and are clearly displayed in Fig. 36.
In the case of copolymer (A), its behaviour is close to that of polyfuran with conductivity higher by 0.5 orders of magnitude, whereas the difference is 1.4 orders of magnitude for copolymer (D).

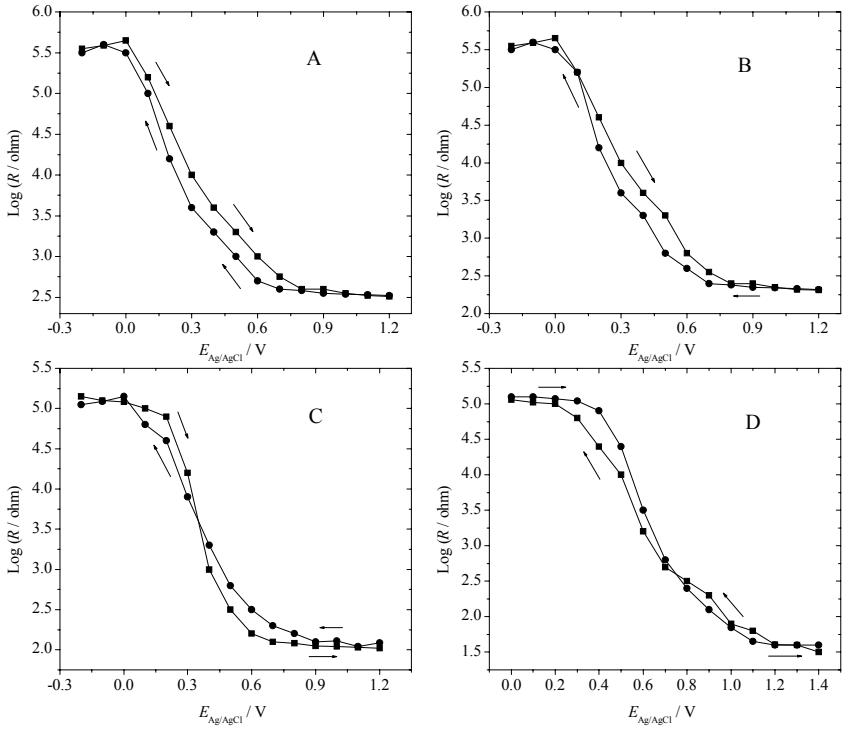

Fig. 36. Resistivity versus electrode potential data in a solution of acetonitrile + 0.1 **M** TBATFB of copolymers obtained from BFEE + EE (ratio 1:2) solution containing furan/thiophene (mole ratio 8:1) at potentials $E_{Ag/AgCl}$ = (A) 1.5 V, (B) 1.55 V, (C) 1.6 V, (D) 1.7 V.

By comparing copolymers (A, D) in Fig. 34 with copolymers (A, D) in Fig. 36, we can conclude that the number of thiophene units in these copolymer chains increases with an increasing thiophene concentration in the polymerization solutions, and the conductivities of the copolymers are between those of polyfuran and polythiophene, implying that oxidation of both monomers is possible and the copolymer chains may accordingly be composed of both furan and thiophene units.

Another noticeable feature is the fact, that *in situ* conductivity properties are not the sum of those of the two individual homopolymers. This result may exclude the possibility that the copolymers can be considered as block copolymers. It may be concluded that the copolymers (D) in Fig. 34 and (A) in Fig. 36 have structures approaching those of polythiophene-based random copolymer and polyfuran-based random copolymer respectively.

The relation between the resistivity and the concentration of thiophene in the electropolymerization solutions is linear (linear fit, Fig. 37) especially at higher concentrations (0.025 - 0.1 **M**), which concurs with our results of cyclic voltammetry indicating that the properties of copolymers depend not only on the electrochemical polymerization potential but also on the monomer feed ratio, see Fig. 11.

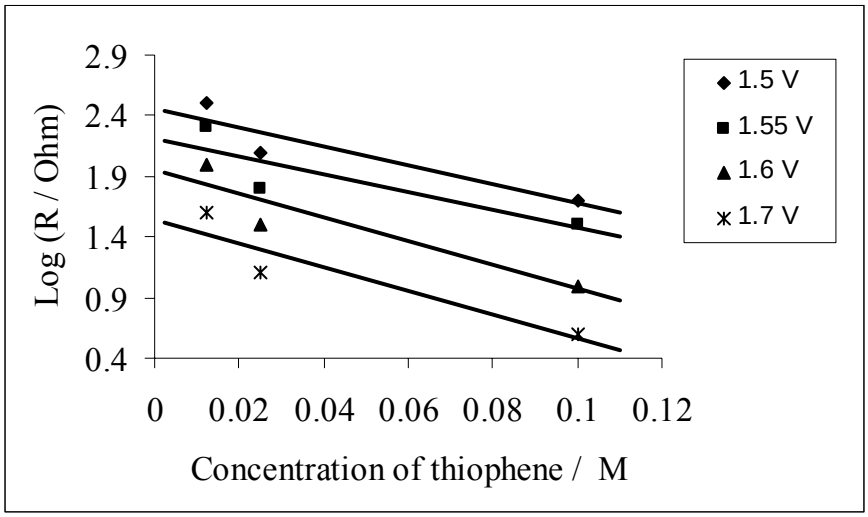

Fig. 37. Dependence of resistivity of copolymers deposited at $E_{Ag/AgCl}$ = 1.5 - 1.7 V respectively on concentration of thiophene in mixed solutions.

Homo- and Copolymer Films of Furan and 3-Chlorothiophene

Polyfuran shows a single conductivity change by about three orders of magnitude starting around $E_{Ag/AgCl}$= 0.1 V with a stable conductivity up to $E_{Ag/AgCl}$= 1.2 V (Fig. 38). When the potential shift is reversed from 1.2 to - 0.2 V, the resistivity is almost restored. The shorter conjugation length, the degradation and ring opening reaction which cannot be totally suppressed in the polymerization solution, and nonconjugated regions, even though in small amounts, exist in the polymer chains. This may be attributed to the lower electrical conductivity of polyfuran [42, 40, 141].

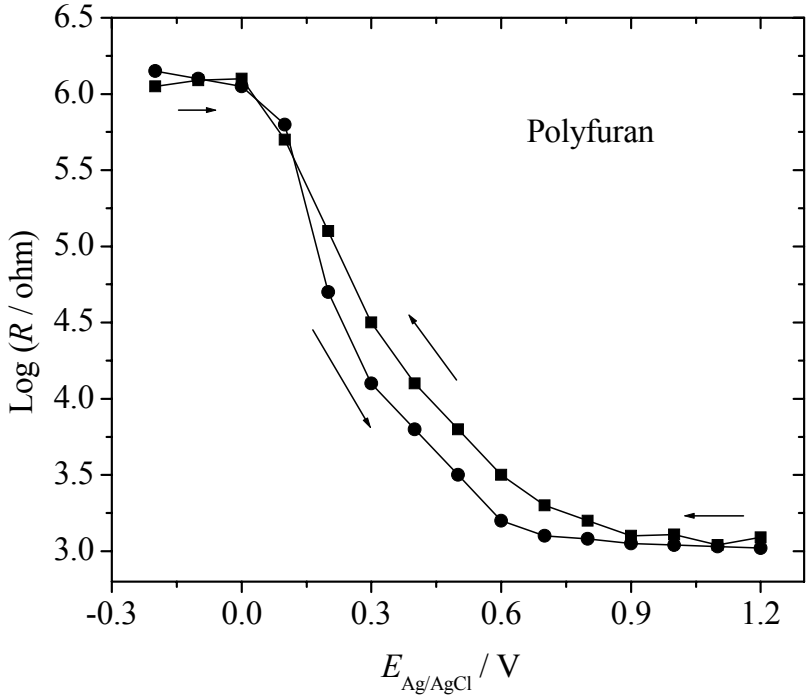

Fig. 38. Resistivity versus electrode potential data in a solution of acetonitrile + 0.1 **M** TBATFB of polyfuran prepared at $E_{Ag/AgCl}$ = 1.35 V from BFEE + EE (ratio 1:2) and TFA (10 % by volume) solution containing 0.1 **M** furan and 0.1 **M** TBATFB.

The resistivity versus the applied potential plot of poly(3-chlorothiophene) deposited potentiostatically at $E_{Ag/AgCl}$= 1.55 V is displayed in Fig. 39. The polymer shows a single change in resistivity. When the applied potential was increased, the resistivity decreased sharply by three orders of magnitude around $E_{Ag/AgCl}$= 0.8 V with a

highly stable conductivity up to $E_{Ag/AgCl}$= 2 V. In a potential scan back from 2.0 to 0.0 V the resistivity is almost completely restored.

The conductivity of poly(3-chlorothiophene) is around one order of magnitude lower than that of polythiophene. This can be explained qualitatively by invoking the difference between the hydrogen and chlorine radii which is around 0.60 Å. This difference may increase the steric hindrance and distortion along the polymer chain which modifies the structure and thus the properties of the polymer [66]. The low conductivity can also be ascribed to the physical discontinuity within the polymer matrices, which increases the resistance of the polymer [142].

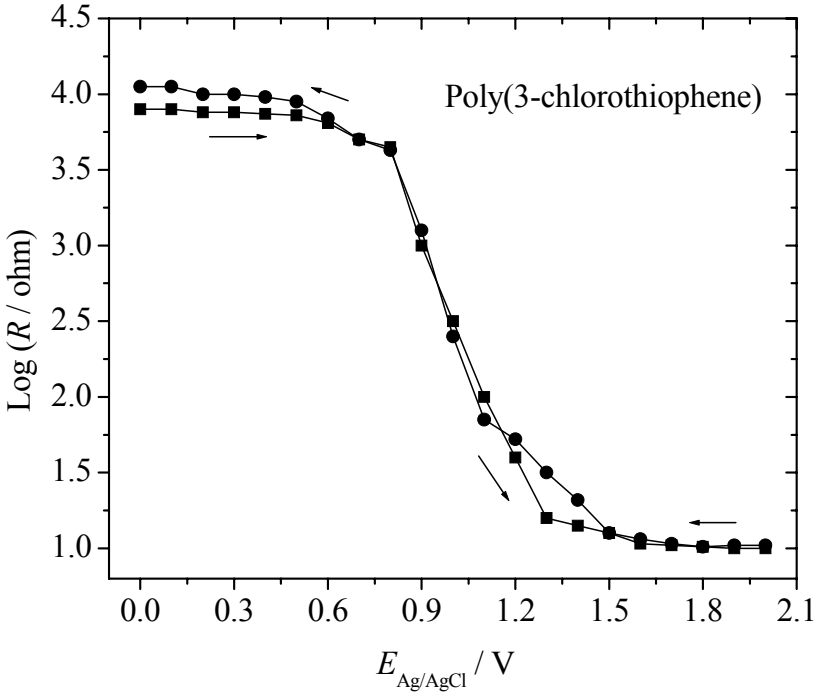

Fig. 39. Resistivity versus electrode potential data in a solution of acetonitrile + 0.1 **M** TBATFB of poly(3-chlorothiophene).

In situ conductivity measurements both at different electrode potentials and with different 3-chlorothiophene concentrations in the polymerization solution were performed. The resistivity versus the applied electrode potential of the copolymers obtained was depicted in Fig. 40(A-D). Copolymer (B) shows a single change in resistivity. When the applied potential is increased, the resistivity decreases sharply at $E_{Ag/AgCl}$= 0.7 V with a stable conductivity up to $E_{Ag/AgCl}$= 2 V. Furthermore, its con-

ductivity is close to that of poly(3-chlorothiophene) and higher than that of polyfuran by 1.8 orders of magnitude. The resistivity is almost completely restored when the potential is shifted back from 2.0 to 0.0 V. The same changes can be observed with copolymer (A). However, its conductivity is higher by 1.2 orders of magnitude as compared to polyfuran. This indicates that more 3-chlorothiophene units are incorporated into the copolymer chains with an increasing preparation potential.

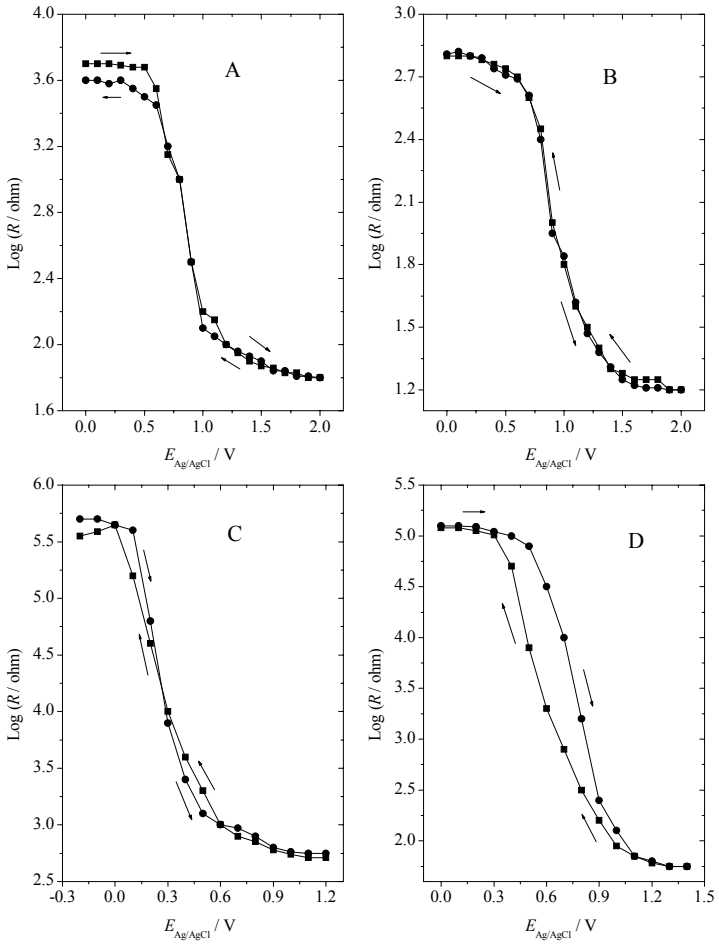

Fig. 40. Resistivity versus electrode potential data in a solution of acetonitrile + 0.1 **M** TBATFB of copolymers deposited at $E_{Ag/AgCl}$ = 1.5 and 1.7 V respectively in a BFEE + EE (ratio 1:2) and TFA (10 % by volume) containing (A, B) furan/3-chlorothiophene (mole ratio 1:1), (C, D) furan/3-chlorothiophene (mole ratio 8:1).

When the furan/3-chlorothiophene feed ratio is changed from (1:1) to (8:1) the same interesting features still exist, i.e. copolymers show a single change in resistivity, when the applied potential is increased, the resistivity decreased and the resistivity is almost restored when the potential is shifted back to - 0.2 V. In the case of copolymer (C), its behaviour is close to that of polyfuran with conductivity higher by 0.3 orders of magnitude, whereas the difference is 1.3 orders of magnitude for copolymer (D).

By comparing copolymers (A, B) with copolymers (C, D), one can conclude that the number of 3-chlorothiophene units in these copolymer chains increases with an increasing 3-chlorothiophene concentration in the polymerization solutions, and the conductivities of the copolymers are between the conductivities of polyfuran and poly(3-chlorothiophene), implying that oxidation of both monomers is possible and the copolymer chains may accordingly be composed of furan and 3-chlorothiophene units.

Another obvious feature is the fact, that *in situ* conductivity properties are not the sum of those of the two individual homopolymers. This result may exclude the possibility that the copolymers can be considered as block copolymers. It may be concluded that copolymers (B) and (C) have structures approaching those of poly(3-chlorothiophene)-based random copolymer and polyfuran-based random copolymer respectively.

3.4 Fourier Transform Infrared Spectroscopy

3.4.1 The FTIR Spectroscopy of Homo- and Copolymer Films

In the spectrum of the (as-prepared) polyfuran, the peak located around 1059 cm^{-1} is assigned to C-O stretching vibration, C-H in-plane deformation and ring deformation [43, 143-144]. The polyfuran C=C stretching vibration was observed at 1510 cm^{-1}; whereas the band around 1399 cm^{-1} is attributed to a C-C stretching vibration and C-H in-plane deformation [145-146]. Furthermore, another remarkable feature in the spectra is an absorption band between 780-989 cm^{-1} related to C-H out-of-plane deformation, which is a characteristic of α-substituted five-membered heterocyclic compounds, suggesting that α-positions in the polymer chains are involved in the polymerization [147-150]. The band near 630 cm^{-1} is probably based on in-plane ring deformation [144]. The weak absorption around 1700 cm^{-1} corresponding to the C=O stretching vibration shows that some defects do exist in the polymer film, see Fig. 41.

For the spectrum of the (as-prepared) polythiophene, the band located at 758 cm^{-1} is assigned to C-S-C out-of-plane deformation [151-152], whereas the broad strong band located around 685 cm^{-1} is assigned to the out-of-plane deformation of the =C-H group, which is a characteristic of monosubstituted polythiophene [153-154]. The stretching frequency of the C=C bond in polythiophene appears in the region 1443 - 1523 cm^{-1}[155-156]. The two bands at 1151 and 1210 cm^{-1} are possibly based on C-H in-plane deformation, while the bands in the region 864 - 987 cm^{-1} are related to C-H out-of-plane deformation [157]. The band near 1350 cm^{-1} is probably due to a stretching vibration of C-C bonds [158]. The band at 538 cm^{-1} is assigned to an in-plane ring deformation [144]. Furthermore, a C=O stretching vibration is assigned to the band at 1717 cm^{-1}, see Fig. 41.

Copolymerization is carried out under potentiostatic conditions. In Fig. 41 the FTIR spectra of a copolymer obtained from a BFEE + EE (ratio 1:2) solution containing 0.10 **M** furan and 0.10 **M** thiophene prepared at $E_{Ag/AgCl}$ = 1.60 V are displayed, for comparison FTIR spectra of the respective homopolymers are shown.

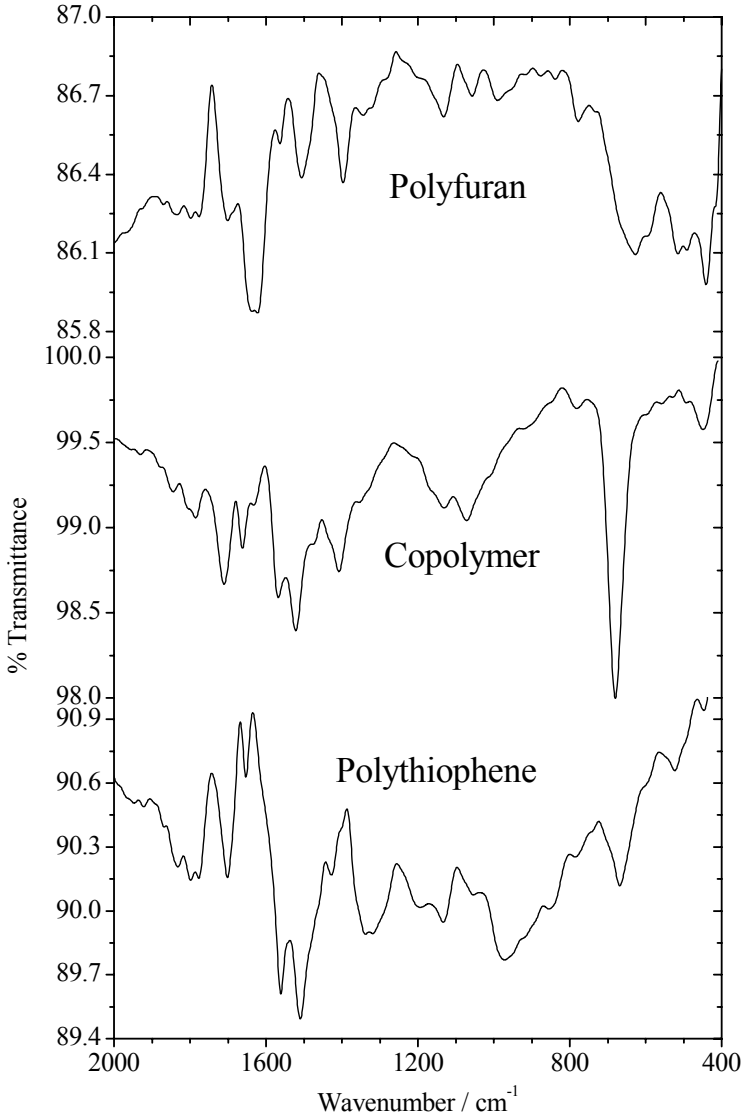

Fig. 41. FTIR spectra of polyfuran, polythiophene, and copolymer deposited at $E_{Ag/AgCl}$ = 1.60 V in a BFEE + EE (ratio 1:2) solution containing 0.10 **M** furan and 0.10 **M** thiophene. Reference: KBr disc, 2 cm^{-1} resolution (eight scans).

The most impressive characteristic of the FTIR spectra of the copolymer is the evolution of a strong absorption band located around 680 cm^{-1}, which is assigned to the overlap between the out-of-plane deformation of the =C-H group and in-plane ring deformation. We can also observe peaks located around 1070 - 1131 cm^{-1} assigned to the combination of C-O stretching vibration, C-H in-plane bending and ring deformation. The stretching frequency of the C=C bond in the copolymer appears in the region of 1470-1570 cm^{-1}. Furthermore, the presence of bands in the region of 840 - 910 cm^{-1} indicates that α-α' coupling of radical cations has taken place in the copolymerization. This is a characteristic of α-substituted five-membered heterocyclic compounds [77]. The infrared band assignments for homopolymers and a selected copolymer (1:1 ratio of comonomers in the feed solution) deposited at $E_{Ag/AgCl}$ = 1.60 V are listed in Table 12.

Table 12. FTIR band assignments of polyfuran, polythiophene and a copolymer deposited at $E_{Ag/AgCl}$ = 1.60 V, all figures in wavenumbers cm^{-1}.

Mode	Polyfuran	Polythiophene	Copolymer[a]
ν(C=O)	1700	1717	1713
$\nu(C=C)_{ring}$	1510	1443-1523	1470-1570
$\nu(C-C)_{ring}$	1399	1350	1350-1406
$\nu(C-O)_{ring}$	1059-1132	-	1070-1131
δ(C-H)	-	1151-1210	1220
γ(C-H)	780-989	864-987	840-910
δ(Ring)	1059	-	1070
δ(Ring)	630	538	-
δ(C-H)	1059-1132	-	1070-1134
γ(C-S-C)	-	758	784
γ(=C-H)	-	685	680[b]

δ: in-plane deformation mode; γ: out-of-plane deformation mode; ν: stretching mode.
[a] copolymer deposited at $E_{Ag/AgCl}$ = 1.60 V in a BFEE + EE (ratio 1:2) solution containing 0.10 **M** furan and 0.10 **M** thiophene.
[b] overlap between γ(=C-H) and δ(ring).

FTIR spectra of copolymers obtained both at different potentials and with different thiophene concentrations have been investigated. Fig. 42(A-C) shows the FTIR spectra of the copolymers obtained with electropolymerization solutions containing 0.1 **M** furan and 0.1 **M** thiophene at potentials ranging from $E_{Ag/AgCl}$ = 1.5 to 1.7 V respectively.

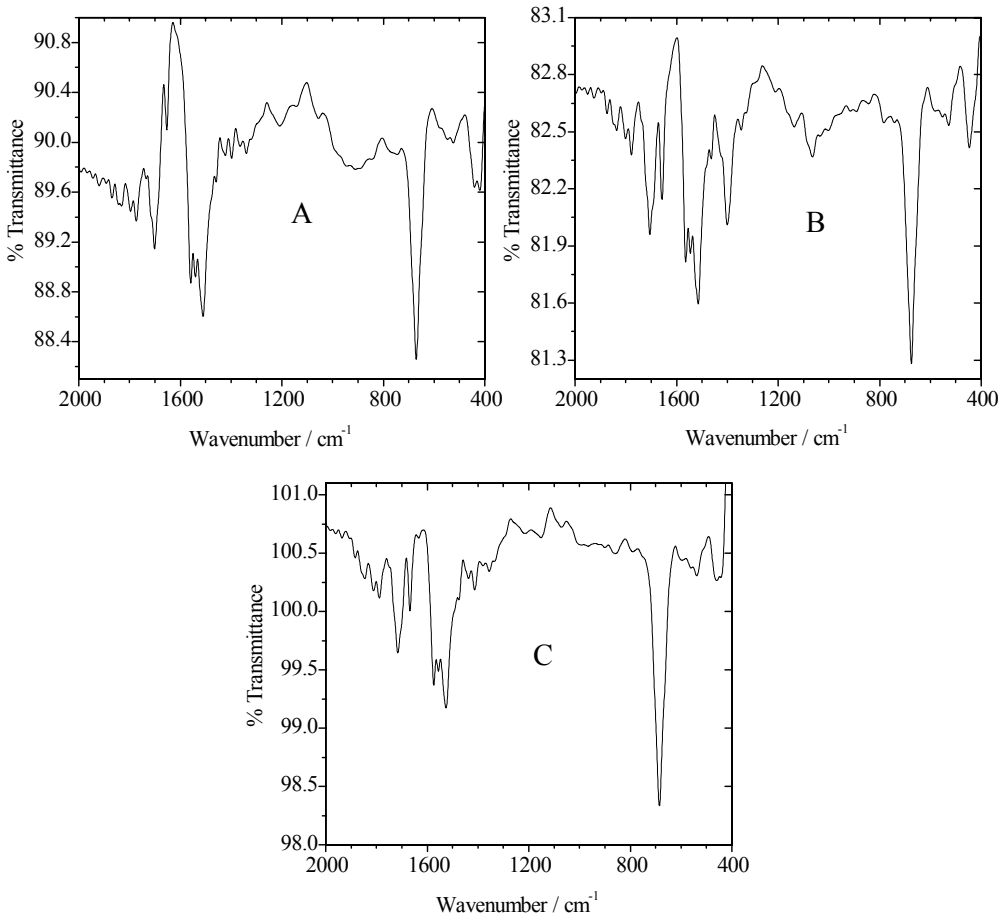

Fig. 42. FTIR spectra of copolymers deposited at $E_{Ag/AgCl}$ = (A) 1.5 V, (B) 1.55 V, (C) 1.7 V in a BFEE + EE (ratio 1:2) solution containing 0.1 **M** furan, 0.1 **M** thiophene, and 0.1 **M** TBATFB. Reference: KBr disc, 2 cm^{-1} resolution (eight scans).

Interestingly, in the FTIR spectra the out-of-plane deformation band which corresponds to the =C-H bond of the copolymers shifts to higher wavenumbers and the intensity of this band also increases with an increasing preparation potential of the co-

polymer due to overlapping with the in-plane ring deformation band. When prepared at $E_{Ag/AgCl}$ = 1.5 V, the copolymer shows an absorption band around 672 cm^{-1}; while prepared at $E_{Ag/AgCl}$ = 1.7 V the copolymer shows an absorption band around 686 cm^{-1} which is closer to pure polythiophene. These peaks differ obviously from those of polythiophene in this region. This may be due to the interaction between the furan and thiophene units in the copolymer, and it may be regarded as evidence of copolymerization; it cannot be explained by simple addition of the spectra of pure homopolymers. These results imply that more thiophene units are incorporated into the copolymer when the electrochemical polymerization potential is increased. The infrared band assignments for the copolymers deposited at $E_{Ag/AgCl}$ = 1.5 to 1.7 V from a polymerization solution containing 0.1 **M** furan and 0.1 **M** thiophene are listed in Table 13.

Table 13. FTIR band assignments of copolymers deposited from polymerization solutions containing 0.1 **M** furan and 0.1 **M** thiophene, all figures in wavenumbers cm^{-1}.

Mode	Polymerization potential $E_{Ag/AgCl}$	1.5 V	1.55 V	1.7 V
ν(C=O)		1703	1710	1717
$\nu(C=C)_{ring}$		1460-1560	1463-1567	1477-1576
$\nu(C-C)_{ring}$		1340-1426	1345-1400	1357-1437
$\nu(C-O)_{ring}$		1061-1140	1067-1134	1077-1147
δ(C-H)		1207	1210	1214
δ(C-H)		1061-1140	1067-1134	1077-1147
γ(C-H)		844-954	845-997	860-967
δ(Ring)		1061	1067	1077
δ(Ring)		525-574	531	535
γ(C-S-C)		761	784	794
γ(=C-H) + δ(Ring)		672	675	686

δ: in-plane deformation mode; γ: out-of-plane deformation mode; ν: stretching mode.

When the furan/thiophene feed ratio changed from 1:1 to 4:1 (Fig. 43) and to 8:1 (Fig. 44), the same interesting features still existed. The strong combination band

which corresponds to the out-of-plane =C-H deformation and the in-plane ring deformation band of the copolymers shifts to higher wavenumbers when the thiophene concentration increases, and the intensity of this band also increases with an increasing preparation potential of the copolymers. A copolymer prepared in a solution containing furan/thiophene (ratio 1:1) prepared at $E_{Ag/AgCl}$ = 1.6 V shows an absorption band around 680 cm^{-1}, whereas a copolymer obtained in a solution containing furan/thiophene (ratio 8:1) shows an absorption band around 673 cm^{-1}.

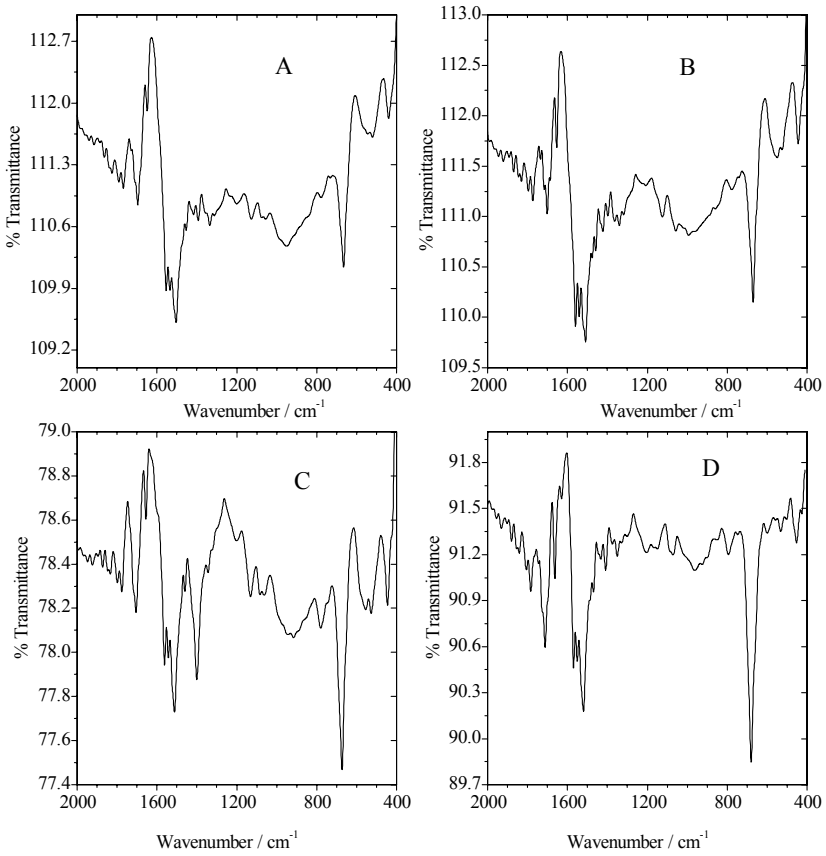

Fig. 43. FTIR spectra of copolymers deposited at $E_{Ag/AgCl}$ = (A) 1.5 V, (B) 1.55 V, (C) 1.6 V, (D) 1.7 V in a BFEE + EE (ratio 1:2) solution containing furan/thiophene (mole ratio 4:1), and 0.1 **M** TBATFB. Reference: KBr disc, 2 cm^{-1} resolution (eight scans). *In some cases there is a small difference in transparency between the reference disc and the sample disc which leads to up shift of the % Transmittance of the spectrum.*

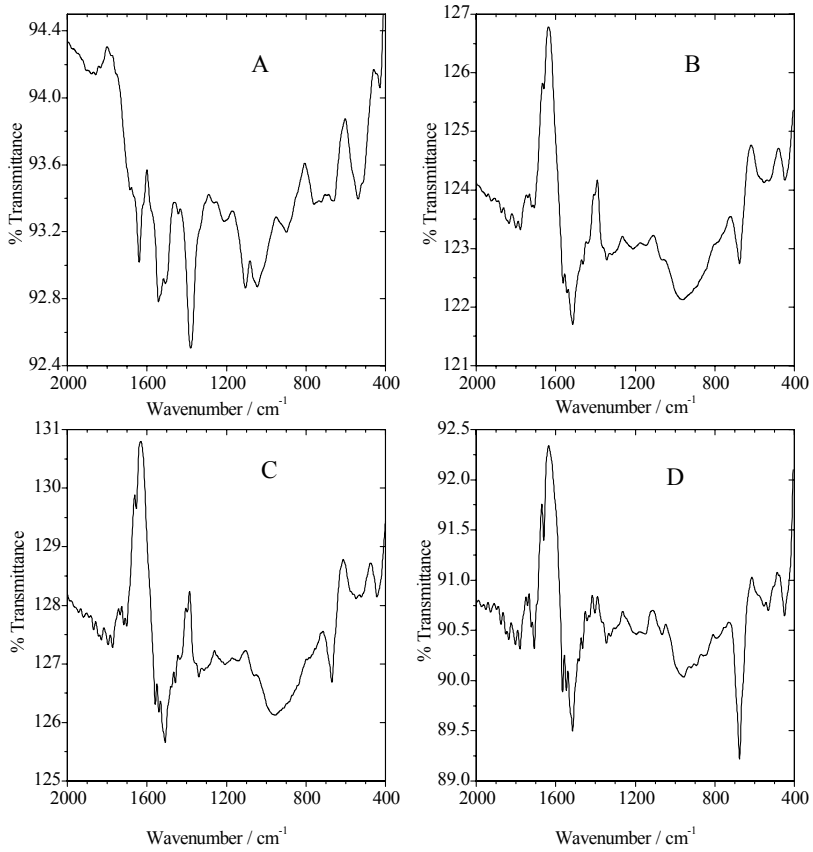

Fig. 44. FTIR spectra of copolymers deposited at $E_{Ag/AgCl}$ = (A) 1.5 V, (B) 1.55 V, (C) 1.6 V, (D) 1.7 V in a BFEE + EE (ratio 1:2) solution containing furan/thiophene (mole ratio 8:1), and 0.1 **M** TBATFB. Reference: KBr disc, 2 cm^{-1} resolution (eight scans). *In some cases there is a small difference in transparency between the reference disc and the sample disc which leads to up shift of the % Transmittance of the spectrum*.

The infrared band assignments for the copolymers deposited at $E_{Ag/AgCl}$ = 1.5 to 1.7 V from polymerization solutions containing furan: thiophene (mole ratio 4:1) and (mole ratio 8:1) are listed in Table 14 and 15 respectively.

Table 14. FTIR bands assignment of copolymers deposited from polymerization solutions containing furan: thiophene at a mole ratio 4:1, all figures in wavenumbers cm^{-1}.

Mode	Polymerization potential $E_{Ag/AgCl}$	1.5 V	1.55 V	1.6 V	1.7 V
ν(C=O)		1730	1715	1705	1713
$\nu(C=C)_{ring}$		1503-1556	1423-1560	1510-1563	1466-1573
$\nu(C-C)_{ring}$		1337-1445	1340-1400	1400-1454	1350-1406
$\nu(C-O)_{ring}$		1061-1131	1061-1123	1070-1134	1077-1143
δ(C-H)		1198	1210	1197	1210
δ(C-H)		1061-1131	1061-1123	1070-1134	1077-1143
γ(C-H)		834-954	844-990	848-921	848-967
δ(Ring)		1061	1061	1070	1077
δ(Ring)		521	548	528-557	531
γ(C-S-C)		774	774	781	794
γ(=C-H) + δ(Ring)		667	671	676	680

δ: in-plane deformation mode; γ : out-of-plane deformation mode; ν: stretching mode.

Table 15. FTIR bands assignment of copolymers deposited from polymerization solutions containing furan: thiophene at a mole ratio 8:1, all figures in wavenumbers cm^{-1}.

Mode	Polymerization potential $E_{Ag/AgCl}$	1.5 V	1.55 V	1.6 V	1.7 V
ν(C=O)		1712	1710	1720	1710
$\nu(C=C)_{ring}$		1510-1545	1516-1540	1507-1560	1513-1570
$\nu(C-C)_{ring}$		1380	1344	1340	1350-1463
$\nu(C-O)_{ring}$		1037-1111	1070-1147	1061-1137	1064-1143
δ(C-H)		1214	1210	1210	1194
δ(C-H)		1037-111	1070-1147	1061-1137	1064-1143
γ(C-H)		897	961	964	840-957
δ(Ring)		1037	1070	1061	1064
δ(Ring)		547	521	545	528
γ(C-S-C)		764	774	774	778
γ(=C-H) + δ(Ring)		663	665	673	676

δ: in-plane deformation mode; γ : out-of-plane deformation mode; ν: stretching mode.

3.4.2 The Electrochemical Degradation Mechanism of Furan-Thiophene Copolymers

Fig. 45 shows the FTIR spectra of the (as-prepared) copolymer film. The weak absorption band around 2900 cm^{-1} corresponding to the saturated C-H stretching vibration indicates a low degree of saturation of the (as-prepared) copolymer. However, the weak absorption around 1700 cm^{-1} and another at 1650 cm^{-1} still show that some defects do exist in the (as-prepared) copolymer film [41, 159-160].

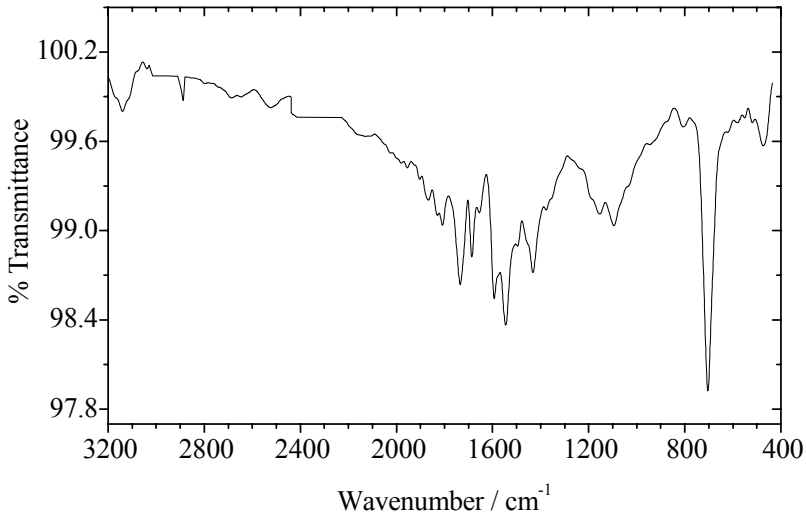

Fig. 45. FTIR spectra of (as-prepared) copolymer deposited at $E_{Ag/AgCl}$ = 1.60 V in a BFEE + EE (ratio 1:2) solution containing 0.1 **M** furan, 0.1 **M** thiophene, and 0.1 **M** TBATFB.

It was reported that the extent of ring fragmentation was higher when the electrochemical polymerization was carried out at higher potentials. Acid catalyzed competitive polymerization after the initial oxidative coupling of furan and/or nucleophilic attack on the positively charged α-carbon by the dopant was considered to be the reason for the formation of nonconjugated structures [38]. However, the intensity of the absorption around 2900 cm^{-1} increases after cycling 100 times in dried acetonitrile (Fig. 46), whereas that of the absorption around 1700 cm^{-1} remains almost the same.

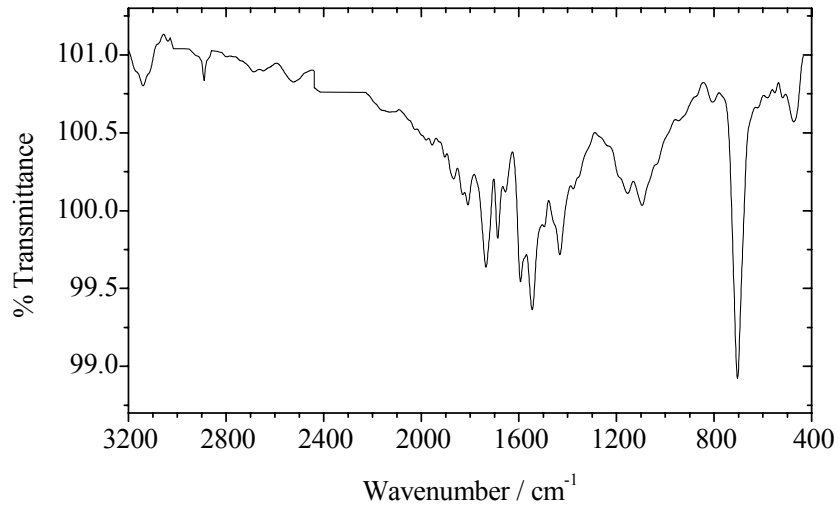

Fig. 46. FTIR spectra of copolymer cycled 100 times in dried MeCN solution deposited at $E_{Ag/AgCl}$ = 1.60 V in a BFEE + EE (ratio 1:2) solution containing 0.1 **M** furan, 0.1 **M** thiophene, and 0.1 **M** TBATFB.

When the copolymer is cycled 100 times in wet acetonitrile and ten times in aqueous solution FTIR spectra as shown in Fig. 47 and Fig. 48 respectively were obtained. The most significant feature is an increase of the intensity of the absorption located at 1650 cm^{-1} with an increase of water content in the solution. The intensity of the absorption around 1700 cm^{-1} remains weak when the copolymer is cycled in wet acetonitrile and increases sharply when the copolymer is cycled in aqueous solution.

It is well known that the degradation of conducting polymers is a complex process related to the nature of the conducting polymer itself, the synthesis conditions, the nature of the solvent, and the counter anion. The mechanism of degradation is not clear yet. Polypyrrole and polythiophene degradation proceeds mostly at electrode potentials positive to the range wherein deposition and reversible redox cycling take place, thus reversible redox processes and the irreversible degradation process can be distinguished clearly. For example, the degradation of polythiophene always takes place when the applied potential is scanned between 0 and 2.2 V in a monomer free electrolyte solution, whereas the reversible redox process happens around $E_{Ag/AgCl}$ = 1.0 V [161-163].

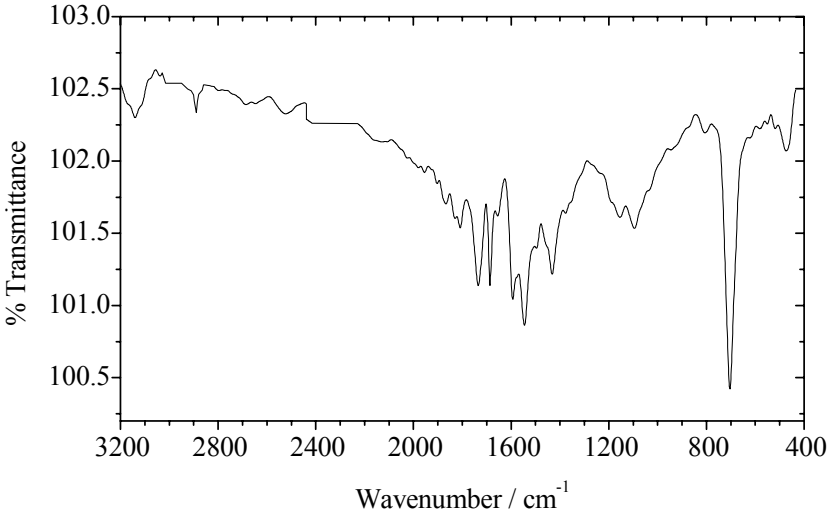

Fig. 47. FTIR spectra of copolymer cycled 100 times in a wet MeCN solution deposited at $E_{Ag/AgCl}$ = 1.60 V in a BFEE + EE (ratio 1:2) solution containing 0.1 **M** furan, 0.1 **M** thiophene, and 0.1 **M** TBATFB.

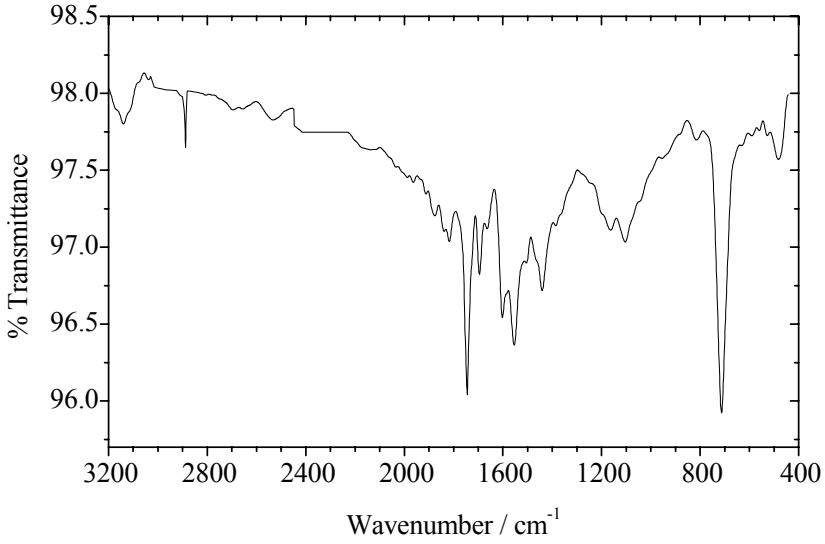

Fig. 48. FTIR spectra of copolymer cycled 10 times in aqueous solution deposited at $E_{Ag/AgCl}$ = 1.60 V in a BFEE + EE (ratio 1:2) solution containing 0.1 **M** furan, 0.1 **M** thiophene, and 0.1 **M** TBATFB.

For copolymers, as indicated in Fig. 46, it can be stated that when the copolymer is cycled in dried acetonitrile solution from $E_{Ag/AgCl}$ = 0 - 1.50 V, saturated C-H structures are produced in the copolymer chains. The degradation process takes place in the same potential range in which the reversible redox process occurs. This implies that the degradation of conjugated structures occurs when the copolymer is oxidized from its undoped state to the doped state. The loss of the electrochemical activity of copolymers in acetonitrile solutions might be related to the production of saturated C-H structures in the copolymer chains.

It is also certain that the absorptions around 1650 cm^{-1} and 1700 cm^{-1} reflect defects existing in the copolymer chains, the absorption around 1700 cm^{-1} presents the C=O stretching vibration. This observation was already reported for polyfuran and polythiophene [162, 122] and it was ascribed to the formation of carbonyl groups at the β-position of the rings with the oxidation of the polymer. In the absence of reports on furan-thiophene copolymer degradation, we speculate that this is also true for the copolymer. However, the assignment of the absorption at 1650 cm^{-1} is more difficult. It may be attributed to the stretching vibration of isolated C=C in the copolymer chain, but it has been reported that the carbonyl peak observed in oxo-pyrroline, the tautomeric form of 3-hydroxy-pyrrole, is at 1675 cm^{-1}[164]. It is more likely that this peak in polyfuran is the characteristic absorption of 3-hydroxyfuran. When polyfuran is reduced in ammonia, this peak is very strong [42]. However, when a furan-thiophene copolymer is electrochemically cycled in acetonitrile solution, this peak is weakened as shown in Fig. 46 and Fig. 47. It seems that the appearance of this absorption is also related to the attack of water molecules on the positively charged copolymer chains.

From these results, we may deduce that the degradation of furan-thiophene copolymers in dried acetonitrile solution mainly produces saturated C-H structures in the copolymer chains, whereas the degradation of copolymer in wet acetonitrile solution results in more C=O structures and fewer saturated C-H structures in the copolymer chains. When the copolymer is cycled in aqueous solution, this phenomenon becomes clearer. This implies that there may be two mechanisms of degradation of the copolymer: cross linking and attack by nucleophilic species such as water molecules [96]. In dry acetonitrile solution (acetonitrile is a weakly nucleophilic medium) the

overoxidation degradation of copolymer caused by the crosslinking mechanism prevails over the nucleophilic mechanism, which mainly results in the saturated C-H structures. In wet acetonitrile solution, the overoxidative degradation by the nucleophilic mechanism also takes place because of the extremely strong nucleophilic property of water molecules, resulting in the ketone structure. The possible byproducts of these degradation processes may be described as shown in Fig. 49(A, B).

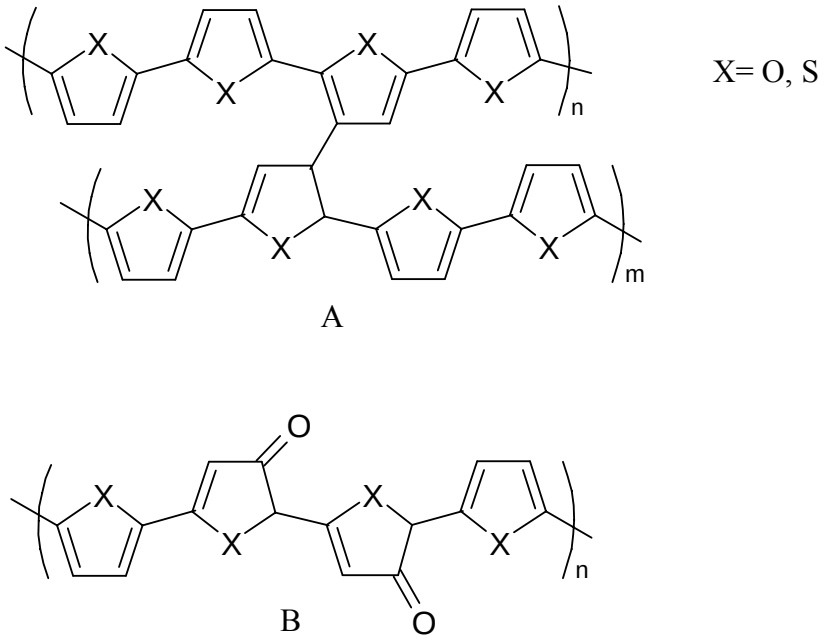

Fig. 49. Possible defects in the copolymer cycled in: (A) dry acetonitrile solution, (B) aqueous solution.

In the analysis of the degradation mechanisms, the overoxidation process happens concurrently with the oxidation process of the copolymer chains. That is, the attack of water molecules takes place at the same time at which the first electron is removed from the copolymer chains. This may be due to the low aromaticity of the furan ring in comparison with pyrrole and thiophene. The possible process may be described as shown in Fig. 50.

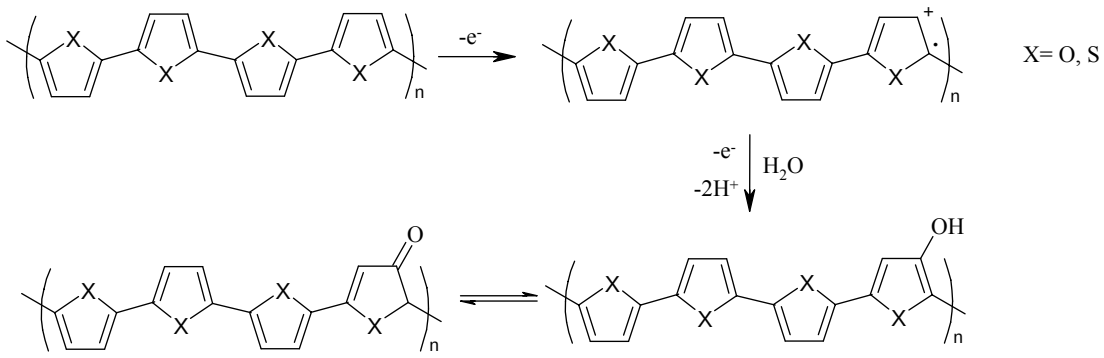

Fig. 50. Possible degradation mechanism of the copolymer cycled in aqueous solution.

3.5 The *In situ* Resonance Raman Spectroscopy

Homo- and Copolymer Films of Furan and Thiophene

Undoped polyfuran films exhibit a very strong visible absorption band, whose maximum is located at approximately 405 nm, related to a $\pi \rightarrow \pi^*$ electronic transition (see section 3.2.1). On the contrary, the doped species only show a very weak absorption band in this region. Therefore, when the polyfuran film is illuminated at 488 or 514.5 nm, the resonance effect enhances more specifically the Raman lines of undoped parts [45]. On the other hand, the band gap of polyfuran is approximately 535 nm, and thus the doped polyfuran films have a broad electronic absorption band with a maximum at approximately 685 nm [36]. In this region the undoped species show a very weak absorption. Thus, the 785 nm or 1064 nm [45] excitation enhance more specifically the Raman lines associated with the doped species.

The 488 nm or 514.5 nm excitation wavelength lies close to the region of the $\pi \rightarrow \pi^*$ absorption band (situated near 447 nm), a characteristic of the polythiophene neutral state [131], (see section 3.2.1). After doping the polymer, the 447 nm absorption band disappears and another band successively grows at 775 nm. Thus, when using 448 nm or 514.5 nm, the resonance conditions are favorable for the neutral polythiophene form, which gives a resonance Raman spectrum stronger than that of the oxidized polythiophene form [165, 166], and vice versa when using 785 nm or 1064 nm laser light [167, 168].

As a result, neither the 785 nor 514.5 nm laser beam is the appropriate Raman excitation source for studying the differences between the Raman spectra of doped and undoped of both polyfuran and polythiophene chains, because of their oxidation state selectivity [45, 165]. However, neither the neutral species nor the oxidized species of both polyfuran and polythiophene show strong absorption at 647.1 nm. Therefore, the special enhancement of Raman bands, relative to the neutral or oxidized species, can be greatly avoided. Thus, λ_0 = 647.1 nm beam is the best choice among the available wavelengths for studying the doping level dependence of the Raman spectra

and the bands resulting from the oxidized species of doped polyfuran and polythiophene, because the Raman spectrum obtained with λ_0 = 647.1 nm can give structural information on neutral and oxidized species simultaneously [92, 169-170].

The Raman spectrum of neutral polyfuran (Fig. 51) shows six major bands at 1592, 1534, 1281, 1021, 970, and 922 cm^{-1}. These bands are assigned to modes of pristine polyfuran [44]. Polyfuran symmetric C=C intraring stretching vibration and C-C intraring stretching vibration were observed at 1534 - 1592 cm^{-1} [171-172]. The band located at 1281 cm^{-1} is assigned to C-C and C-O ring stretching vibration [173-174], whereas C-H in-plane deformation mode is located around 1021 and 970 cm^{-1} [175-176]. The band located around 922 cm^{-1} is assigned to an in-plane ring deformation and C-O ring stretching vibration [43, 177]. Furthermore, another noticeable feature in the spectrum is a band around 922 and 850 cm^{-1}, which is a characteristic of 2-substituted five-membered heterocyclic compounds, suggesting that α-positions in the polymer are involved in the polymerization [178-179].

In this spectrum, several weak or shoulder bands are also present at 1471, 1372, 1139, and 1208 cm^{-1}. The two bands at 1471 and 1208 cm^{-1} are assigned to C-H out-of plane bending, while the bands at 1372 and 1139 cm^{-1} are related to C-C and C-O stretching vibrations respectively [173].

As previously reported in section 3.1.2, the oxidation potential of polyfuran in acetonitrile-based-electrolyte solution was measured to be $E_{Ag/AgCl}$ = ~ 0.50 V. Thus, at potentials of < 0.50 V, the overall features of the Raman spectra are similar to those of neutral polyfuran. With the increase of the applied potential, the Raman bands at 1471, 1372, 1139, and 1208 cm^{-1} are enhanced gradually, whereas the bands associated with the neutral species of polyfuran are still present. Therefore, it is reasonable to conclude that the enhanced bands are attributed to the oxidized species of polyfuran. At $E_{Ag/AgCl}$ = 1.0 V the entire spectrum is similar to that of doped polyfuran [45].

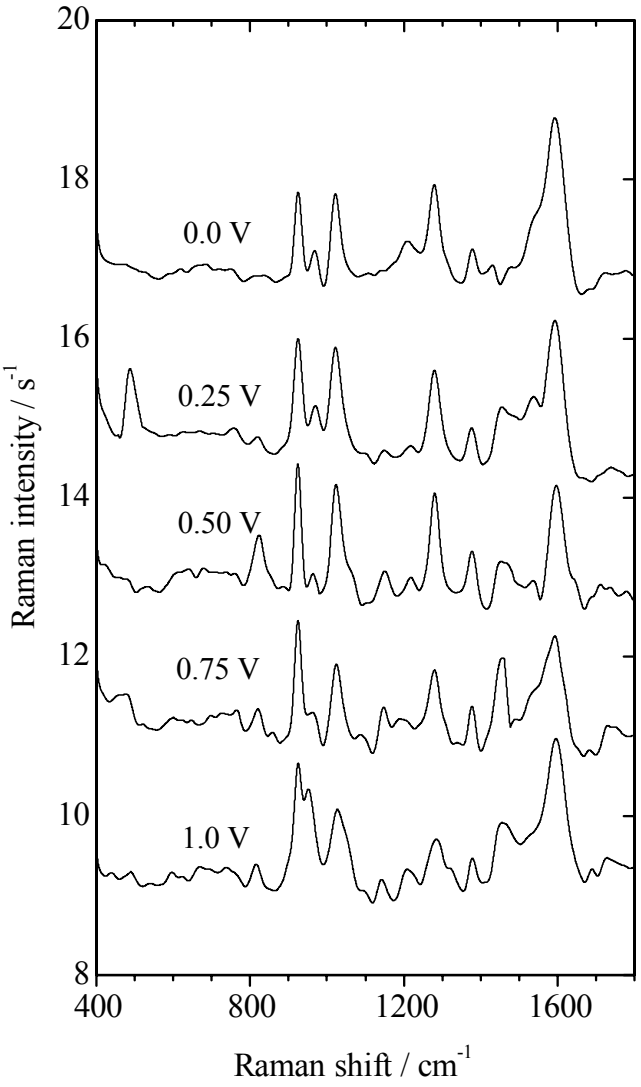

Fig. 51. *In situ* resonance Raman spectra recorded in a solution of acetonitrile + 0.1 **M** TBATFB of polyfuran deposited at $E_{Ag/AgCl}$ = 1.45 V from BFEE + EE (ratio 1:2) solution containing 0.1 **M** furan and 0.1 **M** TBATFB, spectra offset for clarity.

It seems from the *in situ* Raman spectra of polyfuran that most of the conjugation structures in polymer chains remain undestroyed. This may be due to the over-oxidation taking place only at the electrochemically active sites, which may be positively charged sites (polaron) in the chain, and not all the furan rings are defective.

Polyfuran shows a strong localization at the site of the electronic perturbation, i.e., the delocalization of the electrons along the polymer backbone is restricted to several furan rings, as a result, the defects of the electrochemically active sites may cause no considerable changes of the effective conjugation length [122].

In the *in situ* Raman spectra of polythiophene (Fig. 52) the most intense band at 1460 cm^{-1} assigned to the symmetric stretching vibration of the aromatic C=C ring bond [180-182] is of particular interest when studying the oxidation state and the conjugation length of the polymer chains [183]. We have observed a decrease in the intensity and a broadening of the band at higher wavenumbers (tail); weaker bands located therein have been assigned to the corresponding antisymmetric C=C stretching mode when the polythiophene passed from the neutral state to the oxidized form. This is related to changes in the conjugation length distribution in the polythiophene skeleton, since the broadness of the tail has been used as an argument for the presence of shorter polymer units and this tail increased with an increase in electrode potential [180, 99, 90]. Also it is obvious that a bathochromic shift of the C=C skeleton vibration from 1460 to 1443 cm^{-1} is associated with the increase of the applied potential, which is attributed to the symmetric stretching vibration of the C=C bond ring of radical cations (quinoid) [184-185].

The C-C intraring symmetric stretching vibration has been assigned to the band found at 1366 cm^{-1} [186-187]. Another interesting band observed at 1226 cm^{-1} in polythiophene has been attributed to the interring C-C stretching [188-189], whereas the band at 1153 cm^{-1} is assigned to the antisymmetric stretching vibration of C-C bonds [165]. The two bands at 926 and 827 cm^{-1} are assigned to C-H out-of plane deformations [190-191], while the bands at 754 and 706 cm^{-1} are related to C-S-C in-plane deformation [192-193]. Finally, the bands ascribable to the C-H in-plane deformation and in-plane ring deformation vibrations are observed at 1052 and 655 cm^{-1} respectively [194, 153].

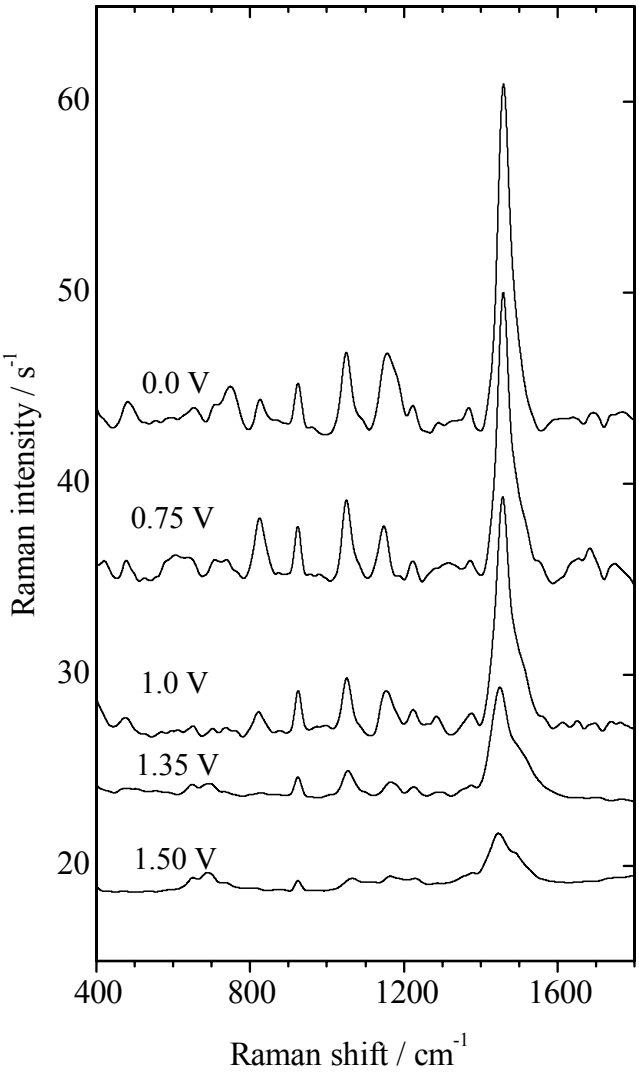

Fig. 52. *In situ* resonance Raman spectra recorded in a solution of acetonitrile + 0.1 **M** TBATFB of polythiophene deposited at $E_{Ag/AgCl}$ = 1.65 V from BFEE + EE (ratio 1:2) solution containing 0.1 **M** thiophene and 0.1 **M** TBATFB, spectra offset for clarity.

Further increase of the applied potential results in a blue shift and a relative intensity increase of the peaks at 1370, 1153 cm^{-1}, and the region between 1000 - 1050 cm^{-1} in comparison with the main band at 1460 cm^{-1}. It is obvious that the intensities strongly depend on the oxidation state of the polythiophene film. These bands can be assigned to defects and are considered to be related to the distorted conformation

around the interring single bonds [195], similar features are observed with doped polythiophene films [92, 182, 192]. The observed broadening and blue shift could be attributed to changes in the conjugation length distribution in the polythiophene chains. This conjugation length associated with π-electron delocalization is favored when the polymer rings are coplanar, owing to the maximum overlap of the C-C interring carbon pz orbitals. The oxidation produces distorted parts in the polymer, thus reducing the coplanarity of the rings and therefore the conjugation length [196].

Comparing the Raman spectra of neutral and oxidized forms of polythiophene, we can observe that the overall intensity decreased upon increasing the applied potential. This intensity difference is probably caused by a larger resonance enhancement of the reduced film, which is associated with a stronger UV-Vis absorption at the laser excitation wavelength. This means that the observed Raman bands originate from the undoped segments of the polymer which become less and less abundant with increasing doping level [192].

Raman band assignments of polyfuran and polythiophene at different electrode potentials are listed in Table 16.

Table 16. Raman band assignments of polyfuran and polythiophene at different electrode potentials, all figures in wavenumbers cm^{-1}.

Mode	Polyfuran					Polythiophene				
$E_{Ag/AgCl}$:	0.0 V	0.25 V	0.50 V	0.75 V	1.0 V	0.0 V	0.75 V	1.0 V	1.35 V	1.50 V
$\nu(C{=}C)_{ring}$	1592	1592	1596	1592	1596	1460	1457	1453	1450	1443
$\nu(C\text{-}C)_{ring}$	1534	1538	1534	1530	1520	-	-	-	-	-
ω(C-H)	1471	1450	1453	1453	1453	-	-	-	-	-
$\nu(C\text{-}C)$	1372	1376	1380	1380	1376	-	-	-	-	-
$\nu(C\text{-}C)_{ring}$	-	-	-	-	-	1370	1370	1376	1372	1376
$\nu(C\text{-}C)_{ring}$	1281	1278	1281	1280	1288	1225	1223	1221	1225	1222
ω(C-H)	1208	1208	1215	1200	1212	-	-	-	-	-
$\nu(C\text{-}O)_{ring}$	1139	1150	1149	1142	1139	-	-	-	-	-
$\nu(C\text{-}C)_{antisym}$	-	-	-	-	-	1153	1146	1158	1164	1168
δ(C-H)	1021	1021	1023	1030	1021	1052	1047	1050	1052	1062
δ(C-H)	970	970	968	974	952	-	-	-	-	-
γ(C-H)	-	-	-	-	-	926	922	923	920	923
$\nu(C\text{-}O)_{ring}$	922	923	926	922	922	-	-	-	-	-
δ(Ring)	920	919	926	922	923	-	-	-	-	-
γ(C-H)	850	835	820	856	813	827	823	821	813	816
δ(C-S-C)	-	-	-	-	-	754	740	736	730	732
δ(C-S-C)	-	-	-	-	-	706	705	703	696	687
$\delta(C\text{-}C)_{ring}$	-	-	-	-	-	655	650	651	647	651

δ, in-plane deformation; γ, out-of-plane deformation; ν, stretching; ω, out-of plane bending

Fig. 53 shows the Raman spectra of the homopolymers and copolymer in a solution of acetonitrile + 0.1 **M** TBATFB recorded at $E_{Ag/AgCl}$ = 0.0 V in their neutral states. The copolymer was prepared at $E_{Ag/AgCl}$ = 1.60 V in a BFEE + EE (ratio 1:2) solution containing 0.10 **M** furan and 0.10 **M** thiophene.

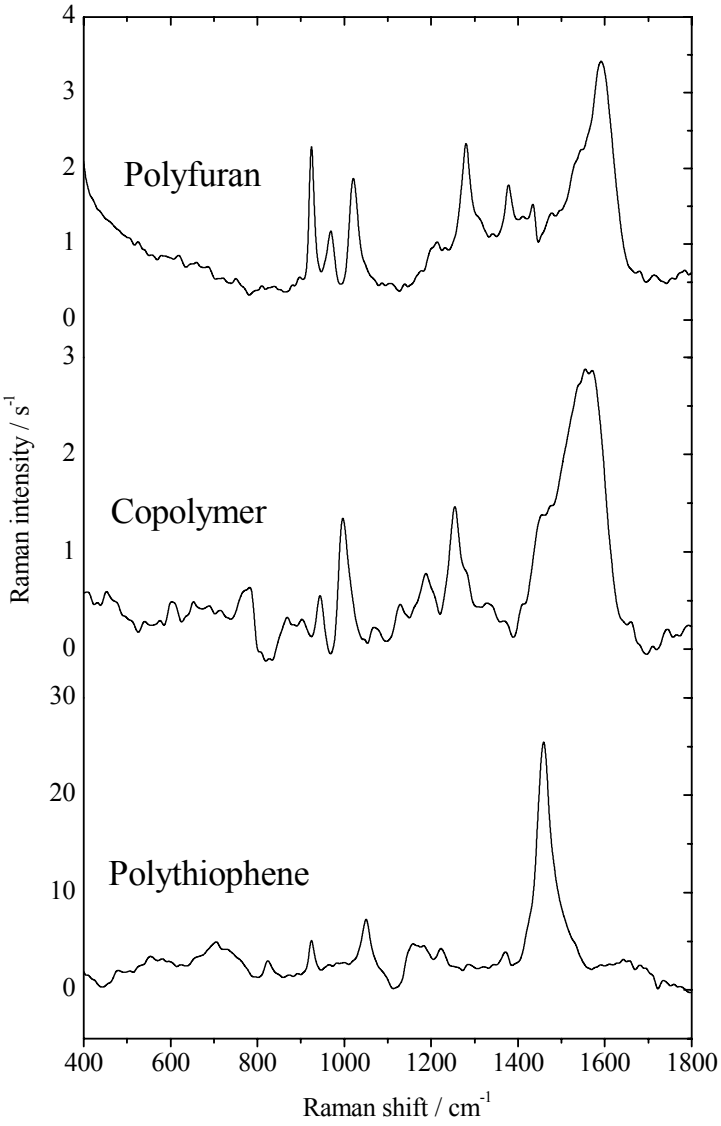

Fig. 53. Resonance Raman spectra recorded at $E_{Ag/AgCl}$ = 0.0 V in a solution of acetonitrile + 0.1 **M** TBATFB of polyfuran, polythiophene, and copolymer deposited at $E_{Ag/AgCl}$ = 1.60 V in a BFEE + EE (ratio 1:2) solution containing 0.10 **M** furan, 0.10 **M** thiophene, and 0.1 **M** TBATFB.

The copolymer has a broad band around 1562 cm^{-1} in the neutral state. This band corresponding to the symmetric C=C intraring stretching vibration suggests the coexistence of both long and short effective conjugated lengths due to furan and thiophene monomeric units. The greater the red shift of this peak, the longer the effective conjugation length of the conducting polymer [77]. The C-C intraring symmetric stretching vibration has been assigned to the band found at 1342 cm^{-1}. The two bands at 947 and 1000 cm^{-1} are assigned to C-H in-plane deformations, whereas the C-O ring stretching vibration band is located around 1127 cm^{-1}. The bands at 774 and 650 cm^{-1} are related to C-S-C in-plane deformation, while the band ascribable to the C-H out-of plane deformation is observed at 864 cm^{-1}. This indicates that α-α' coupling of radical cations has taken place during copolymerization. This is a characteristic of α-substituted five-membered heterocyclic compounds.
It is noticed that the features of the Raman spectra of the copolymer are between the features of the Raman spectra of both polyfuran and polythiophene, implying that oxidation of both monomers is possible and the copolymer chains may accordingly be composed of furan and thiophene units.

Raman spectra both at different polymerization potentials and with different thiophene concentrations have been investigated. Fig. 54 shows the Raman spectra recorded at $E_{Ag/AgCl}$ = 0.0 V of the copolymers obtained with electropolymerization solutions containing 0.1 **M** furan and 0.1 **M** thiophene at potentials ranging from $E_{Ag/AgCl}$ = 1.5 to 1.7 V. A remarkable characteristic of the Raman spectra is that the broad band which corresponds to the symmetric C=C intraring stretching vibration in the neutral state of the copolymers shifts to lower wave numbers, and the intensity of this band also increases with increasing the preparation potential of the copolymers. When prepared at $E_{Ag/AgCl}$ = 1.5 V, the copolymer shows a broad band around 1574 cm^{-1}, which is close to the position of the respective band of pure polyfuran. When prepared at $E_{Ag/AgCl}$ = 1.7 V the copolymer shows a band around 1554 cm^{-1}. Furthermore, the intensity of the two bands corresponding to the C-H in-plane deformation located around 927 - 954 cm^{-1} and 1000 - 1061 cm^{-1} increases with increasing the preparation potential of the copolymers. By increasing the preparation potential, the band attributed to C-C ring stretching vibration shifts to lower wavenumbers by 27 cm^{-1} (see Table 17) and moves closer to that of pure polythiophene. In addition, the intensity of this band is also enhanced with an increasing polymerization potential.

This indicates that more thiophene units are incorporated into the copolymer chains with an increasing preparation potential.

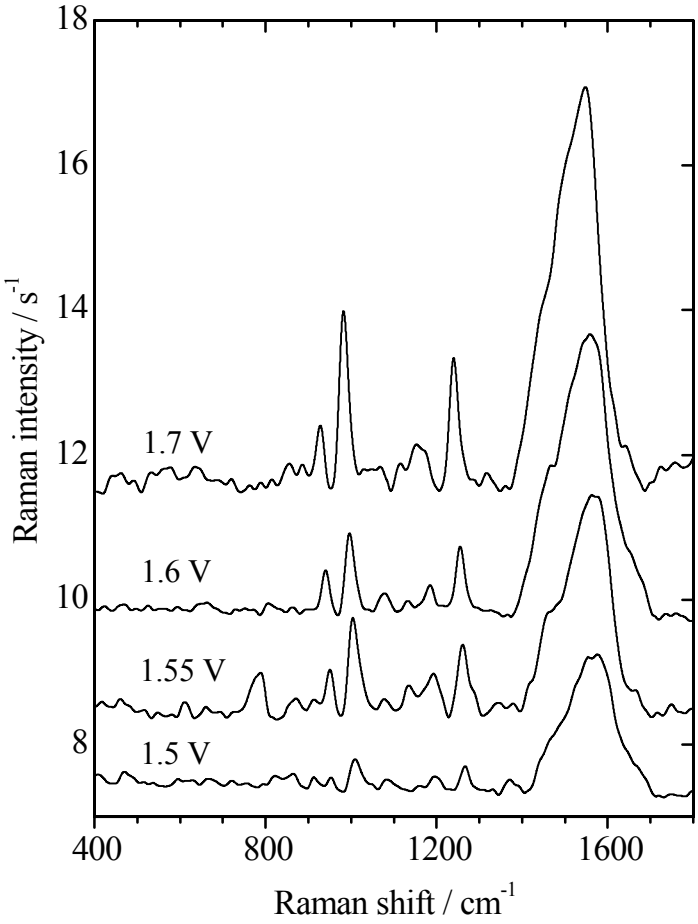

Fig. 54. Resonance Raman spectra recorded at $E_{Ag/AgCl}$ = 0.0 V in a solution of acetonitrile + 0.1 **M** TBATFB of (a) copolymers deposited at $E_{Ag/AgCl}$ = 1.5- 1.7 V in a BFEE + EE (ratio 1:2) solution containing furan/thiophene (mole ratio 1:1), spectra offset for clarity.

Raman band assignments of copolymer deposited at $E_{Ag/AgCl}$ = 1.5 - 1.7 V in a solution containing 0.1 **M** furan and 0.1 **M** thiophene recorded at $E_{Ag/AgCl}$ = 0.0 V are listed in Table 17.

Table 17. Raman band assignments of copolymer deposited at $E_{Ag/AgCl}$ = 1.5 - 1.7 V in a solution containing 0.1 **M** furan and 0.1 **M** thiophene, all figures in wavenumbers cm^{-1}.

Mode	1.5 V				1.55 V				1.70 V			
	$E_{Ag/AgCl}$ = 0.0 V	$E_{Ag/AgCl}$ = 0.50 V	$E_{Ag/AgCl}$ = 1.0 V	$E_{Ag/AgCl}$ = 1.25 V	$E_{Ag/AgCl}$ = 0.0 V	$E_{Ag/AgCl}$ = 0.50 V	$E_{Ag/AgCl}$ = 1.0 V	$E_{Ag/AgCl}$ = 1.25 V	$E_{Ag/AgCl}$ = 0.0 V	$E_{Ag/AgCl}$ = 0.75 V	$E_{Ag/AgCl}$ = 1.0 V	$E_{Ag/AgCl}$= 1.25 V
$\nu_{(C=C)ring}$	1574	1575	1573	1572	1569	1570	1568	1568	1554	1554	1552	1554
$\nu_{(C-C)ring}$	1523	1527	1520	1540	1511	1517	1529	1523	1528	1537	1535	1532
$\omega_{(C-H)}$	1468	1460	1460	1488	1464	1455	1458	1462	1438	1445	1436	1445
$\nu_{(C-C)}$	1341	1325	1326	1357	1336	1355	1337	1388	1300	1349	1328	1346
$\nu_{(C-C)}$	1267	1268	1275	1280	1259	1263	1263	1264	1240	1250	1241	1244
$\omega_{(C-H)}$	1197	1191	1200	1203	1188	1193	1193	1200	1171	1178	1169	1154
$\nu_{(C-O)ring}$	1145	1120	1018	1123	1134	1141	1110	1074	1115	1139	1112	1074
$\delta_{(C-H)}$	1013	1012	-	1039	1024	1087	1007	1014	1061	1062	1056	1029
$\delta_{(C-H)}$	954	954	964	950	927	952	946	934	929	936	967	954
$\gamma_{(C-H)}$	879	874	877	879	878	910	863	807	843	847	838	847
$\delta_{(C-S-C)}$	757	752	720	777	743	776	716	730	756	739	733	763
$\delta_{(C-S-C)}$	720	710	700	650	670	693	620	658	672	680	673	676

δ, in-plane deformation; γ, out-of-plane deformation; ν, stretching; ω, out-of plane bending.

When the furan/thiophene feed ratio is changed from 1:1 to 4:1 (0.1 **M**/ 0.025 **M**) and to 8:1 (0.1 **M**/ 0.0125 **M**) Raman spectra as shown in Fig. 55 are obtained.

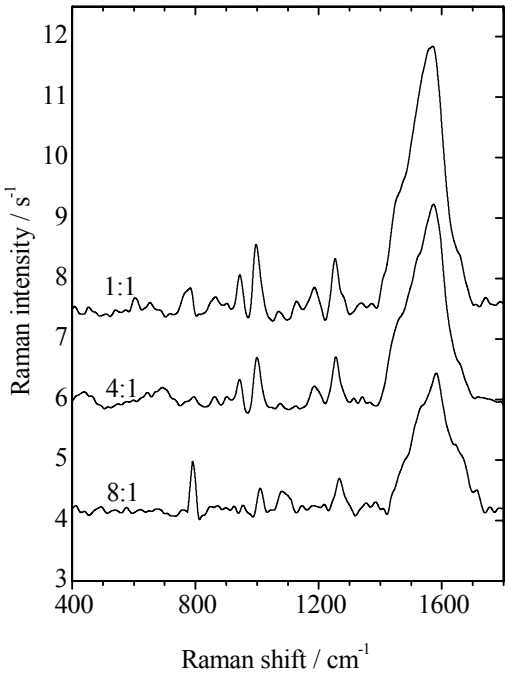

Fig. 55. Resonance Raman spectra recorded at $E_{Ag/AgCl}$ = 0.0 V in a solution of acetonitrile + 0.1 **M** TBATFB of copolymers deposited at $E_{Ag/AgCl}$ = 1.6 V in a BFEE + EE (ratio 1:2) solution containing furan/thiophene (mole ratio 1:1, 4:1, and 8:1); spectra offset for clarity.

The same interesting features still exist, i.e. the stretching vibration band which is assigned to the C=C stretching mode and which is considered as an indicator of effective conjugation length shifts to lower wavenumbers as the concentration of thiophene increases in the polymerization solutions. The band which is attributed to C-C ring stretching vibration shifts to lower wavenumbers by 11 cm^{-1} and becomes closer to that of pure polythiophene. In addition, its intensity also increases with an increasing thiophene concentration. These results show that the number of thiophene units in these copolymer chains increases with an increasing thiophene concentration in the polymerization solutions [197]. Raman band assignments of the copolymers prepared at $E_{Ag/AgCl}$ = 1.6 V with different thiophene concentrations are listed in Table 18.

Table 18. Raman band assignments of copolymer deposited at $E_{Ag/AgCl}$ = 1.6 V with different mole ratios, all figures in wavenumbers cm^{-1}.

Mode	1:1[a]				4:1[a]				8:1[a]			
	$E_{Ag/AgCl}$ = 0.0 V	$E_{Ag/AgCl}$ = 0.75 V	$E_{Ag/AgCl}$ = 1.15 V	$E_{Ag/AgCl}$ = 1.50 V	$E_{Ag/AgCl}$ = 0.0 V	$E_{Ag/AgCl}$ = 0.45 V	$E_{Ag/AgCl}$ = 0.90 V	$E_{Ag/AgCl}$ = 1.35 V	$E_{Ag/AgCl}$ = 0.0 V	$E_{Ag/AgCl}$ = 0.50 V	$E_{Ag/AgCl}$ = 0.75 V	$E_{Ag/AgCl}$ = 1.25 V
$\nu(C=C)_{ring}$	1562	1561	1560	1562	1570	1571	1570	1568	1580	1580	1577	1579
$\nu(C-C)_{ring}$	1510	1514	1511	1514	1512	1516	1514	1507	1526	1523	1506	1512
ω(C-H)	1453	1452	1467	1466	1445	1449	1445	1443	1464	1471	1474	1461
ν(C-C)	1342	1344	1346	1338	1346	1308	1326	1334	1356	1353	1346	1359
$\nu(C-C)_{ring}$	1252	1254	1262	1261	1255	1257	1256	1251	1263	1269	1257	1272
ω(C-H)	1185	1189	1186	1184	1186	1174	1179	1177	1144	1196	1211	1198
$\nu(C-O)_{ring}$	1127	1126	1100	1082	1128	1116	1125	1117	1083	1144	1180	1147
δ(C-H)	1000	1074	1024	1005	1027	1068	1024	1050	1024	1040	1035	1020
δ(C-H)	947	963	945	935	967	969	959	950	967	953	950	969
γ(C-H)	864	853	859	867	855	879	883	882	886	828	867	860
δ(C-S-C)	774	722	764	723	723	752	739	710	764	757	787	787
δ(C-S-C)	650	639	665	684	662	703	649	642	639	700	694	690

[a]furan/thiophene mole ratio; δ, in-plane deformation; γ, out-of-plane deformation; ν, stretching; ω, out-of plane bending.

The Raman spectra of the copolymers are more complex than those of pure polyfuran and polythiophene, making the assignment difficult. This complexity may be due to the change of effective conjugation length and the more complex chemical environment of each unit encountered in the copolymer chains. However, the *in situ* Raman spectra of the copolymers are reminiscent of the *in situ* Raman spectra of polyfuran and polythiophene; see Fig. 56. The copolymers have a broad band in the range of 1544-1588 cm^{-1} in the neutral state, which corresponds to the symmetric C=C intraring stretching vibration indicating the coexistence of both long and short effective conjugation lengths due to furan and thiophene monomeric units. We observe a decrease in the intensity and a broadening of this band at higher wavenumbers with an increase of the applied potential. The overall intensity of the spectra decreases upon increasing the applied potential.

The results demonstrate that the Raman spectra of the copolymers in the doped state are different from those of neutral copolymers. Bands related to the oxidized and thus distorted species were identified with the *in situ* Raman spectroscopy.

Raman band assignments of copolymers deposited at $E_{Ag/AgCl}$ = 1.5 - 1.7 V in a solution containing furan/thiophene (mole ratio 4:1, 8:1) are listed in Table 19 and 20 respectively.

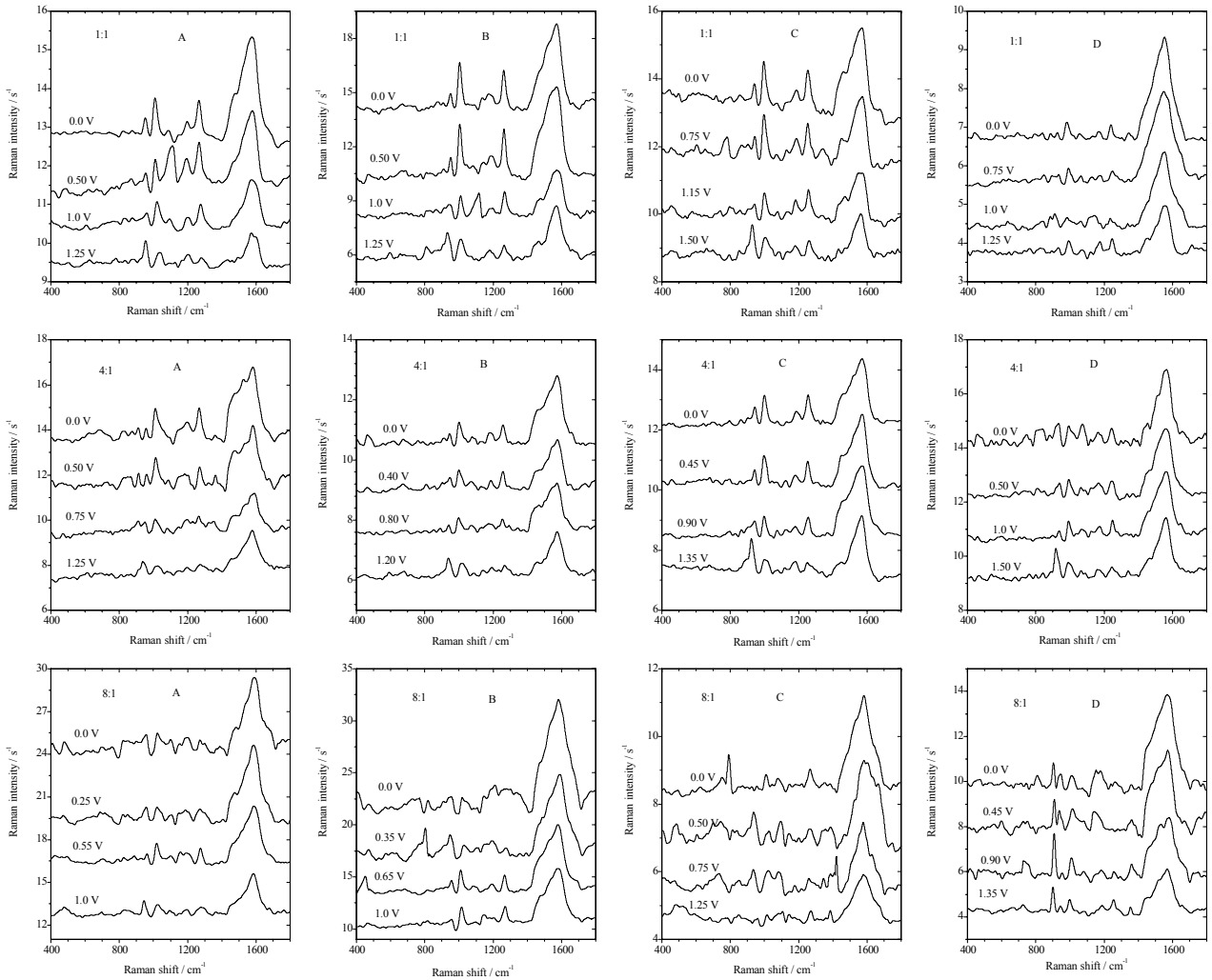

Fig. 56. Resonance Raman spectra recorded at different electrode potentials in a solution of acetonitrile + 0.1 **M** TBATFB of copolymers deposited at $E_{Ag/AgCl}$ = (A) 1.5 V, (B) 1.55 V, (C) 1.6 V, (D) 1.7 V in a BFEE + EE (ratio 1:2) solution containing furan/thiophene (mole ratio 1:1, 4:1, and 8:1), and 0.1 **M** TBATFB; spectra offset for clarity.

Table 18. Raman band assignments of copolymer deposited at $E_{Ag/AgCl}$ = 1.5 - 1.7 V in a solution containing furan/thiophene (mole ratio 4:1), all figures in wavenumbers cm^{-1}.

Mode	1.5 V				1.55 V				1.70 V			
	$E_{Ag/AgCl}$ = 0.0 V	$E_{Ag/AgCl}$ = 0.50 V	$E_{Ag/AgCl}$ = 0.75 V	$E_{Ag/AgCl}$ = 1.25 V	$E_{Ag/AgCl}$ = 0.0 V	$E_{Ag/AgCl}$ = 0.40 V	$E_{Ag/AgCl}$ = 0.80 V	$E_{Ag/AgCl}$ = 1.20 V	$E_{Ag/AgCl}$ = 0.0 V	$E_{Ag/AgCl}$ = 0.50 V	$E_{Ag/AgCl}$ = 1.0 V	$E_{Ag/AgCl}$= 1.50 V
$\nu_{(C=C)ring}$	1580	1581	1578	1579	1574	1575	1572	1574	1562	1562	1560	1561
$\nu_{(C-C)ring}$	1536	1534	1528	1524	1519	1508	1502	1536	1512	1501	1505	1503
$\omega_{(C-H)}$	1452	1464	1458	1453	1455	1444	1447	1448	1457	1452	1447	1456
$\nu_{(C-C)}$	1358	1360	1348	1369	1347	1358	1347	1364	1324	1335	1307	1343
$\nu_{(C-C)}$	1265	1270	1268	1270	1260	1258	1255	1268	1247	1251	1249	1247
$\omega_{(C-H)}$	1177	1178	1193	1194	1178	1190	1170	1189	1166	1166	1176	1165
$\nu_{(C-O)ring}$	1105	1097	1138	1130	1137	1127	1077	1139	1072	1066	1073	1066
$\delta_{(C-H)}$	1021	1021	1027	1028	1026	1071	1017	1023	1026	1020	1023	1029
$\delta_{(C-H)}$	970	960	963	951	970	973	965	947	968	939	965	953
$\gamma_{(C-H)}$	887	867	823	825	857	877	881	805	874	834	830	872
$\delta_{(C-S-C)}$	759	727	726	773	781	809	781	735	778	761	758	763
$\delta_{(C-S-C)}$	698	671	680	668	688	697	714	691	705	700	645	703

δ, in-plane deformation; γ, out-of-plane deformation; ν, stretching; ω, out-of plane bending.

Table 19. Raman band assignments of copolymer deposited at $E_{Ag/AgCl}$ = 1.5 - 1.7 V in a solution containing furan/thiophene (mole ratio 8:1), all figures in wavenumbers cm^{-1}.

Mode	1.5 V				1.55 V				1.70 V			
	$E_{Ag/AgCl}$ = 0.0 V	$E_{Ag/AgCl}$ = 0.25 V	$E_{Ag/AgCl}$ = 0.55 V	$E_{Ag/AgCl}$ = 1.0 V	$E_{Ag/AgCl}$ = 0.0 V	$E_{Ag/AgCl}$ = 0.35 V	$E_{Ag/AgCl}$ = 0.65 V	$E_{Ag/AgCl}$ = 1.0 V	$E_{Ag/AgCl}$ = 0.0 V	$E_{Ag/AgCl}$ = 0.45 V	$E_{Ag/AgCl}$ = 0.90 V	$E_{Ag/AgCl}$= 1.35 V
$\nu_{(C=C)ring}$	1588	1587	1586	1585	1584	1584	1580	1581	1574	1572	1572	1570
$\nu_{(C-C)ring}$	1536	1537	1508	1501	1523	1520	1519	1520	1507	1510	1528	1515
$\omega_{(C-H)}$	1469	1459	1455	1451	1468	1462	1455	1460	1446	1461	1447	1445
$\nu_{(C-C)}$	1364	1366	1365	1361	1369	1353	1362	1350	1359	1362	1360	1357
$\nu_{(C-C)}$	1275	1270	1278	1285	1214	1275	1265	1272	1260	1277	1255	1256
$\omega_{(C-H)}$	1199	1182	1196	1198	1189	1192	1195	1208	1184	1123	1185	1188
$\nu_{(C-O)ring}$	1147	1101	1158	1099	1147	1144	1088	1147	1155	1085	1083	1084
$\delta_{(C-H)}$	1098	1032	1020	1025	1026	1033	1023	1026	1029	1026	1020	1023
$\delta_{(C-H)}$	968	965	968	950	969	956	966	965	968	950	968	970
$\gamma_{(C-H)}$	833	831	883	851	878	862	850	820	823	846	851	886
$\delta_{(C-S-C)}$	769	730	796	750	782	765	759	765	761	735	755	752
$\delta_{(C-S-C)}$	706	694	709	703	682	637	650	655	677	700	644	691

δ, in-plane deformation; γ, out-of-plane deformation; ν, stretching; ω, out-of plane bending.

Homo- and Copolymer Films of Furan and 3-Chlorothiophene

As previously reported in this section, laser light with λ_0 = 647.1 nm is the best choice among the available wavelengths for studying the doping level dependence of the Raman spectra and the bands resulting from the oxidized species of doped polyfuran and polythiophenes. The *in situ* resonance Raman spectra of polyfuran and poly(3-chlorothiophene) are displayed for reference in Fig. 57.

The Raman spectrum of neutral polyfuran shows six major bands at 1590, 1532, 1283, 1020, 975, and 9202 cm^{-1}. These bands are assigned to modes of pristine polyfuran (see Table 20). Polyfuran symmetric C=C intraring stretching vibration and C-C intraring stretching vibration were observed at 1532 - 1590 cm^{-1}. The band located at 1283 cm^{-1} is assigned to C-C and C-O ring stretching vibration, whereas C-H in-plane deformation modes are located around 1020 and 975 cm^{-1}. The band located around 920 cm^{-1} is assigned to an in-plane ring deformation and C-O ring stretching vibration. Furthermore, another noticeable feature in the spectrum is a band around 920 and 850 cm^{-1}, which is characteristic of 2-substituted five-membered heterocyclic compounds, suggesting that α-positions in the polymer are involved in the polymerization. These results are totally in agreement with our previous polyfuran prepared in this project (see page 94).

In this spectrum, several weak bands or shoulders are also present at 1470, 1370, 1140, and 1210 cm^{-1}. The two bands at 1470 and 1210 cm^{-1} are assigned to C-H out-of-plane bending, while the bands at 1370 and 1140 cm^{-1} are related to C-C and C-O stretching vibrations respectively. The oxidation potential of polyfuran in acetonitrile-based electrolyte solution is measured to be $E_{Ag/AgCl}$ = ~ 0.57 V (see page 43). Thus, at potentials < 0.57 V, the overall features of the Raman spectra are similar to those of neutral polyfuran. With the increase of the applied potential, the Raman bands at 1470, 1370, 1140, and 1210 cm^{-1} are enhanced gradually, whereas the bands associated with the neutral species of polyfuran are still present. Therefore, it is reasonable to conclude that the enhanced bands are caused by the oxidized species of polyfuran. At $E_{Ag/AgCl}$ = 0.8 V the entire spectrum is similar to that of doped polyfuran.

The *in situ* Raman spectra of poly(3-chlorothiophene) show a weak fluorescence background and a high signal-to-noise ratio. The band around 1400-1500 cm^{-1} is a common feature of Raman spectra of aromatic and heteroaromatic systems; it is always strong and dominates the entire Raman spectrum [198]. As can be seen in Fig. 57(B), the most intense band is located at approximately 1468 cm^{-1} and is assigned to the totally symmetric in-plane C=C vibration of bulk thiophene rings spread over the whole polymer chain. A decrease in the intensity and a broadening of the band at higher wavenumbers (tail) is observed; weaker bands located there have been assigned to the corresponding asymmetric C=C stretching mode when the polymer film passed from the neutral state to the oxidized form. This is related to changes in the conjugation length distribution in the poly(3-chlorothiophene) skeleton, since the broadness of the tail has been used as an argument for the presence of shorter polymer units and this tail increased with an increase in the electrode potential. The bathochromic shift of the C=C skeleton vibration from 1468 to 1450 cm^{-1} (see Table 20) is associated with the increase of the applied potential, which is attributed to the symmetric stretching vibration of C=C bond ring of radical cations (quinoid). The band at 1357 cm^{-1} in the spectrum of neutral state is also found at 1376 cm^{-1} in the spectrum of oxidized state and is assigned to the C-C intraring symmetric stretching vibration. The well defined scattering near 1157 cm^{-1} is associated with the asymmetric stretching vibration of C-C bonds. Upon doping, this band shifts upwards to 1162 cm^{-1}. The two bands at 927 and 827 cm^{-1} are assigned to C-H out-of plane deformations, while the bands at 754 and 710 cm^{-1} are related to C-S-C in-plane deformation. Finally, the band ascribable to the C-Cl in-plane deformation observed at 439 cm^{-1} remains basically unchanged when the neutral polymer is oxidized [70, 71].

Comparing the Raman spectra of neutral and oxidized forms of poly(3-chlorothiophene), we can observe that the overall intensity decreased upon increasing the applied potential. This intensity difference is probably caused by a larger resonance enhancement of the reduced film, which is associated with a stronger UV-Vis absorption at the laser excitation wavelength. This means that the observed Raman bands are caused by the undoped segments of the polymer which become less and less abundant with increasing doping level. These results are totally compatible with our previous polythiophene prepared in this project (see page 98).

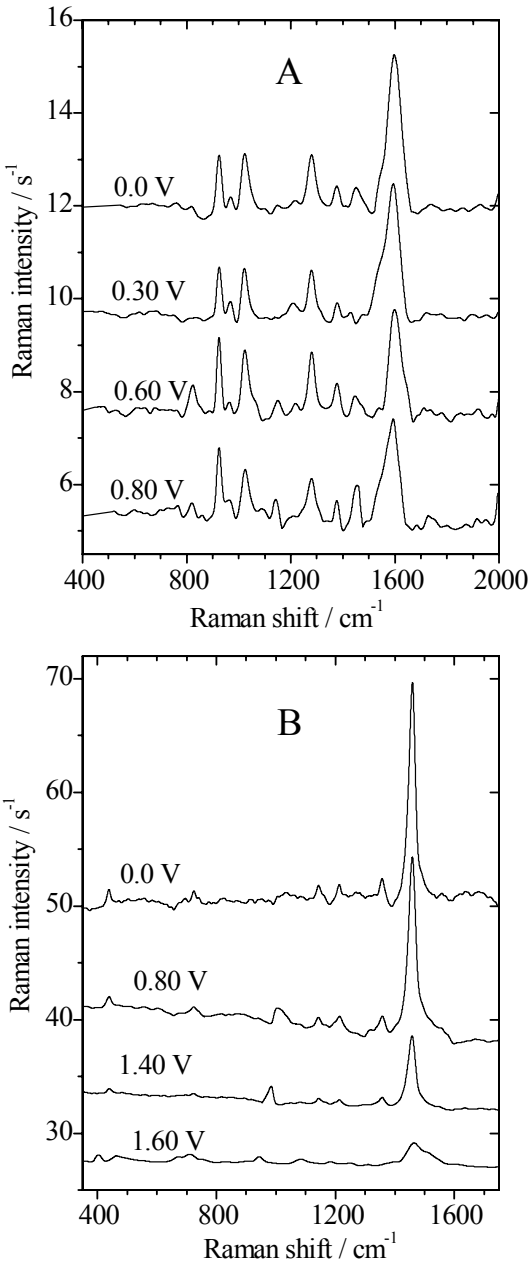

Fig. 57. *In situ* resonance Raman spectra recorded in a solution of acetonitrile + 0.1 **M** TBATFB of (A) polyfuran deposited at $E_{Ag/AgCl}$ = 1.35 V from BFEE + EE (ratio 1:2) and TFA (10 % by volume) containing 0.1 **M** furan, (B) poly(3-chlorothiophene) deposited at $E_{Ag/AgCl}$ = 1.55 V from BFEE + EE (ratio 1:2) and TFA (10 % by volume) containing 0.1 **M** 3-chlorothiophene, spectra off-set for clarity.

Table 20. Raman band assignments of polyfuran and poly(3-chlorothiophene) at different electrode potentials, all figures in wavenumbers cm^{-1}.

Mode	Polyfuran				Poly(3-chlorothiophene)			
$E_{Ag/AgCl}$:	0.0 V	0.30 V	0.60 V	0.80 V	0.0 V	0.80 V	1.40 V	1.60 V
$\nu(C=C)_{ring}$	1590	1593	1597	1590	1468	1458	1453	1450
$\nu(C-C)_{ring}$	1532	1540	1534	1532	-	-	-	-
$\omega(C-H)$	1470	1455	1453	1450	-	-	-	-
$\nu(C-C)$	1370	1376	1380	1383	-	-	-	-
$\nu(C-C)_{ring}$	-	-	-	-	1373	1370	1376	1378
$\nu(C-C)_{ring}$	1283	1278	1280	1280	1220	1223	1224	1225
$\omega(C-H)$	1210	1208	1215	1202	-	-	-	-
$\nu(C-O)_{ring}$	1140	1152	1149	1142	-	-	-	-
$\nu(C-C)_{antisym}$	-	-	-	-	1157	1150	1158	1162
$\delta(C-H)$	1020	1021	1025	1030	1050	1047	1051	1052
$\delta(C-H)$	975	970	968	973	-	-	-	-
$\gamma(C-H)$	-	-	-	-	927	925	923	926
$\nu(C-O)_{ring}$	920	923	924	922	-	-	-	-
$\delta(Ring)$	918	919	926	923	-	-	-	-
$\gamma(C-H)$	850	835	830	856	827	823	821	813
$\delta(C-S-C)$	-	-	-	-	754	740	736	730
$\delta(C-S-C)$	-	-	-	-	710	707	703	700
$\delta(C-C)_{ring}$	-	-	-	-	656	650	650	647
$\delta(C-Cl)$	-	-	-	-	439	437	437	439

δ: in-plane deformation; γ: out-of-plane deformation; ν: stretching; ω: out-of-plane bending.

Raman spectra of copolymers obtained both at different polymerization potentials and with different thiophene concentrations have been investigated. Fig. 58(A) shows that the copolymer has a broad band around 1552 cm^{-1} in the neutral state. This band corresponding to the symmetric C=C intraring stretching vibration suggests the coexistence of both long and short effective conjugated lengths due to furan and 3-chlorothiophene monomeric units. The greater the red shift of this peak, the longer the effective conjugation length of the conducting polymer. The C-C intraring symmetric stretching vibration has been assigned to the band found at 1315 cm^{-1}. The two bands at 930 and 1055 cm^{-1} are assigned to C-H in-plane deformations, whereas the C-O ring stretching vibration band is located around 1121 cm^{-1}. The bands at 756 and 662 cm^{-1} are related to C-S-C in-plane deformation, while the band ascribable to the C-H out-of plane deformation is observed at 843 cm^{-1}. This indicates that α-α' coupling of radical cations has taken place during copolymerization. This is a characteristic of α-substituted five-membered heterocyclic compounds. It is noticed that the features of the Raman spectra of the copolymer are between the features of the Raman spectra of both homopolymers, implying that oxidation of both monomers is possible and the copolymer chains may accordingly be composed of furan and 3-chlorothiophene units.

Comparing Fig. 58(A) with Fig. 58(B) one can notice that the broad band which corresponds to the symmetric C=C intraring stretching vibration in the neutral state of the copolymers shifts to lower wave numbers and the intensity of this band also increases with increasing the preparation potential of the copolymers. When prepared at $E_{Ag/AgCl}$ = 1.5 V, the copolymer shows a broad band around 1572 cm^{-1}, which is close to the position of the respective band of pure polyfuran. When prepared at $E_{Ag/AgCl}$ = 1.7 V the copolymer shows a band around 1552 cm^{-1}. By increasing the preparation potential, the band attributed to C-C ring stretching vibration shifts to lower wavenumbers by 20 cm^{-1} and moves closer to that of pure poly(3-chlorothiophene). Furthermore, the band corresponding to the C-Cl in-plane deformation observed at 450 cm^{-1} shifts downwards to 441 cm^{-1} (see Table 21). In addition, the intensity of this band is also enhanced with an increasing polymerization potential. This indicates that more 3-chlorothiophene units are incorporated into the copolymer chains with an increasing preparation potential.

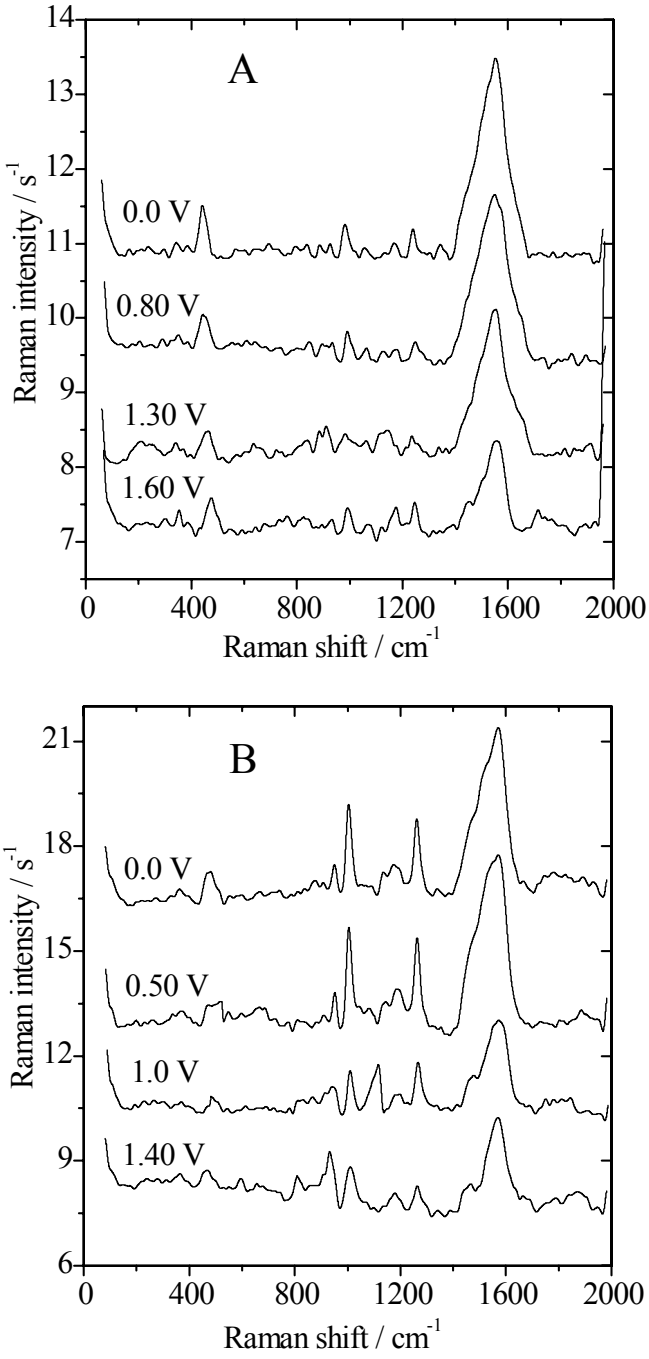

Fig. 58. *In situ* resonance Raman spectra recorded in a solution of acetonitrile + 0.1 **M** TBATFB of copolymers deposited at $E_{Ag/AgCl}$ (A) 1.7 V, (B) 1.5 V in a BFEE + EE (ratio 1:2) and TFA (10 % by volume) containing furan/3-chlorothiophene (mole ratio 1:1)

Table 21. Raman band assignments of copolymers deposited at $E_{Ag/AgCl}$ = 1.5 and 1.7 V in a solution containing 0.1 **M** furan and 0.1 **M** 3-chlorothiophene, all figures in wavenumbers cm^{-1}.

Mode	**1.50 V**				**1.70 V**			
$E_{Ag/AgCl}$:	0.0 V	0.50 V	1.0 V	1.40 V	0.0 V	0.80 V	1.30 V	1.60 V
$\nu(C=C)_{ring}$	1572	1570	1568	1570	1552	1554	1550	1550
$\nu(C-C)_{ring}$	1514	1517	1527	1525	1525	1530	1531	1532
$\omega(C-H)$	1460	1455	1458	1460	1442	1445	1436	1438
$\nu(C-C)$	1340	1355	1335	1388	1315	1330	1328	1332
$\nu(C-C)_{ring}$	1261	1263	1260	1264	1241	1248	1239	1242
$\omega(C-H)$	1190	1193	1195	1204	1176	1172	1169	1158
$\nu(C-O)_{ring}$	1130	1121	1110	1084	1121	1133	1112	1084
$\delta(C-H)$	1032	1050	1007	1012	1055	1060	1056	1039
$\delta(C-H)$	932	950	946	937	930	936	960	954
$\gamma(C-H)$	878	870	863	817	843	847	838	847
$\delta(C-S-C)$	750	776	732	735	756	739	733	763
$\delta(C-S-C)$	670	693	640	658	662	670	663	666
$\delta(C-Cl)$	450	449	449	450	441	444	440	445

δ: in-plane deformation; γ: out-of-plane deformation; ν stretching; ω: out-of-plane bending.

When the furan/3-chlorothiophene feed ratio is changed from 1:1 to 8:1 (0.1 **M**/ 0.0125 **M**) Raman spectra as shown in Fig. 59(A-B) are obtained. The same previous interesting features still exist, i.e. the C=C stretching vibration which is considered as an indicator of effective conjugation length shifts to lower wavenumbers as the concentration of 3-chlorothiophene increases in the polymerization solutions. The band which is attributed to the C-C ring stretching vibration shifts to lower values by 9 cm^{-1} closer to that of pure poly(3-chlorothiophene), furthermore the mode associated with the C-Cl bond appears at 441 cm^{-1} when the copolymer is prepared at a 1:1 monomer feed ratio (see Table 22). These results show that the number of 3-chlorothiophene

units in these copolymer chains increases with an increasing 3-chlorothiophene concentration in the polymerization solutions.

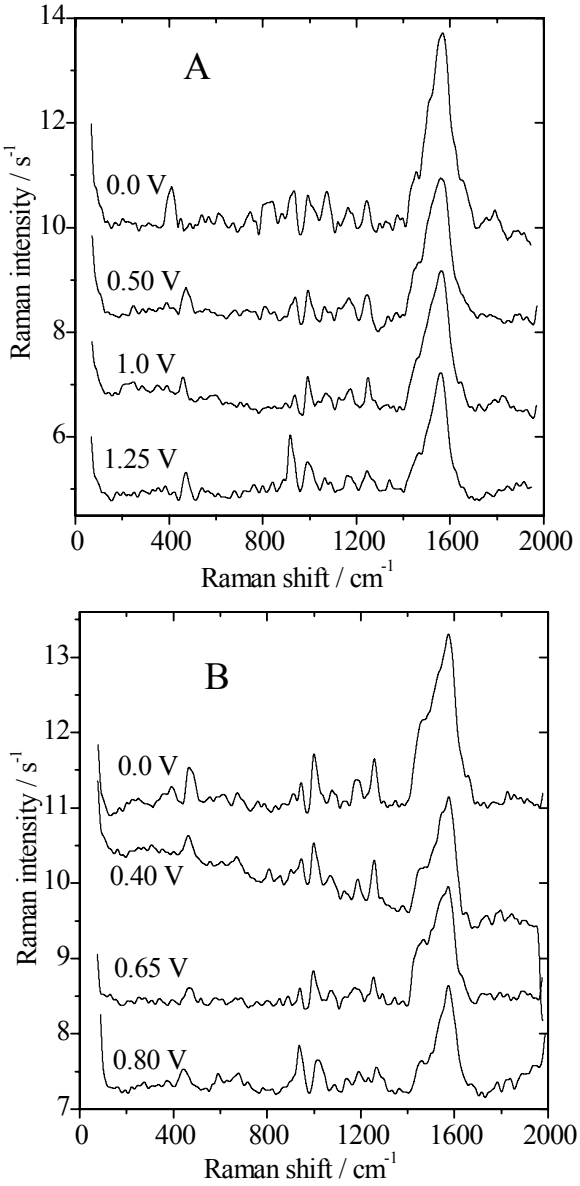

Fig. 59. *In situ* resonance Raman spectra recorded in a solution of acetonitrile + 0.1 **M** TBATFB of copolymers deposited at $E_{Ag/AgCl}$ (A) 1.7 V, (B) 1.5 V in a BFEE + EE (ratio 1:2) and TFA (10 % by volume) containing furan/3-chlorothiophene (mole ratio 8:1)

Table 22. Raman band assignments of copolymer deposited at $E_{Ag/AgCl}$ = 1.7 V with different mole ratios, all figures in wavenumbers cm^{-1}.

Mode	**8:1**[a]				**1:1**[a]			
$E_{Ag/AgCl}$:	0.0 V	0.50 V	1.0 V	1.40 V	0.0 V	0.45 V	0.90 V	1.20 V
$\nu(C=C)_{ring}$	1564	1562	1560	1560	1552	1554	1550	1550
$\nu(C-C)_{ring}$	1510	1501	1505	1513	1525	1530	1531	1532
ω(C-H)	1451	1452	1447	1449	1442	1445	1436	1438
ν(C-C)	1330	1335	1327	1343	1315	1330	1328	1332
$\nu(C-C)_{ring}$	1250	1251	1249	1241	1241	1248	1239	1242
ω(C-H)	1170	1166	1172	1160	1176	1172	1169	1158
$\nu(C-O)_{ring}$	1070	1069	1073	1061	1121	1133	1112	1084
δ(C-H)	1030	1025	1023	1022	1055	1060	1056	1039
δ(C-H)	958	939	955	943	930	936	960	954
γ(C-H)	864	834	830	842	843	847	838	847
δ(C-S-C)	772	761	758	763	756	739	733	763
δ(C-S-C)	710	702	675	703	662	670	663	666
δ(C-Cl)	451	451	454	449	441	444	440	445

[a]furan/3-chlorothiophene mole ratio; δ: in-plane deformation; γ: out-of-plane deformation; ν: stretching; ω: out-of-plane bending.

It is obvious that the Raman spectra of the copolymers are more complex than those of pure polyfuran and poly(3-chlorothiophene), making the assignment difficult. However, the *in situ* Raman spectra of the copolymers are reminiscent of the *in situ* Raman spectra of homopolymers, see Figs. 58-59. We observe a decrease in the intensity and a broadening of the symmetric C=C intraring stretching vibration at higher wavenumbers with an increase of the applied potential. The overall intensity of the spectra decreases upon increasing the applied potential.

Summary

Conducting polymers have been studied intensively since the 1970s for possible applications in electronics. Initially it was the inorganic polysulfurnitrile $(SN)_x$ that was discovered to be highly conducting but interest soon turned to organic polymers, in the hope of exploiting conventional plastics processing technology for the processing of the materials. The introduction has given an overview on conducting polymers and their structures, in addition to synthesis and characterization of these conducting polymers. This thesis has described the behaviour of polyfuran, polythiophenes and their copolymers at platinum surface, which is based on electrochemical and spectroelectrochemical measurements. The experimental parameters of these measurements are summarized in the experimental part.

Section 3.1 summarizes the results obtained with cyclic voltammetry for the homo- and copolymer films at different applied polymerization potentials and different monomer feed ratios. The small difference between the oxidation potentials of furan and thiophene/ 3-chlorothiophene suggests a large probability of copolymerization of the two monomers, and the oxidation potential of the mixture is between the oxidation potential of the monomers implying that oxidation of both monomers is likely, the copolymer chains may accordingly be composed of furan and thiophene/or 3-chlorothiophene units. The addition of TFA (10 % by volume) to the polymerization solution decreased the oxidation potential of the monomers; the polymerization rate was also accelerated because TFA increases the ionic conductivity of the electrolyte.

The oxidation and reduction potentials of the homo- and copolymer films have been obtained and discussed in detail. The homopolymers have only one redox peak caused by polymer oxidation and reduction. The difference in the peak potentials of polyfuran indicates a high reversibility of the associated redox processes, while for polythiophenes the peak separation is larger and less close to reversibility. Electrochemical copolymerization both at different potentials and with different thiophene/or 3-chlorothiphene concentrations has been investigated. The copolymers show a typical cyclic voltammograms as depicted in the homopolymers; only one anodic/cathodic peak couple appears with the copolymer film at a position quite different from the positions observed with homopolymers. The redox peak potential of the copolymers

shifts to higher potentials with an increasing polymerization potential of the copolymer and becomes closer to that of polythiophene/ poly(3-chlorothiophene). This indicates that more thiophene/ 3-chlorothiphene units are incorporated into the copolymer with an increasing preparation potential. It is also observed that a lower concentration of thiophene/ 3-chlorothiphene in the feed leads to a negative shift of the redox peak potentials of the copolymer. This implies that more thiophene/ 3-chlorothiphene units are incorporated into the copolymer film when the concentration of thiophene/ 3-chlorothiphene increases.

The electropolymerization mechanism of copolymers is proposed to be based on already known coupling reactions of aromatic compounds. The first electrochemical step (E) is the oxidation of the monomer into its radical cation. The second step involves the coupling of two radicals to produce a dihydrodimer dication that leads to a dimer after the loss of two protons and rearomatization. This rearomatization constitutes the driving force of the chemical step (C). Electropolymerization then proceeds through successive electrochemical and chemical steps according to a general E(EC)n mechanism, until the oligomer becomes insoluble in the electrolyte solution and precipitates onto the electrode surface.

Furan-thiophene copolymers show fairly good long-term stability of the redox activity after cycling in acetonitrile; the retention of the redox activity of furan-thiophene copolymers after cycling in dry acetonitrile for 100 times is about 60%, whereas about 20% of the redox activity of the copolymer remains after 100 cycles in wet acetonitrile solution. However, when the furan-thiophene copolymer is cycled in an aqueous solution, the redox activity is almost totally lost since it shows a very large anodic peak current but no associated cathodic one indicating that the loss rate of redox activity increases with the amount of water in acetonitrile. The associated loss of redox capacity during the oxidation process may be caused by the destruction of conjugated structures.

In section 3.2 *in situ* UV-Vis spectra measured at different applied polymerization potentials and different monomer feed ratios of all investigated homo- and copolymer films have been presented. λ_{1max} which corresponds to the $\pi \rightarrow \pi^*$ transition has been determined. The optical transition with λ_{2max} from the valence band into the higher bipolaron band has also been assigned. The band gap (E_g) for homo- and copolymer films from a direct interband transition is estimated from the absorption edge

of the spectrum. The redox thermodynamics of the homo- and copolymer films suggest that one electron is removed from the polymer segments containing four monomer units. The correlation between the standard electrode potential and the slope of the copolymer films indicates that the oxidation of copolymers with higher standard potential requires more energy.

The investigated conducting films show a single conductivity change with a stable conductivity up to $E_{Ag/AgCl}$= 2 V is described in section 3.3. The conductivity of these films is almost restored when the potential shift direction is reversed. Polyfuran has a lower conductivity compared to polythiophenes, which attributed to the shorter conjugation length. Another reason is that the degradation and ring opening reaction cannot be totally suppressed in the polymerization solution, and nonconjugated regions, even though in small amounts, exist in the polymer chains.

The conductivity of poly(3-chlorothiophene) is around one order of magnitude lower than that of polythiophene. This can be explained qualitatively by the difference between the hydrogen and chlorine radii. This difference may increase the steric hindrance and distortion along the polymer chain which modifies the structure and thus the properties of the polymer. The low conductivity can also be ascribed to the physical discontinuity within the polymer matrices, which increases the resistance of the polymer. Another noticeable feature is the fact, that *in situ* conductivity properties are not the sum of those of the two individual homopolymers. This result may eliminate the possibility that the copolymers can be considered as block copolymers.

Vibrational spectra of homo- and copolymer films investigated in this study were obtained using standard techniques as displayed in section 3.4. The presence of bands in the region of 840 - 910 cm^{-1} indicates, that α-α' coupling of radical cations has taken place in the copolymerization. This is a characteristic of α-substituted five-membered heterocyclic compounds. The electrochemical degradation of furan-thiophene copolymers is described by two mechanisms: cross linking and attack by nucleophilic species such as water molecules. In dry acetonitrile solution (acetonitrile is a weakly nucleophilic medium) the overoxidative degradation of copolymer caused by the crosslinking mechanism prevails over the nucleophilic mechanism which mainly results in the saturated C-H structures. In wet acetonitrile solution, the over-oxidative degradation by the nucleophilic mechanism also takes place because of the

extremely strong nucleophilic property of water molecules, resulting in the ketone structure.

In section 3.5 *in situ* resonance Raman spectroscopy of the copolymers shows spectroscopic properties intermediate between those of homopolymers. At higher polymerization potentials and at higher concentrations of thiophene/ 3-chlorothiophene in the feed more thiophene/ 3-chlorothiophene units are incorporated into the copolymer chains. The results confirmed that the Raman spectra of the homo- and copolymer films in the doped state were different from those of neutral films. It is also obvious that the Raman spectra of the copolymers are more complex than those of homopolymers, making the assignment difficult. This complexity may be due to the change of effective conjugation length and the more complex chemical environment of each unit encountered in the copolymer chains.

Future Work

Future exploration will require the employment of complementary *in situ* electron spin resonance (ESR) spectroscopy. Much information about the radicals generated during electrochemical processes can be gained from this *in situ* characterization method [41, 119]. This information will give further approaching into the electropolymerization mechanism of copolymers, which were discussed in section 3.1.

Another investigation is to study the thermal stability of electrochemically synthesized homo- and copolymer films by thermogravimetry (TG), the influence of temperature on the film structure by infrared spectroscopy, and morphology by scanning electron microscopy (SEM) [199-202].

The research can be continued to examine the polymeric films by using surface enhanced Raman spectroscopy (SERS) since it enables us to obtain not only selective structural insights into these polymers but also information concerning the orientation of the polymeric nuclei with respect to the metal surface (for example gold and silver) [42, 190, 195].

References

1. H. Shirakawa, E. J. Louis, A. G. MacDiarmid, C. K. Chiang, and A. J. Heeger, *J. Chem. Soc. Chem. Commun*., (1977) 578.
2. C. K. Chiang, C. R. Fischer, Y. W. Park, A. J. Heeger, H. Shirakawa, E. J. Louis, S. C. Gau, and A. G. MacDiarmid, *Phys. Rev. Letters*, 39 (1977) 1098.
3. T. A. Skotheim, R. L. Elsenbaumer, and J. R. Reynolds (eds.), *Handbook of Conducting Polymers*, 2nd ed., Marcel Dekker, New York, (1998).
4. J. C. W. Chien, Polyacetylene: Chemistry, Physics, and Materials Science, Academic: Orlando, (1984).
5. J. Amanokura, Y. Suzuki, S. Imabayashi, and M. Watanabe, *J. Electrochem. Soc*., 148 (2001) D43.
6. G. A. Sotzing, S. M. Briglin, R. H. Grubbs, and N. S. Lewis, *Anal. Chem*., 72 (2000) 3181.
7. C. W. Lin, B. J. Hwang, and C. R. Lee, *J. Appl. Polym. Sci*., 73 (1999) 2079.
8. A. Malinauskas, J. Malinauskiene, and A. Ramanavicius, *Nanotechnol.*, 16 (2005) R51.
9. D. James, S. M. Scott, Z. Ali, and W. T. Ohare, *Microchim. Acta*, 149 (2005) 1.
10. N. J. L. Guernion and W. Hayes, *Curr. Org. Chem.*, 8 (2004) 637.
11. J. C. Vidal, E. Garciaruiz, and J. R. Castillo, *Microchim. Acta*, 143 (2003) 93.
12. L. M. Dai, P. Soundarrajan, and T. Kim, *Pure Appl. Chem.*, 74 (2002) 1753.
13. M. Trojanowicz, T. K. Velkrawczyk, and P. W. Alexander, *Chem. Anal.*, 42 (1997) 199.
14. M. Trojanowicz, *Microchim. Acta*, 143 (2003) 75.
15. S. Cosnier, *Anal. Bioanal. Chem.*, 377 (2003) 507.
16. P. N. Bartlett and P. R. Birkin, *Synth. Met.*, 61 (1993) 15.
17. O. A. Sadik, *Electroanal.*, 11 (1999) 839.
18. G. G. Wallace, M. Smyth, and H. Zhao, *TRAC-Trend. Anal. Chem.*, 18 (1999) 245.
19. H. Shinohara, M. Aizawa, and H. Shirakawa, *J. Chem. Soc. Chem. Commun*., (1986) 87.

20. H. N. T. Le, B. Garcia, C. Deslouis, and Q. L. Xuan, *J. Appl. Electrochem.*, 32 (2002) 105.
21. L. J. Buckley and M. Eashoo, *Synth. Met*., 78 (1996) 1.
22. W. Chen and G. Xue, *Prog. Polym. Sci*., 30 (2005) 783.
23. J. D. Stenger, *Prog. Polym. Sci*., 23 (1998) 57.
24. A. Pron and P. Rannou, *Prog. Polym. Sci*., 27 (2002) 135.
25. A. G. MacDiarmid, *Angew. Chem. Int. Ed*., 40 (2001) 2581.
26. R. J. Waltman, J. Bargon, and A. F. Diaz, *J. Phys. Chem*., 87 (1983) 1459.
27. G. Tourillon and F. Garnier, *J. Electroanal. Chem*., 135 (1982) 173.
28. S. Glenis, D. S. Ginley, and A. J. Frank, *J. Appl. Phys*., 62 (1987**)** 190.
29. R. Holze, *Handbook of Electronic and Photonic Materials and Devices*, H.S. Nalwa Hrsg., Academic Press, San Diego, Vol. 8, (2000), p. 209.
30. A. F. Diaz, J. Castillo, K. K. Kanazawa, J. A. Logan, M. Salmon, and O. Fajardo, *J. Electroanal. Chem.*, 133 (1982) 233.
31. R. Holze, *Handbook of Advanced Electronic and Photonic Materials*, H.S. Nalwa Hrsg., Gordon and Breach, Singapur, Vol. 2, (2001), p. 171.
32. C. Kuo, S. Chen, G. Hwang, and H. Kuo, *Synth. Met*., 93 (1998) 155.
33. D. Kumar and R. Sharma, *Eur. Polym. J*., 34 (1998) 1053.
34. J. L. Bredas, R. R. Chance, and R. Sileby, *Phys. Rev., Part B*, 26 (1982) 5843.
35. E. Blanca, I. Carrillo, M. J. Gonzalez-Tejera, and I. Hernandez-Fuentes, *J. Polym. Sci. : Part A: polymer chemistry*, 38 (2000) 291.
36. T. Ohsawa, K. Kaneto, and K. Yoshino, *Jpn. J. Appl. Phys*., 23 (1984) L663.
37. B. Nessakh, Z. Kotkowska-Machnik, and F. Tedjar, *J. Electroanal. Chem*., 269 (1990) 263.
38. G. Zotti, G. Schiavon, and N. Comisso, *Synth. Met.*, 36 (1990) 337.
39. S. Glenis, M. Benz, E. LeGoff, J. L. Schindler, C. R. Kannewurt, and M. G. Kanatzidis, *J. Am. Chem. Soc*., 115 (1993) 12519.
40. M. J. Gonzalez-Tejera, I. Carrillo, and I. Hernandez-Fuentes, *Synth. Met.*, 73 (1995) 135.
41. B. Demirboga and A. M. Onal, *Synth. Met.*, 99 (1999) 237.
42. X. Wan, F. Yan, S. Jin, X. Liu, and G. Xue, *Chem. Mater*., 11 (1999) 2400.
43. V. Hernandez, F. J. Ramirez, G. Zotti, and J. T. L. Navarrete, *J. Chem. Phys*., 98 (1993) 769.

44. V. Hernandez, F. J. Ramierez, G. Zotti, and J. T. L. Navarrete, *Chem. Phys. Lett*., 191 (1992) 419.
45. C. Liu, J. Zhang, G. Shi, and Y. Zhao, *J. Phys. Chem. B*, 108 (2004) 2195.
46. J. Roncali, *Chem. Rev*., 92 (1992) 711.
47. R. McCullough, *Adv. Mater*., 10 (1998) 93.
48. J. Roncali, *J. Mater. Chem*., 9 (1999) 1875.
49. S. Higgins, *Chem. Soc. Rev*., 26 (1997) 247.
50. D. McQuade, A. Pullen, and T. Swager, *Chem. Rev.*, 100 (2000) 2537.
51. A. Malinauskas, *Synth. Met*., 107 (199 9) 75.
52. G. Grundmeier, W. Schmidt, and M. Stretmann, *Electrochim. Acta,* 45 (2000) 2515.
53. K. Gurunathan, A. V. Mrurgan, R. Marimuthu, U. P. Mulik, and D. P. Amalnerkar, Mater. *Chem. Phys*., 61 (1999) 173.
54. T. F. Otero and I. Cantero, *J. Power Sources* , 81 (1999) 838.
55. B. Fritz and R. Paul, *Electrochim. Acta,* 45 (2000) 2467.
56. G. G. Wallace, *Trends Anal. Chem*., 18 (1999) 443.
57. S. Cosnier, *Biosen. Bioelectron*., 14 (1999) 443.
58. R. V. Parthasarathy and C. R. Martin, *Nature*, 369 (1994) 298.
59. G. Zotti and G. Schiavon. *J. Electroana.l Chem*., 163 (1984) 385.
60. G. Q. Shi, S. Jin, G. Xue, and C. Li. *Science*, 267 (1995) 994.
61. C. Li, G. Q. Shi, G. Xue, S. Jin, B. Yu, and S. Yang, *J. Polym. Sci. : Part B: Polym. Phys*.,33 (1995) 2199.
62. S. Hotta, M. Soga, and N. Sonoda, *Synth. Met*., 26 (1988) 267.
63. M. Feldhues, G. Kamf, H. Litterer, T. Mecklenburg, and P. Wegener, *Synth. Met*., 28 (1989) C487.
64. G. Heffner and D. Pearson, *Synth. Met*., 44 (1991) 341.
65. D. Deffieux, D. Bonafoux, M. Bordeau, C. Biran, and J. Dunogues, *Organometallics*, 15 (1996) 2041.
66. A. Kassmi, F. Fache, and M. Lemaire, *J. Electroanal. Chem*., 373 (1994) 241.
67. L. Shi, J. Roncali, and F. Garnier, *J. Electroanal. Chem*., 263 (1989) 155.
68. L. Zhou and G. Xue, *Synth. Met*., 87 (1997) 193.
69. M. Lemaire, W. Buchner, R. Garreau, H. Hoa, A. Guy, and J. Roncali, *J. Electroanal. Chem*., 281 (1990) 293.
70. J. Xu, G. Shi, Z. Xu, F. Chen, and X. Hong, *J. Electroanal. Chem*., 514 (2001)

16.

71. J. Xu, G. Shi, F. Chen, F. Wang, J. Zhang, and X. Hong, *J. Appl. Polym. Sci*., 87 (2003) 502.
72. C. Li, G. Shi, and Y. Liang, *J. Electroanal. Chem*., 455 (1998) 1.
73. C. Li, G. Shi, and Y. Liang, *Synth. Met*., 104 (1999) 113.
74. M. Berggren, O. Inganas, G. Gustafsson, J. Rasmusson, M. Andorsson, and T. Hjerthery, *Nature*, 372 (1994) 444.
75. L. Zhou, Y. Q. Li, and G. Xue, *Thin Solid Films*, 335 (1998) 112.
76. L. Li, W. Chen, N. Xu, Z. G. Xaio, and G. Xue, *J. Mat. Sci.*, 39 (2004) 2395.
77. X. Wan, W. Zhang, S. Jin, G. Xue, Q. You, and B. Che, *J. Electroanal. Chem*., 470 (1999) 23.
78. T. Okada, T. Ogata, and M. Ueda, *Macromolecules*, 40 (1996) 3963.
79. R. Sugimoto, S. Takeda, H. B. Gu, and K. Yoshino, *Chem. Express*, 1 (1986) 635.
80. N. Toshima and S. Hara, *Prog. Polym. Sci*., 20 (1995) 155.
81. P. Kovacic and M. B. Jones, *Chem. Rev*., 87 (1987) 357.
82. S. Asavapiriyonont, G. K. Chandler, G. A. Gunawardena, and D. Pletcher, *J. Electroanal. Chem*., 177 (1984) 229.
83. E. Genies, G. Bidan, and A. F. Diaz, *J. Electroanal. Chem*., 149 (1983) 113.
84. C. Pinzino, R. Angelone, F. Benvenuti, C. Carlini, A. M. R. Galletti, and G. Sbrana, *J. Polym. Chem., Polym. Phys*., 36 (1986) 1901.
85. N. N. Greenwood, R. L. Martin, and H. J. Emeleus, *J. Chem. Soc*., 1 (1950) 3030.
86. G. Q. Shi, C. Li, and Y. Q. Liang, *Adv. Mater*., 11 (1999) 1145.
87. G. Q. Shi, G. Xue, C .Li, S. Jin, and B. Yu, *Macromolecules*, 27 (1994) 3678.
88. G. Q. Shi, G. Xue, C. Li, and S. Jin, *Polym Bull*., 33 (1994) 325.
89. Z. M. Huang, L. T. Qu, G. Q. Shi, F. Chen, and X. Y. Hong. *J Electroanal Chem*., 556 (2003) 159.
90. J. B. He, H. J. Zhou, F. Wan, Y. Lu, and G .Xue, *Vib. Spectrosc*., 31 (2003) 265.
91. J. B. He, W. Chen, N. Xu, L. Li, X. W. Li, and G. Xue, *Appl. Surf. Sci*., 221 (2004) 87.
92. G. Louarn, M. Trznadel, J. P. Buisson, J. Laska, A. Porn, M. Lapkowski, and S. Lefrant, *J. Phys. Chem*., 100 (1996) 12532.

93. R. Holze and J. Lippe, *Synth. Met.*, 38 (1990) 99.
94. J. Lippe and R. Holze, *Synth. Met*., 41 (1991) 2927.
95. J. Heeger, *J. Phys. Chem. B*, 105 (2001) 8475.
96. A. A. Pud, *Synth. Met*., 66 (1994) 1.
97. P. A. Christensen and A. Hamnett, *Electrochim. Acta*, 36 (1991) 1263.
98. R. Qian, J. Qiu, and B. Yan, *Synth. Met*., 14 (1986) 81.
99. J. Bukowska and K. Jakowska, *Synth. Met.*, 35 (1990) 143.
100. S. Wang, K. Tanaka, and T. Yamabe, *Synth. Met*., 32 (1989) 32.
101. T. Kobayashi, H. Yoneyama, and H. Tamura, *J. Electroanal. Chem*., 161 (1984) 419.
102. A. Kitani, M. Kaya, K. Yoshikawa, and K. Sasaki, *Synth. Met*., 18 (1987) 341.
103. J. Roncali, *Chem. Rev.*, 97 (1997) 173.
104. E. E. Moore and D. Yaron, *J. Phys. Chem.* A, 106 (2002) 5339.
105. M. Kobayashi, N. Colaneri, M. Boysel, F. Wudl, and A. J. Heeger, *J. Chem. Phys.*, 82 (1985) 5717.
106. D. R. Baigent, P. J. Hamer, R. H. Friend, S. C. Moratti, and A. B. Holmes, *Synth. Met*., 71 (1995) 2175.
107. I. T. Kim and R. L. Elsenbaumer, *Macromolecules*, 33 (2000) 6407.
108. A. J. Hagan, S. C. Moratti, and I. C. Sage, *Synth. Met*., 119 (2001) 147.
109. K. Lee and G. A. Sotzing, *Macromolecules,* 34 (2001) 5746.
110. U. Salzner, J. B. Lagowski, P. G. Pickup, and R. A. Poirier, *Synth. Met*., 96 (1998) 177.
111. T. Tani, P. M. Grant, W. D. Gill, G. B. Street, and T. C. Clarke, *Solid state Commun*., 33 (1980) 499.
112. G. Gritzner and J. Kuta, *Pure Appl. Chem*., 56 (1984) 461.
113. P. Marque and J. Roncali, *J. Phys. Chem*., 94 (1990) 8614.
114. J. Casado, M. Bengoechea, J. T. L. Navarette, and T. F. Otero, *Synth. Met*., 95 (1998) 93.
115. M. Zhou and J. Heinze, *Electrochim. Acta* , 44 (1999) 1733.
116. E.A. Bazzaoui, S. Aeiyach, and P.C. Lacaze, *J. Electroanal. Chem*., 364 (1994) 63.
117. S. Shreepathi and R. Holze, *Chem. Mater*. 17 (2005) 4078.
118. H. Chan and C. Siu, *Prog. Polym. Sci*. 23 (1998) 1167.

119. M. A. Del Valle, L. Ugalde, F. R. Daiz, M. E. Bodini, and J. C. Bernede, *J. Appl. Polym. Sci.,* 92 (2004) 1346.

120. E. M. Genies, G. Bidan, and A. F. Diaz, *J. Electroanal. Chem.*, 149 (1983) 101.

121. R. S. Glass, *Topics in Current Chemistry*, Springer, 205 (1999) 1-87.

122. X-B. Wan, L. Li, J-B. He, D-S. Zhou, G. Xue, and T-W. Wang, *J. Appl. Polym. Sci.,* 86 (2002) 3160.

123. S. Yang, P. Olishevski, and M. Kertesz, *Synth. Met*. 141 (2004) 171.

124. L. E. Lyons, *Aust. J. Chem*. 33 (1980) 1717.

125. V. Saxena and B. D. Malhotra, *Current. Appl. Phys*. 3 (2003) 293.

126. J. C. Scott, P. Pfluger, M. T. Krounbi, and G. B. Street, *Phys. Rev*. B, 28 (1983) 2140.

127. W. P. Su, J. R. Schrieffer, and A. J. Heeger, *Phys. Rev*. B, 22 (1980) 2099.

128. J. L. Bredas, J. C. Scott, K. Yakushi, and G. B. Street, *Phys. Rev*. B, 30 (1984) 1023.

129. J. L. Bredas and G. B. Street, *Acc. Chem*. *Res.*, 18 (1985) 309.

130. Y. S. Negi and P. V. Adhyapak, *J. Macromol. Sci.-Polym. Rev*. C, 42 (2002) 35.

131. S. Vogel and R. Holze, *Electrochim. Acta*, 50 (2005) 1587.

132. J. Bredas, R. Silbey, D. Bourdreaux, and R. Chance, *J. Am. Chem. Soc*., 105 (1983) 6555.

133. W. Salaneck, O. Inganas, J. Nillson, J. Osterholm, B. Themans, and J. Bredas, *Synth. Met*., 28 (1989) C451.

134. H. Chan, S. Ng, S. Seow, and J. Moderscheim, *J. Mater. Chem*., 2 (1992) 1135.

135. G. Tourillon and F. Garnier, *J. Phys. Chem*., 87 (1983) 2289.

136. R. B. Kaner, S. J. Porter, D. P. Nairns, and A. G. MacDiarmid, *J. Chem. Phys*., 90 (1989) 5102.

137. A. F. Diaz, J. I. Castillo, J. A. Logan, and W-Y. Lee, *J. Electroanal. Chem*., 129 (1981) 115.

138. E. M. Genies and J. M. Pernaut, *Synth. Met*., 10 (1984/85) 117.

139. M. Nechtschein, F. Deverux, F. Genoud, E. Vieil, J. M. Pernaut, and E. Genies, *Synth. Met*., 15 (1986) 59.

140. J. R. Reynolds, A. D. Child, J. P. Ruiz, S. Y. Hong, and D. S. Marynic, *Macromolecules*, 26 (1993) 2095.

141. M. J. Gonzalez-Tejera, I. Carrillo, and I. Hernandez-Fuentes, *Synth. Met.*, 92 (1998) 187.

142. H. Masuda, S. Tanaka, and K. Kaeriyama, *Synth. Met*., 31 (1989) 29.

143. R. M. Silverstein, G. C. Bassler, and T. C. Morrill, *Spectrocsopic Identification of Organic Compounds*, 4th ed., John Wiley & Sons (1981).

144. G. Socrates, *Infrared Characteristic Group Frequencies*, , John Wiley & Sons (1980).

145. S. K. Manohar, A. G. MacDiarmid, K. R. Cromack, J. M. Ginder, and A. J. Epstein, *Synth. Met*., 29 (1989) E349.

146. A. R. Katritzky and J. M. Lagowski, *J. Chem. Soc*., (1959) 657.

147. S. Kuwabata, S. Ito, and H. Yoneyama, *J. Electrochem. Soc.*, 135 (1988) 1691.

148. F. Garnier, G. Tourillon, M. Gazard, and J. C. Dubois, *J. Electroanal. Chem*., 148 (1983) 299.

149. K. Kaneto, K. Yoshino, and Y. Inuishi, *Solid State Commun*., 46 (1983) 389.

150. A. Gok, B. Sari, and M. Talu, *J. Appl. Polym. Sci*., 88 (2003) 2924.

151. F. Mohammad, *J. Phys. D: Appl. Phys*., 31 (1998) 951.

152. Y. Yagci, F. Yilmaz, S. Kiralp, and L. Toppare, *Macromol. Chem. Phys*., 206 (2005) 1178.

153. M. Rico, J. M. Orza, and J. Morcillo, *Spectrochim. Acta*, 21 (1965) 689.

154. C. Yong and Q. Renyaun, *Solid State Commun*., 54 (1985) 211.

155. A. Hidalgo, *J. Phys. Rad*., 16 (1955) 366.

156. M. H. Gutierrez, W. T. Ford, and H. A. Pohl, *J. Polym. Sci. Polym. Chem. Ed*., 22 (1984) 3789.

157. F. Martinez, G. Neculqueo, and M. Veas, *Bol. Soc. Chil. Quim*., 45 (2000).

158. F. Beck, U. Barsch, and R. Michaelis, *J. Electroanal. Chem*., 351 (1993) 169.

159. I. Carrillo, E. S. Blanca , M. J. Gonzalez-Tejera, and I. Hernandez-Fuentes, *Chem. Phys. Lett.*, 229 (1994) 633.

160. A. F. Diaz and B. Hall, *IBM J. Res. Dev*., 27 (1983) 342.

161. S. Wang, K. Tanaka, and T. Yamabe, *Synth. Met*., 32 (1989) 141.

162. M. Can, K. Pekmez, N. Pekmez, and A. Yildiz, *J. Appl. Polym. Sci.*, 77 (2000) 312.
163. M. Can, K. Pekmez, N. Pekmez, and A. Yildiz, *Tr. J. Chem*., 22 (1998) 47.
164. R. S. Atkinson and E. Bullock, *Can. J. Chem*., 41 (1963) 625.
165. F. Chen, G. Q. Shi, J. X. Zhang, and M. X. Fu, *Thin Solid Films*, 424 (2003) 283.
166. Y. Shen, F. Chen, P. Wu, and G. Shi, *J. Chem. Phys*., 119 (2003) 11415.
167. M. Fu, G. Shi, F. Chen, and X. Hong, *Phys. Chem. Chem. Phys*., 4 (2002) 2685.
168. E. A. Bazzaoui, J. Aubard, A. Elidrissi, A. Ramdani, and G. Levi, *J. Raman Spectrosc*., 29 (1998) 799.
169. Y. Furukawa, *J. Phys. Chem*., 100 (1996) 15644.
170. P. A. Lane, X. Wei, and Z. V. Vardeny, *Phys. Rev. Lett.*, 77 (1996) 1544.
171. F. R. Dollish, W. G. Fateley, and F. F. Bentley, *Characteristic Raman frequencies of organic compounds*, Newyork, John Wiley & sons, Inc (1974).
172. G. B. Guthrie, D. W. Scott, W. N. Hubbard, C. Katz, J. P. McCullough, M. E. Gross, K. D. Williamson, and G. Waddington, *J. Am. Chem. Soc*., 74 (1952) 4662.
173. V. Hernandez, F. J. Ramirez, G. Zotti and J. T. L. Navarrete, *Synth. Met.*, 55 (1993) 4467.
174. M. Ceppatelli, M. Santoro, R. Bini, and V. Schettino, *J. Chem. Phys*., 18 (2003) 1499.
175. J. H. S. Green and D. J. Harrison, *Spectrochim. Acta*, 33A (1977) 843.
176. V. Hernandez, J. T. L. Navarrete, G. Zotti, M. Veronelli, and G. Zerbi, *Synth. Met.*, 69 (1995) 391.
177. V. Hernandez, M. Veronelli, L. Favaretto, J. T. L. Navarrete, D. Jones, and G. Zerbi, *Acta Polymer.*, 47 (1996) 62.
178. K. Matsuno and K. Han, *Bull. Chem. Soc. Jap*., 9 (1934) 327.
179. K. Han, *Bull. Chem. Soc. Jap*., 11 (1936) 701.
180. R. Holze, *Synth. Met.*, 40 (1991) 379.
181. J. L. Sauvajol, G. Poussigue, C. Benoit, J. P. Lere-Porte, and C. Chorro, *Synth. Met.*, 41 (1991) 1237.

182. S. Hasoon, M. Galtier, J. L. Sauvajol, J. P. Lere-Porte, A. Bonniol, and B. Moukala, *Synth. Met.*, 28 (1989) C317.

183. G. Louarn, J. Y. Mevellec, J. P. Buisson, and S. Lefrant, *Synth. Met.*, 55-57 (1993) 587.

184. J. Casado, V. Hernandez, Y. Kanemitsu, and J. T. L. Navarrete, *J. Raman Spectrosc*., 31 (2000) 565.

185. M. X. Fu, F. Chen, J. X. Zhang, and G. Shi, *J. Mater. Chem*., 12 (2002) 2331.

186. B. Dufour, P. Rannou, J. P. Travers, A. Pron, M. Zagorska, G. Korc, I. Kulszewicz-Bajer, S. Quillard, and S. Lefrant, *Macromolecules*, 35 (2002) 6112.

187. M. X. Fu, Y. F. Zhu, R. Q. Tan, and G. Q. Shi, *Adv. Mater*., 13 (2001) 1874.

188. W. Fujita, N. Teramae, and H. Haraguchi, *Chem. Lett.*, (1994) 511.

189. E. A. Bazzaoui, J. P. Marsault, S. Aeiyach, and P. C. Lacaze, *Synth. Met.*, 66 (1994) 217.

190. E. A. Bazzaoui, S. Aeiyach, J. Aubard, N. Felidj, P. C. Lancaze, N. Sakmeche, and G. Levi, *J. Raman Spectrosc*., 29 (1998) 177.

191. C. Botta, S. Luzzati, G. Dellepiane, and C. Taliani, *Synth. Met.*, 28 (1989) D331.

192. G. Louarn, J. P. Buisson, S. Lefrant, and D. Fichon, *J. Phys. Chem*., 99 (1995) 11399.

193. V. Hernandez, J. Casado, Y. Kanemitsu, and J. T. L. Navarrete, *J. Chem. Phys.*, 110 (1999) 6907.

194. E. F. Steigmeir, H. Auderset, W. Kobel, and D. Baeriswyl, *Synth. Met.*, 18 (1987) 219.

195. E. A. Bazzaoui, G. Levi, S. Aeiyach, J. Aubard, J. P. Marsault, and P. C. Lacaza, *J. Phys. Chem.*, 99 (1995) 6628.

196. Y. Furukawa, M. Akimoto, and I. Harada, *Synth. Met.*, 18 (1987) 151.

197. N. Ozcicek, K. Pekmez, R. Holze, and A. Yildiz, *J. Appl. Polym. Sci*., 90 (2003) 3417.

198. A. Bongini, G. Barbarella, M. Zambianchi, V. Hernandez, and J. T. L. Navarrete, *Synth. Met*., 108 (2000) 27.

199. I. Carrillo, F. Fernandez, C. Barba, E. Blanca, M. Gonzalez-Tejera, and I. Hernandez-Fuentes, *Polym*. *Bull.*, 43 (1999) 269.

200. A. Gok, B. Sari, and M. Talu, *J. Appl. Polym. Sci*., 98 (2005) 2048.

201. M. Talu, M. Kabasakaloglu, F. Yildirim, and B. Sari, *Appl. Surf. Sci.*, 181 (2001) 51.

202. M. Kabasakaloglu, M. Talu, F. Yildirim, and B. Sari, *Appl. Surf. Sci*., 218 (2003) 84.

List of publications

1. **F. Alakhras** and R. Holze, Spectroelectrochemistry of Intrinsically Conducting Furan-3-Chlorothiophene Copolymers, *J. Solid State Electrochem.*, 12 (2008) 81.

2. **F. Alakhras** and R. Holze, Furan-Thiophene copolymers: electrosynthesis and electrochemical behavior, *J. Appl. Polym. Sci*., 107 (2008) 1133.

3. **F. Alakhras** and R. Holze, *In situ* UV-Vis- and FT-IR- Spectroscopy of Electrochemically Synthesized Furan-Thiophene Copolymers, *Synth. Met*., 157 (2007) 109.

4. **F. Alakhras** and R. Holze, Redox Thermodynamics, Conductivity and Raman Spectroscopy of Electropolymerized Furan-Thiophene Copolymers, *Electrochim. Acta*, 52 (2007) 5896.

5. **F. Alakhras**, K. Abu- Dari, and M. Mubarak, Synthesis and Chelating Properties of Some Poly(amidoxime-hydroxamic acid) Resins Toward Some Trivalent Lanthanide Metal Ions, *J. Appl. Polym. Sci*., 97 (2005) 691.

Selbstständigkeitserklärung

Hiermit erkläre ich an Eides statt, die vorliegende Arbeit selbstständig und ohne unerlaubte Hilfsmittel durchgeführt zu haben.

Chemnitz, den 20.09.2007

M.Sc. Fadi Alakhras

Curriculum Vitae

Personal Information

Name:	Fadi Alakhras
Date of Birth:	July 05, 1979
Marital Status:	Single, no Children
Current Address:	Vettersstrasse 52/532
	09126 Chemnitz, Germany
Email:	fadi.alakhras@s2005.tu-chemnitz.de
	fadialakhras@yahoo.com

Education

1996–1997	Al-Ittihad High Secondary School (Scientific Stream), Amman, Jordan
1997–2001	Yarmouk University. Irbid, Jordan. **B.Sc.** (Chemistry)
2001–2004	University of Jordan. Amman, Jordan **M.Sc.** (Chemistry) M.Sc. Thesis titled with: "Chelation Properties of Some Poly (Amidoxime-Hydroxamic Acid) Polymers toward Some Trivalent Lanthanide Ion.
2005–2008	**Ph.D.** Student, Institute of Physical Chemistry/Electrochemistry, TU Chemnitz, Germany. Supervisor: Prof. Dr. Rudolf Holze.

Professional Experience

1. **Scientific Coworker** (Wissenschaftlicher Mitarbeiter), TU Chemnitz, Physical Chemistry/Electrochemistry. April 2006–August 2006, October 2007–January 2008.

2. **Senior Analyst** (Analytical Lab.), International Pharmaceutical Research Center (Jordan). June 2004–March 2005.

3. **Researcher** (Analytical Unit), ACDIMA Center for Bioequivalence and Pharmaceutical Studies (Jordan). July 2003–May 2004.

4. **Analyst** (Analytical Division), Pharmaceutical Research Unit. (Jordan). April 2001–May 2002.

5. **Teaching Assistant,** University of Jordan (Jordan), Chemistry Department, Inorganic Chemistry labs. 2002/2003.

Conferences and Seminars

1. "Elektrochemie in Sachsen". Kurt-Schwabe Institut. Meinsberg, Germany. 05.12.2005. Seminar presented: *Spectroelectrochemistry of intrinsically conducting Furan-Thiophene copolymers*.

2. Graduate Student Seminar. TU Chemnitz, 14.06.2007. Seminar presented: *Calculation vs. Experiment: Predictive Tools in Spectroelectrochemistry of Molecules and Conducting Polymers.*

Scholarships

1. German Academic Exchange Service (DAAD). Scholarship for study conclusion aid, June - July (2007).